Status of Thesis

Title of thesis | Engine Performance and Combustion Characteristics of Hydrogen in a Direct Injection Engine

I MUHAMAD ADLAN BIN ABDULLAH

hereby allow my thesis to be placed at the Information Resource Center (IRC) of Universiti Teknologi PETRONAS (UTP) with the following conditions:

1. The thesis becomes the properties of UTP.

2. The IRC of UTP may make copies of the thesis for academic purposes only.

3. This thesis is classified as

[ ] Confidential

[√] Non-confidential

If this thesis is confidential, please state the reason:

-

The contents of the thesis will remain confidential for - years.

Remarks on disclosure:

-

Endorsed by

Signature of Author

Permanent Address: No 8 Jalan Desaria 13, Taman Desaria Nilai, Nilai, N Sembilan

Date: 11 Feb 2009

Signature of Supervisor

Name of Supervisor: Assoc. Prof. Dr. A Rashid B A Aziz

Date: 11/2/2009

APPROVAL PAGE

UNIVERSITI TEKNOLOGI PETRONAS

Approval by Supervisor (s)

The undersigned certify that they have read, and recommend to The Postgraduate Studies Programme for acceptance, a thesis entitled "**Engine Performance and Combustion Characteristics of Hydrogen in a Direct Injection Engine**" submitted by **Muhamad Adlan Bin Abdullah** for the fulfillment of the requirements for the degree of Master of Science in Mechanical Engineering.

11/2/2009

Date

Signature : _____

Main supervisor : Assoc. Prof. Dr A Rashid B A Aziz

Date : 11/2/2009

Signature : -

Co-Supervisor : -

Date : -

TITLE PAGE

UNIVERSITI TEKNOLOGI PETRONAS

Engine Performance and Combustion Characteristics of Hydrogen in a Direct Injection Engine

By

Muhamad Adlan Bin Abdullah

A THESIS

SUBMITTED TO THE POSTGRADUATE STUDIES PROGRAMME AS A REQUIREMENT FOR THE

DEGREE OF MASTER OF SCIENCE

MECHANICAL ENGINEERING

BANDAR SERI ISKANDAR,

PERAK

NOVEMBER, 2008

DECLARATION

I hereby declare that the thesis is based on my original work except for quotations and citations which have been duly acknowledged. I also declare that it has not been previously or concurrently submitted for any other degree at UTP or other institutions.

Signature : 

Name : MUHAMAD ADLAN BIN ABDULLAH

Date : 11 Feb 2009

ACKNOWLEDGEMENT

I thank Allah almighty for His guidance and blessings that made all this work possible. I am also grateful to my supervisor, Assoc. Prof. Dr A Rashid A Aziz for his constant support and guidance for me to complete this MSc degree.

I am especially indebted to my colleagues En Razali and En Firmansyah for tirelessly assisting me in the preparation and running of the experiments. Their understanding and knowledge of the facility and the equipment was superb! I sincerely wish them luck in their future undertakings. I also wish to express my gratitude to the other postgraduate students for their friendship and sharing of ideas that assisted me in this work.

ABSTRACT

Hydrogen's high flammability, low ignition energy, clean burning and high flame speed are attractive advantages for use in internal combustion engines to attain high performance and efficiency. To overcome volumetric efficiency loss, high NO_x emissions and abnormal combustion, direct injection option is being studied. Optimisation of the direct injection strategies and understanding of the combustion processes are currently being studied in the automotive industry and research institutions.

In this study, the engine performance and combustion characteristics of hydrogen in a single cylinder direct injection engine was investigated. The engine was originally designed for CNG fuel with a compression ratio of 14:1. To demonstrate practicality and ease of adoption, no modification was made to the engine. Tests were carried out at full throttle for speeds from1800 rpm to 4000 rpm. The effects of varying injection timing and air fuel ratio were studied for the purpose of finding optimised operations. Comparisons with CNG operation were made to demonstrate the potential of hydrogen direct injection to improve the engine performance.

The study has demonstrated that despite having to 'de-rate' the engine for pre-ignition control at higher speeds, 10% performance improvement can be achieved when operating on hydrogen at low engine speeds and WOT. It was shown that full and late partial direct injection at stoichiometric operation would be desired for maximum performance. At intermediate speed, 3000 rpm, the operation at lambda 1.2 would be optimum for engine efficiency while maintaining the performance. An indicated thermal efficiency of 46% would be possible at lower loads by running the engine with unthrottled lean operation.

While the CO and THC emissions were an order of magnitude lower than CNG, the NO_x emission would be higher at low speed. Due to the degree of stratification, at close to stoichiometric, the NO_x emission increased as SOI was advanced despite lower performance and peak cylinder pressure. Operating at lambda higher than 1.3 yield low NO_x emission, however the performance was much compromised.

Keywords: Hydrogen, direct injection, spark ignition engine, injection timing

ABSTRAK

Kelebihan hidrogen dari segi mudah terbakar, mempunyai pembakaran yang bersih dan halaju pembakaran yang tinggi boleh menghasilkan prestasi dan kecekapan enjin yang tinggi. Sistem pancitan terus umumnya dipertimbangkan untuk mengatasi masalah kehilangan kecekapan isipadu, pelepasan NO_x dan pembakaran tidak normal. Mengenalpasti strategi tepat untuk sistem pancitan terus ini dan pemahaman proses pembakaran hidrogen di dalam enjin merupakan satu bidang kajian terkini dalam industri dan di pusat-pusat penyelidikan.

Kajian ini melihat kepada prestasi enjin dan ciri-ciri pembakaran hidrogen dalam sebuah enjin satu silinder dengan system pancitan terus. Potensi hidrogen untuk meningkatkan prestasi enjin pada kelajuan enjin yang rendah juga dikaji. Enjin yang direka untuk kegunaan CNG dengan nisbah mampatan 14:1 digunakan untuk tujuan ini. Tiada sebarang pengubahsuaian dilakukan keatas enjin ini bagi menunjukkan potensi bahawa penggunaan hidrogen adalah praktikal dan sedia digunakan.

Ujian enjin dijalankan dengan bukaan pendikit yang maksima pada kelajuan enjin 1800 ke 4000 rpm (pusingan per minit). Kesan daripada mempelbagaikan pemasaan pancitan bahanapi dan nisbah udara dan bahanapi dikaji supaya operasi yang optima dapat dikenalpasti. Perbandingan dengan penggunaan CNG dibuat untuk menunjukkan potensi pancitan terus hidrogen bagi meningkatkan prestasi enjin.

Sebanyak 10% peningkatan prestasi pada kelajuan enjin yang rendah telah dibuktikan melalui kajian ini. Penggunaan pancitan terus penuh dan separa penuh lewat adalah diperlukan untuk prestasi maksimum. Pada kelajuan 3000 rpm, operasi pada lambda 1.3 adalah optima untuk kecekapan enjin yang maksima. Pada bebanan yang rendah, tahap kecekapan tertunjuk sebanyak 46% boleh dicapai dengan operasi tanpa pendikit dan nisbah bahanapi dengan udara yang tinggi.

Walaupun pelepasan CO and THC dalam julat 10 kali lebih rendah daripada CNG, tahap pelepasan NO_x pula adalah lebih tinggi terutamanya pada kelajuan rendah. Pada keadaan stoikiometrik, pelepasan NO_x menaik dengan pancitan lebih awal, walaupun

tekanan puncak silinder dan prestasi menurun. Ini disebabkan oleh tahap stratifikasi campuran bahan api dan udara dalam silinder. Operasi pada lambda lebih daripada 1.3 dapat mengurangkan pelepasan NO_x, namun prestasi enjin terjejas.

TABLE OF CONTENTS

LIST OF TABLES

LIST OF FIGURES

ABBREVIATIONS

H_2ICE	Hydrogen Internal Combustion Engine
CNG	Compressed Natural Gas
NGV	Natural Gas Vehicle
LPG	Liquified Petroleum Gas
LNG	Liquified Natural Gas
HCNG	A fuel of mixture of Hydrogen and Compressed Natural Gas
DI	Direct Injection
SOI	Start of Injection
BTDC	Before Top Dead Centre
ATDC	After Top Dead Centre
EGR	Exhaust Gas Recirculation
IANGV	International Association for Natural Gas Vehicle
MBT	Maximum Brake Torque
WOT	Wide Open Throttle
AFR	Air Fuel Ratio
IMEP	Indicated Mean Effective Pressure
BMEP	Brake Mean Effective Pressure
BSFC	Brake Specific Fuel Consumption
HC	Hydrocarbon
CO	Carbon Monoxide
NO_x	Nitric Oxide
COV	Coefficient of variation

NOMENCLATURES

Lambda	The ratio of the mixture air fuel ratio to the stoichiometric air fuel ratio
γ	The polytropic index. In this study a value of 1.33 was used
ρ	The density of intake air
mw_{exh}	The molecular weight of exhaust gas
$\dot{m}_{exh}$	The mass flow rate of the exhaust gas
$\dot{m}_a$	The mass flow rate of the intake air
$\dot{m}_f$	The mass flow rate of the fuel
$conc_e$	The volumetric concentration of the exhaust emission constituent
$\dot{n}_{exh}$	The mole flow rate of the total exhaust gas
$\dot{n}_e$	The mole flow rate of the exhaust emission constituent
S_e	The brake specific emissions, expressed in g/kWhr
P	Power output of the engine
N	Engine speed
T	Torque output of the engine
V_s	The swept volume of the engine
FC	The fuel consumption
V_d	The displacement volume of the engine or the engine capacity
η_v	The volumetric efficiency
W_c	The indicated work
σ_{IMEP}	The standard variation of the *IMEP*
Δp	The change in total pressure
Δp_c	The change in pressure due to combustion
Δp_v	The change in pressure due to the volume change
Q_{out}	The heat released by the combustion
Q_{in}	The heat input from the fuel
Q_{ch}	The chemical energy of the fuel
q_{HV}	The lower heating value of the fuel
P_i	The indicated power
P_b	The brake power
η_{ind}	The indicated thermal efficiency of the engine

CHAPTER I

INTRODUCTION

1.1 Background

Hydrogen economy is the most accepted and talked about hypothetical energy economy in the world today. Efforts to realise the hydrogen economy have led to research initiatives across the globe. Iceland, with its vast renewable energy resources from geothermal and hydroelectricity, but lacking the conventional fossil reserves, has launched its ambitious program to transition its energy source to hydrogen by the year 2030 [1].

It is envisioned that the fossil fuel will be replaced by renewable energy for power and transportation. Hydrogen itself is not the source of energy, but rather the carrier. Malaysia has its own road map for hydrogen economy which includes the use of fuel cells and internal combustion engines (Figure 1-1) [2]. However, this vision of transition from fossil fuels to hydrogen is not without its challenges. Figure 1-2 shows the US plan for the transition to hydrogen [3] which indicates that most of the technologies required for the hydrogen economy are yet to mature. As an example, the much hyped fuel cells are currently not as durable and cost effective as the internal combustion engines [4], and efficient and cost effective means of storing and transporting hydrogen are still under much research.

In the use of hydrogen for transportation fuel, there is a widely accepted argument that direct combustion of hydrogen in internal combustion engine could serve as a pathway to hydrogen economy before fuel cells technologies mature and become cost effective [5,6]. Current automotive technologies and manufacturing processes can be used and the experience of operating and handling gaseous fuels such as natural gas can prove beneficial. This would also facilitate the proliferation of the hydrogen production and refuelling infrastructures.

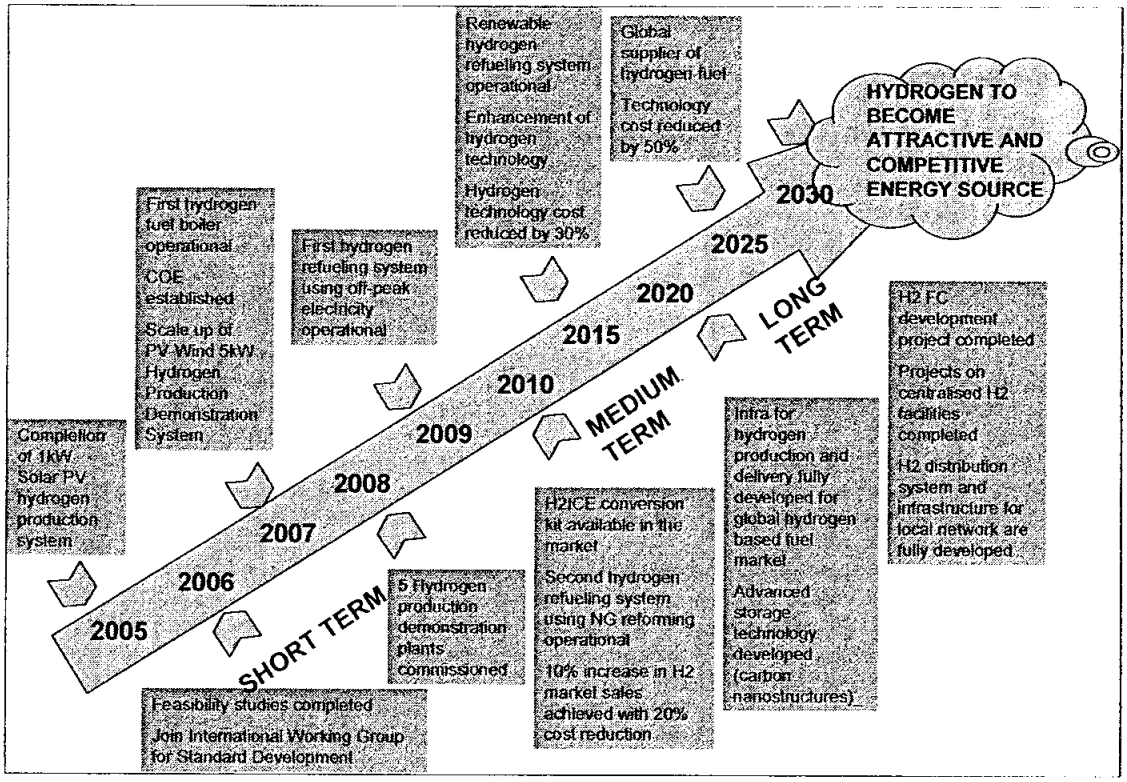

Figure 1-1 Malaysia road map for hydrogen economy [4]

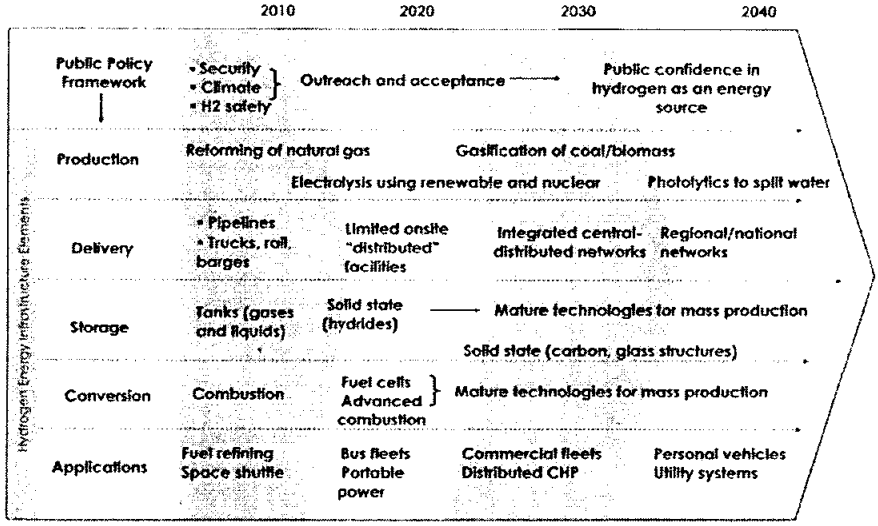

Figure 1-2 The transition to hydrogen economy for the USA[3]

The use of hydrogen in internal combustion engines was pioneered in Germany during the 1920's [7] and research into such uses is recently becoming more of interest ever since the concept of hydrogen economy becomes popular. Most of the works were done on external mixture preparation in which either a carburettor or port fuel injection was used. As the direct injection (DI) technology becomes available in the automotive industry, the new researches are focusing on adapting the technology for hydrogen to increase the power density and reduce the oxides of nitrogen (NO_x) emission.

Since hydrogen is not widely accessible today and the cost is prohibitive for widespread use in transportation sector, bi-fuel approach is used. BMW, for example, demonstrated the gasoline-hydrogen bi-fuel vehicle in 2006 [8] to show that hydrogen vehicles are practical to be used. Researches on dual fuel diesel-hydrogen were also conducted. For gaseous fuel engine, mixture of CNG-hydrogen is proposed.

As hydrogen has unique and sometimes contradicting characteristics in relation to its use as internal combustion fuel [9], it poses new challenges and opportunities. On one hand, hydrogen's wide flammability range gives opportunity for throttleless operation (or power control by fuel quantity controlled means similar to diesel engines) with significant volumetric efficiency improvements potential. The high flame propagation speed gives rise to near constant volume combustion, yielding a potential thermal efficiency improvement. A further thermal efficiency improvement is also possible due to the inherent hydrogen's high auto-ignition temperature (a higher compression ratio engine is possible).

On the other hand, hydrogen's very low density and viscosity, low ignition energy and low radiant heat push for new sets of thinking and approach to using it as a fuel for internal combustion engines. For example, while high compression ratio is desired considering the high octane of hydrogen, its low ignition energy may result in preignition due to glow ignition. In this case, optimised compression ratio or combustion chamber design may need to be determined. Even though the combustible limits of hydrogen are wide, its low density and viscosity may require optimization of injection parameters in order to reduce NO_x and the occurrence of preignition.

Most of the previous works adopted lean burn strategies for hydrogen operation to avoid abnormal combustion. Even for direct injection engines, only compression ratios similar to gasoline engine were used.

In this present study, the performance of hydrogen in a direct injection, spark ignition was studied. In this case, bi-fuel approach was proposed. The engine was originally designed and optimised for compressed natural gas (CNG) use. However, CNG has limitations in terms of its properties related to combustion such as low flame speed, high ignition energy and narrow combustible limit. These properties put a cap on the attainable power. Results from a previous study on DI CNG shows performance deficit at low speed - low indicated mean effective pressure (*IMEP*), low combustion efficiency and high carbon monoxide (CO) and total hydrocarbons (THC) emissions [10]. This is probably related to the poor mixing at low engine speed as there is less turbulence.

In view of hydrogen favourable properties, it is proposed to run the engine on hydrogen to overcome the performance deficit of the DI CNG engine especially at low end speeds (<2500rpm) where CNG combustion inefficiency resulted in lower torque and power. Low end speed performance is targeted for the following reasons:

1. More incomplete combustion with CNG at those operating speeds, as demonstrated by high THC and CO emissions [10].
2. Low end torque is deemed important for vehicle launch and is an important criterion for driveability ratings. Poor low end performance gives the initial perception of low performing engine [11].
3. Operation at low speed would produce lower heat and reduce the engine susceptibility to preignite, thus operation at or close to stoichiometric may be possible for maximum performance. In addition, lower heat will also reduce the risk of engine damage.

Hydrogen operation is proposed due to its readiness to combust at any given mixture, its low ignition energy and its very wide combustible limits. This would give more complete combustion at low speed where mixing is poor due to lower turbulence [12].

In addition, hydrogen has approximately 20% more energy per unit mass of air at stoichiometric that would give higher torque and power at any given speed [13].

1.2 Problem Statement

For natural gas engines, direct injection improved the performance of the engine due to increased volumetric efficiency. However, due to the properties of natural gas which has low flame speed, narrow combustible range and high ignition energy, the improvement is limited especially at lower engine speeds where the combustion becomes less complete resulting in lower performance and higher CO and THC emissions. Hydrogen, on the other hand, is known to have wide combustible limit, low ignition energy and has more energy per unit mass than CNG. It is thus of interest to see whether the use of hydrogen at these low speed could improve the performance of the engine.

However, the unique qualities of hydrogen require a new set of thinking and approach to using it as a fuel for an internal combustion engine. For example, while high compression ratio is desired considering the high octane of hydrogen, its low ignition energy may result in preignition due to glow ignition thus optimum compression ratio or combustion chamber design may need to be determined. Even though the combustible limits of hydrogen are wide, its low density and viscosity may require optimization of injection parameters in order to reduce NO_x and the occurrence of preignition As such, hydrogen combustion in DI high compression engine need optimisation and trade off due to its unique properties.

1.3 Objectives

The objectives of the study are as follows:

1. To investigate the combustion and engine performance characteristics of hydrogen in a direct injection natural gas engine.

2. To investigate the effects of hydrogen on emissions characteristics of a direct injection engine.
3. To compare the performance of the hydrogen direct injection engine against the natural gas direct injection engine.

1.4 Scope of Works

This research investigates the hydrogen combustion in the direct injection CNG engine and looks for its potential to improve the full load performance of the engine. Since no engine modification is desired, particular focus is given on the injection parameters and the air fuel ratio optimisation. In this case, full load wide open throttle operation was assessed with air fuel ratio close to stoichiometric. The ignition timing was set to maximum best torque (MBT) where possible, as limited by abnormal combustion. Particular interest is given at low engine speeds between 1800 rpm to 3000 rpm with injection pressure set at 18 bar to allow maximum fuel delivery.

1.5 Thesis Organisation

This thesis consists of six chapters which are the introduction, literature review, theoretical background, experimental works, results and discussions, as well as conclusions and recommendations.

Chapter 1 gives the background of the research project by describing the position of hydrogen fuelled internal combustion engines in the hydrogen economy and issues related to its use. The motivation for the research is also discussed while the objectives and scope of works are described.

Chapter 2 discusses the previous research in the area of hydrogen internal combustion engines and explains the position of the current research work in this area. Mainly it

describes the issues and advantages of hydrogen in comparison to conventional fuels as well as discusses the issues in the different technologies adopted.

Chapter 3 presents the theoretical background which will be used in this research work. Particularly, it gives the theoretical justifications for conducting the research and also discusses the theory of engine performance and combustion analysis.

Chapter 4 elaborates on the equipments used in this research and the method adopted for the engine tests and combustion analysis.

Chapter 5 details the results obtained from the study. Combustion analysis and engine performance assessment is discussed with respect to the parameters of interest. Comparison to CNG operation is also made.

Chapter 6 concludes the study based on the results and recommends areas for future works on this engine technology.

CHAPTER II

LITERATURE REVIEW

2.1 Engines and Gaseous Fuels

It is an interesting fact that quite a number of early internal combustion engines in the 1800's were designed and operated using gaseous fuels such as hydrogen, coal gas and stove gas (Table 2-1). In fact, the first practical internal combustion engine was using gaseous fuel [14]. Today, gaseous fuelled engines constitute about 17 million of the total population of automobiles in the world which consist of mainly natural gas (CNG and LNG) and liquefied petroleum gas (LPG) [15, 16]. The key drivers for the adoption of gaseous fuelled engines are primarily the environmental conservation and the security of energy supply. Gaseous fuels such as CNG and LPG combust more cleanly than their liquid counterparts, producing cleaner exhaust emissions [17]. CNG and LPG also have higher hydrogen to carbon ratio, giving lower CO_2 emissions when burned, which in turn reduce global warming. A test programme involving buses demonstrated that CNG engines can produce less CO_2 than their diesel counterparts [18].

Table 2-2 shows the comparison of the properties between gaseous fuels and liquid fuels [19]. The main constituents of CNG and LPG are methane and propane respectively. Thus they have higher energy content per unit mass than gasoline and diesel. However, due to the higher stoichiometric air fuel ratios, the heating value of the stoichiometric mixture is similar to the liquid counterparts. The flammability limit of methane is reasonably wide, allowing lean burn strategies for CNG engines to be adopted [20]. This can increase the thermal efficiency of the engine.

Table 2-1 The history of internal combustion engine [14]

Year	IC Engine Development
1680	Dutch physicist, Christian Huygens designed (but never built) an internal combustion engine that was to be fueled with gunpowder.
1807	Francois Isaac de Rivaz of Switzerland invented an internal combustion engine that used a mixture of hydrogen and oxygen for fuel. Rivaz designed a car for his engine - the first internal combustion powered automobile.
1824	English engineer, Samuel Brown adapted an old Newcomen steam engine to burn gas, and he used it to briefly power a vehicle up Shooter's Hill in London.
1858	Belgian-born engineer, Jean Joseph Étienne Lenoir invented and patented (1860) a double-acting, electric spark-ignition internal combustion engine fueled by coal gas.
1862	Alphonse Beau de Rochas patented but did not build a four-stroke engine.
1864	Austrian engineer, Siegfried Marcus*, built a one-cylinder engine with a crude carburetor, and attached his engine to a cart for a rocky 500-foot drive. Several years later, Marcus designed a vehicle that briefly ran at 10 mph that considered as the forerunner of the modern automobile by being the world's first gasoline-powered vehicle.
1866	German engineers, Eugen Langen and Nikolaus August Otto improved on Lenoir's and de Rochas' designs and invented a more efficient engine.
1873	George Brayton, an American engineer, developed an unsuccessful two-stroke kerosene engine (it used two external pumping cylinders). However, it was considered the first safe and practical oil engine.
1876	Nikolaus August Otto invented and later patented a successful four-stroke engine, known as the "Otto cycle".
1876	The first successful two-stroke engine was invented by Sir Dougald Clerk.
1883	French engineer, Edouard Delamare-Debouteville, built a single-cylinder four-stroke engine that ran on stove gas
1885	Gottlieb Daimler invented what is often recognized as the prototype of the modern engine - with a vertical cylinder, and with gasoline injected through a carburetor (patented in 1887).

Table 2-2 The properties of gaseous and liquid fuels [19]

Fuel	**Molecular weight**	**Specific gravity (density, kg/m^3*)**	**Lower heating value, MJ/kg**	**Stoich. Air to fuel ratio**	**LHV of stoich. Mixture, MJ/kg**
Gasoline	~110	0.72 – 0.78	44.0	14.6	2.83
Light diesel	~170	0.84 – 0.88	42.5	14.5	2.74
Natural Gas$^+$	~18	(~0.79)	45	14.5	2.9
Methane	16.04	(0.72)	50	17.23	2.72
Propane	44.10	(2.0)	46.4	15.67	2.75
Hydrogen	2.015	(0.090)	120.0	34.3	3.40

* density in kg/m^3 at 0°C and 1 atm

$^+$ typical values

However, as the gaseous fuel displaces more air than liquid fuel, the volumetric efficiency loss is a major issue in its application in internal combustion engines. For example, a CNG or LPG engine would lose approximately 10% of power over its equivalent petrol fuelled engine [17,21]. This has shifted the method of introducing the gaseous fuels into internal combustion engine from fumigation (carburettor) based to timed port fuel injection, and recently, to direct injection. By virtue of having the gaseous fuel injected once the intake valves closed, the maximum air intake is realised and subsequently maximise performance.

Substantial research and development efforts were done on direct injection gas engines [10, 22, 23, 24]. Although direct injection engines are expected to improve the performance, more optimisation works are needed. Longer combustion duration especially for homogenous CNG charge remains to be solved. High hydrocarbon emission is also a concern to be dealt with. Firmansyah [10], showed that at low speed, the combustion is less efficient, giving higher CO and THC emissions. The results showed that maximum torque was achieved at 3000rpm, the point which maximum volumetric efficiency occurred. At lower speed, the performance drop was higher than expected from the lower volumetric efficiency alone. The low combustion efficiency can be attributed to mixture formation in the cylinder. It was also demonstrated that the injection timing, pressure and injector design have substantial effects on the combustion and performance.

2.2 Hydrogen in Internal Combustion Engines

In the light of the hydrogen economy, hydrogen fuelled internal combustion engines is said to be the pathway or bridging technology before fuel cells technology becomes mature and widely available. This helps proliferate the hydrogen refuelling infrastructure while gaining the much needed experience and reputation. The experience of NGV industry can be proven valuable as the operation of the compressed gaseous fuel is not much different from hydrogen, especially in the refuelling and storage [5, 6]. With the increasing concern over global warming and

the push for hydrogen economy, the interest in hydrogen internal combustion engine (H_2ICE) has recently been renewed. Some research groups in the automotive industry are looking into H_2ICE and some prototypes were launched [25, 26].

Hydrogen internal combustion engine started as early as in the 1800s when W. E. Cecil used hydrogen for his engine [9]. The interest in hydrogen engine subsided as gasoline and diesel fuels that have better versatility in terms of storage and energy density became widely available. With the advent of environmental and energy security issues coupled with the availability of the state of the art engine controls, hydrogen internal combustion engines have recently regained much interest. This is compounded by the fact that H_2ICE is regarded as the transition technology before fuel cells technology is mature and ready for wide adoption [27-30]. An excellent technical and historical review of literatures on H_2ICE research can be obtained from the work by White [31] and Verhelst [32]. They provide an overview of the 'state of the art' of engine specific research covering the hydrogen fuel properties and advanced engine technologies employed.

The main driving force for H_2ICE is the ability to operate the engine at significantly leaner air fuel ratio so that higher efficiency in comparison to gasoline [33, 34] can be achieved. This is due to the low lean limit and ignition energy of hydrogen that allows the engine to be run with stable combustion with little or no throttling. As such, most of the research works involving hydrogen internal combustion engines were aimed at increasing the lean limit of the spark ignition engines [35,36].

Table 2-3 [31] shows the comparison of hydrogen and other types of fuels. Since the objective of the present research is to improve the CNG based engine, comparison with CNG is made here. In the case of hydrogen, the stiochiometric heating value is 17% higher than natural gas. Thus it follows that for hydrogen, higher power output is expected for the same engine capacity. However, the specific output is generally low since hydrogen at stoichiometric occupies 30% volume in comparison to 10% volume for natural gas. For comparison, gasoline occupies only 1.76% volume [37, 38]. This is true in the case of carburettor or port fuel injection. For direct injection, the intake charge can be maximised and hence the full load performance can be increased [39].

Table 2-3 Comparison between hydrogen and other fuels [31]

Fuel properties at 25 °C and 1 atm

Property	Hydrogen	CNG	Gasoline
Density (kg/m^3)	0.0824	0.72	730[a]
Flammability limits (volume % in air)	4–75	4.3–15	1.4–7.6
Flammability limits (ϕ)	0.1–7.1	0.4–1.6	$\approx$ 0.7–4
Autoignition temperature in air (K)	858	723	550
Minimum ignition energy (mJ)[b]	0.02	0.28	0.24
Flame velocity ($m\,s^{-1}$)[b]	1.85	0.38	0.37–0.43
Adiabatic flame temperature (K)[b]	2480	2214	2580
Quenching distance (mm)[b]	0.64	2.1[c]	$\approx$ 2
Stoichiometric fuel/air mass ratio	0.029	0.069	0.068
Stoichiometric volume fraction %	29.53	9.48	$\approx$ 2[d]
Lower heating value (MJ/kg)	119.7	45.8	44.79
Heat of combustion (MJ/kg_{air})[b]	3.37	2.9	2.83

[a]Liquid at 0 °C.
[b]At stoichiometry.
[c]Methane.
[d]Vapor.

Hydrogen's very wide flammability limit allows the engine to operate at ultra-lean combustion leading to high efficiency and low NO_x emissions. The engine can be run mostly, if not all the time, unthrottled. Its high octane number can be exploited to increase efficiency. Hydrogen combustion has high flame velocity that leads to almost constant volume combustion, thus higher thermodynamic efficiency.

On the other hand, hydrogen's ignition energy is about 1 order of magnitude lower, thus it is susceptible to preignition from hot spots such as spark plug electrodes, combustion chamber deposits, oil contaminants, combustion in crevice volumes and residuals energy in ignition systems [40]. This abnormal combustion could also lead to backfire should the combustion 'flash back' to the intake system. As shown in the ignition energy vs. equivalence ratio (Figure 2-1), operating the engine at close to stoichiometric air fuel ratio increases the risk of the abnormal combustion [41, 42, 43]. Optimised fuel injection timing[43], water injection[44], improved scavenging by variable valve timings, use of liquid hydrogen, ultra lean combustion strategy [45] and

direct injection have been shown to be effective in reducing the preignition. Direct injection strategy also eliminates the possibility of back fire.

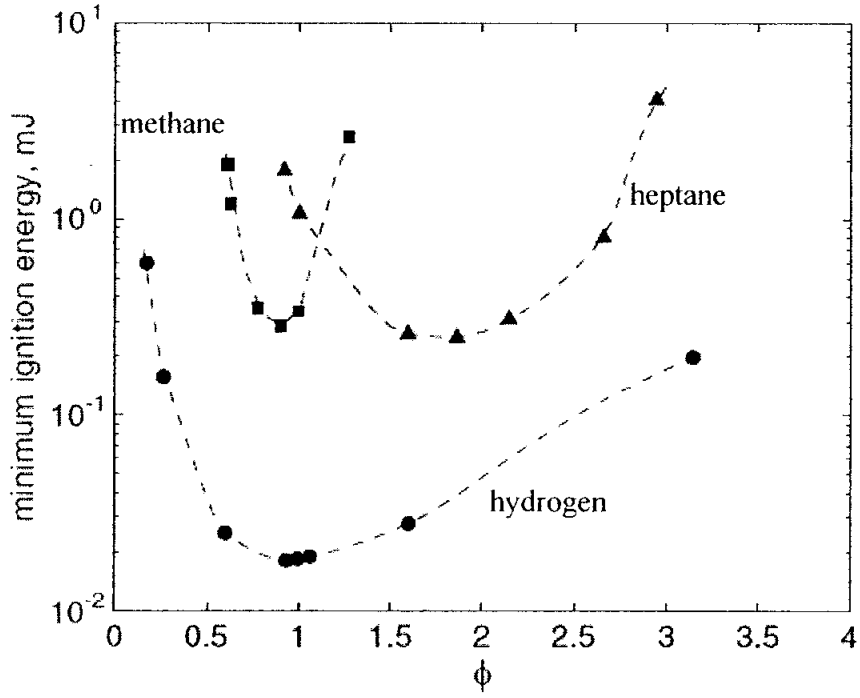

Figure 2-1 The ignition energy of fuels in air in relation to the equivalence ratio at atmospheric conditions [31]

In addition, hydrogen combustion has higher flame temperature and lower quenching distance that lead to narrow thermal boundary layers. This results in more heat loss to the combustion chamber walls [46]. Charge stratification strategies by employing direct injection technique was shown to be able to reduce the heat loss [47, 48].

As hydrogen has no carbon content, its combustion results in zero fuel derived carbon emissions. As expected, extremely low THC, CO and CO_2 emissions are produced. The source of the minimal carbon emissions are from the engine lubricants [49].

NO_x emissions can be an issue in hydrogen engine since it has high peak cylinder temperatures. It has been demonstrated that this can be effectively controlled by

several means. Ultra lean operation [50], EGR [51], water injection[44], use of liquid hydrogen [52], use of catalytic converter and direct injection strategies [53,54] are the various methods used to minimise the emission of NO_x.

In short, running an engine on hydrogen requires different strategies and design features than traditional fuels. Direct injection is generally preferred [31, 33, 39, 43] while the load control via mixture quality control means is desired for improved efficiency and fuel economy.

Hydrogen can be used in internal combustion engines as a sole fuel or through two other options – bi-fuel or dual fuel. In bi-fuel mode, the user can switch either to operate the engine on hydrogen or on gasoline. In this way, the vehicle is more flexible and can have longer mileage range. Engine manufacturer, MAN, tested a transit bus operating on bi-fuel hydrogen and gasoline for two years on public service routes covering more than 10,000km [55]. Auto manufacturer BMW had introduced a bi-fuel hydrogen vehicle in 2006 that provided a range of 400 km [56].

Dual fuel mode is when both hydrogen and the traditional fuel is mixed and burned together. Diesel, natural gas and gasoline engines have been experimented with hydrogen enriched fuels to improve the engine efficiency and emissions.

Majority of previous works in diesel engine based H_2ICE dealt with dual fuel option [57, 58]. Hydrogen is introduced into the intake air and diesel is used as a pilot ignition. It was reported that the thermal efficiency increased by almost 30% compared to the original diesel engine, while NO_x, smoke and particulate emissions were decreased [59].

In compressed natural gas engines, mixture of hydrogen and CNG (termed HCNG) was evaluated extensively [37, 60-63]. The unique properties of both fuel compliments each other. For example, the high flame speed of hydrogen compensates for low flame speed of natural gas especially at leaner ratios, thus extending the lean limit of CNG [64]. CNG on the other hand, reduces the susceptibility of hydrogen to preignite. As a result, operating on HCNG greatly reduce the CO and NO_x emissions

while modest thermal efficiency gain is realised [37, 64]. Slight drop in torque is expected as mixture of hydrogen and CNG has lower LHV than CNG alone. In the industry, Hythane®, a patented fuel consisting of 80% natural gas and 20% hydrogen, is being marketed by Hythane Company LLC [64]. The company deploys Hythane® technology that integrates the blending system with the existing natural gas refuelling stations.

The other route of employing hydrogen power in engine is via hydrogen boosted gasoline engine. This idea pivots on the ability of hydrogen to extend the lean limit of the gasoline [65]. In this approach, small amount of hydrogen is fed into the engine together with gasoline and combusted with a spark. It was shown that 20-30% fuel economy benefits can be realised [35] due to reduced pumping losses. At the same time, emissions of NO_x also reduced due to lower peak cylinder temperature of the lean burn engine. For hydrogen generation, on board reforming of gasoline is proposed.

2.3 Hydrogen Fuel Delivery Methods

Port Injection/Carburetted

The most practical means to introduce hydrogen in existing internal combustion engine is through external mixture preparation via the port injection or carburettor. However as hydrogen displaces significant amount of air [66], this approach of fuel delivery caused approximately 20% drop in engine performance [31, 33]. Knocking/preignition is also a serious issue with port injection hydrogen engine. The existence of combustible hydrogen-air mixture in the intake manifold increases the risk of backfire [43]. This has resulted in most of the earlier works in hydrogen ICE to revolve around lean mixtures.

Timed sequential port injection was shown to reduce the tendency of hydrogen to preignite [43] and the engine can be safely operated at stoichiometric. Other option is by using liquid hydrogen injection technique [52, 67]. The cool hydrogen was proven

to reduce the preigintion problem as well as to reduce volumetric efficiency loss. This system, however, requires extensive cryogenic system.

External mixture preparation also has the advantage of better mixing. For low load operation where very lean mixture is desired, the inherent low volumetric efficiency reduces throttle requirement [42]. It has also been demonstrated that at low loads, external mixture formation resulted in higher efficiency, has extended lean operation, lower *COV* and lower NO_x when compared to direct injection [42, 68].

Due to the need to reduce NO_x emissions as well as overcome engine knock, ultra lean combustion strategies are sometimes adopted for hydrogen engines [38]. This unfortunately reduces the power of the engine. In order to restore performance, turbocharged hydrogen engine with ultra lean combustion is used.

Direct injection

To overcome the volumetric efficiency issues, the preignition tendency and NO_x emissions, direct injection has become the main interest over the past decade. In fact, the work on direct injection H_2ICE can be found in the literatures as early as in 1980s. Homan [69] conducted some experiments on ASTM Cooperative Fuel Research (CFR) engine that was converted to hydrogen use. He showed that by having late injection and almost instantaneous ignition with combustion rate controlled by injection rate, the undesired combustion could be avoided. Efficiencies up to 43% were noted. It was also observed that NO_x emissions were highly dependent on the equivalence ratio.

A good review of the literatures on different methods of fuel delivery including direct injection can be found in [31, 32] which covered the literatures up to year 2005. In general, direct injection was demonstrated to be able to increase the power density by 15% in comparison to gasoline while reducing the tendency to knock. The latter is achieved by the minimised residence time of the hydrogen with the hotspots point as well as improved mixing of residual gas with air.

Most of the experiments carried out on hydrogen direct injection covered engines which were originally designed for gasoline, with compression ratios close to typical gasoline values i.e. between 9 to 11.5. One exception is the work by Eschelseder [34], who tested the engine with variable compression ratio up to 13.5. On the other hand, Tang et.al [70] demonstrated that for port injection engines, a compression ratio of 14.5 was optimum for efficiency.

NO_x is generally reduced by direct injection. In order to reduce it further, ultra lean combustion is generally adopted. To control NO_x emissions while keeping air fuel ratio close to stoichiometric, water injection strategies was tested [50]. Dual fluid injector (water and hydrogen) was employed in which water is pre-metered and introduced together with the hydrogen into the combustion chamber. It was shown that water injection and EGR could allow stoichiometric equivalence ratio while keeping the NO_x emissions low.

Conflicting reports on the effects of start of injection to NO_x emissions and thermal efficiency indicated that there is still a need to understand the fundamentals of the mixing that is dependent on the chamber geometry, injector design & location and the flow dynamics in the cylinder. Wallner [71] investigated the effects of injector nozzle design and location to the combustion of hydrogen. Westport direct injector was used in a 0.5 litre single cylinder engine with 100 bar injection pressure. The compression ratio adopted was 11.5:1. The injector has two designs of nozzles (6 and 5 holes) placed at 2 possible locations – side and centre. It was demonstrated that for low loads, the injector location and design plays a more important role than at high loads in terms of thermal efficiency. At high loads, injector design could play an important role to improve NO_x emissions while keeping the efficiency unaffected.

The other important aspect of direct injection hydrogen engine is the mixture formation. As the time available for mixing is very much limited especially in cases where late injection is desired, understanding of the fundamentals of the mixing of hydrogen inside the combustion chamber is important. White [72] utilised PIV and PLIF systems to investigate the mixture formation inside an optical engine. It was demonstrated that for early direct injection, the mixture are generally premixed. For

later injections, rich region is located spatially close to the injector. It was suggested that the jet wall interactions played a role that causes the mixture to be rich near the injector. It was also demonstrated that the injector tip geometry, location and injection timing are critical parameters to the mixture formation.

At very low load such as idle, the coefficient of variation (*COV*) of the combustion of hydrogen engine is known to be high, especially in direct injection. Kim [73] showed that the high *COV* in direct injection H_2ICE is dependent on the variation in the early stage of combustion. It was also shown that at early SOI, the COV is less than for late injection.

Yi et. al [74] and Rottengruber et. al [75] compared between direct injection and port fuel injection of hydrogen. It was determined that for low loads external mixture preparation has the advantage while for full load, internal mixture preparation is desired. In this case to take advantage of both systems, a dual injector strategy is proposed.

Summary

Direct injection gaseous engine still requires optimisation and research. CNG direct injection has been shown to improve performance, however, performance at low speed is relatively poor due to poor mixture formation. Hydrogen, due to its wide combustible limits, low ignition energy and fast flame speed can be considered to outperform natural gas at this speed.

The list of the previous research conducted on the hydrogen use in internal combustion engines can be found in the references section. BMW and MAN in Europe and Ford in the USA have aggressively pursued hydrogen engine research programmes. BMW had demonstrated cryogenic hydrogen mixture preparation that improved the efficiency and the combustion stability with ongoing research on direct injection strategy. MAN has ongoing low pressure (15 bar) direct injection research as well as research into diesel engine to hydrogen conversion.

In the reviewed literatures, most of the work utilized compression ratio around that of gasoline engines, i.e. 10-11 ratio. Comparisons with similar base engine on gasoline operation were also conducted. Discussion and comparison with natural gas is not widely reported, except may be in [76] and[77] which were either carburetted or port injection based, however, the effects with respect to the injection and other control parameters were not discussed. The reviewed literatures also did not discuss the emissions of the direct injection hydrogen engines with respect to the control parameters chosen, other than the NO_x emissions.

It was reasonable to conclude that the processes of the mixture formation in direct injection hydrogen engine is highly dependent on the engine design, geometry, injection nozzle tip design, injection timing, injection pressure and the engine flow dynamics. Efforts to cover the fundamental understanding of the process are still ongoing across the field of computational fluid dynamics [78], modelling [79-82] and in cylinder flow visualisation [83-85]. As such, it is important to experiment across various engine design and configurations.

CHAPTER III

THEORETICAL BACKGROUND

In this chapter, the theoretical background applied in this study is presented. The theoretical advantages of hydrogen in comparison to CNG are discussed. The theory and calculation behind the analysis of the engine performance and combustion are also described.

3.1 Hydrogen as Internal Combustion Engine Fuel

As was discussed in previous section, hydrogen is a unique fuel when used in internal combustion engine. This unique properties and characteristics require a different approach to engine design and optimisation.

In an internal combustion engine, the energy introduced into the cylinder is closely related to the stoichiometric air fuel ratio of the fuel in air. The theoretical air fuel ratio for hydrogen in air can be calculated based on its stoichiometric chemical reaction equation.

$$2H_2 + O_2 = 2H_2O \qquad (3\text{-}1)$$

Thus for complete combustion, 2 moles of hydrogen is needed for every mole of oxygen. Taking into consideration that air contains nitrogen, the equation for the combustion of hydrogen in air becomes

$$2H_2 + (O_2 + 3.76N_2) = 2H_2O + 3.76N_2 \qquad (3\text{-}2)$$

4.76 moles of air requires 2 moles of hydrogen for complete combustion. Therefore for the air fuel ratio on mass basis;

Hydrogen mass = no of moles of hydrogen x molecular weight

= 2 x 2

= 4 g

Air mass = no of moles of air x molecular weight of air

= 1 x (16x2 + 3.76x14x2)

= 137.28g

Stoichiometric air fuel ratio (mass basis) is thus = 137.28/4

= 34.32 : 1

For molar basis or volume basis, the air fuel ratio is as follows:

Air fuel ratio, volume basis = 4.76 moles of air/2moles of hydrogen

= 2.38 : 1

Thus, the volume occupied by hydrogen for a stoichiometric condition;

= moles of hydrogen/total no of moles

$$= \frac{2}{(4.76+2)}$$

= 29.6%

For internal combustion engine, the energy introduced into the cylinder is the parameter that determines the mean effective pressure and power produced by the engine. For port/external mixture preparation, this depends on the mixture volume. In this case, since hydrogen occupies 30% of the mixture volume, the energy content is significantly diminished. In contrast, for direct injection, the energy introduced into the cylinder depends on the mass of air inducted into the engine.

Figure 3-1 shows the mixture calorific values of various fuels for external mixture preparation and for direct injection [13]. For other fuels, even methane, the difference in the mixture calorific value for direct injection and external mixture preparation is not as large as hydrogen. Thus, for hydrogen, direct injection is the solution for best power density. In case of direct injection, hydrogen is also shown to have the highest

mixture calorific value in comparison to other fuels. For example, hydrogen has 20% more mixture calorific value than natural gas (methane). Thus it follows that for the same direct injection engine capacity, operating with hydrogen would result in 20% more torque and power than with natural gas.

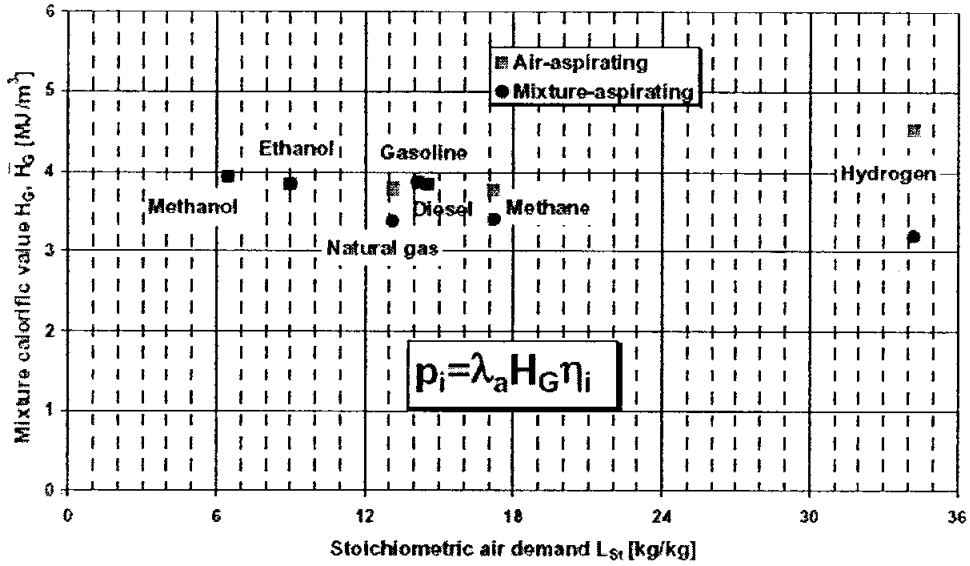

Figure 3-1 The mixture calorific values for various fuel. *Air aspirating* represents direct injection while *mixture aspirating* represents external mixture preparation [13].

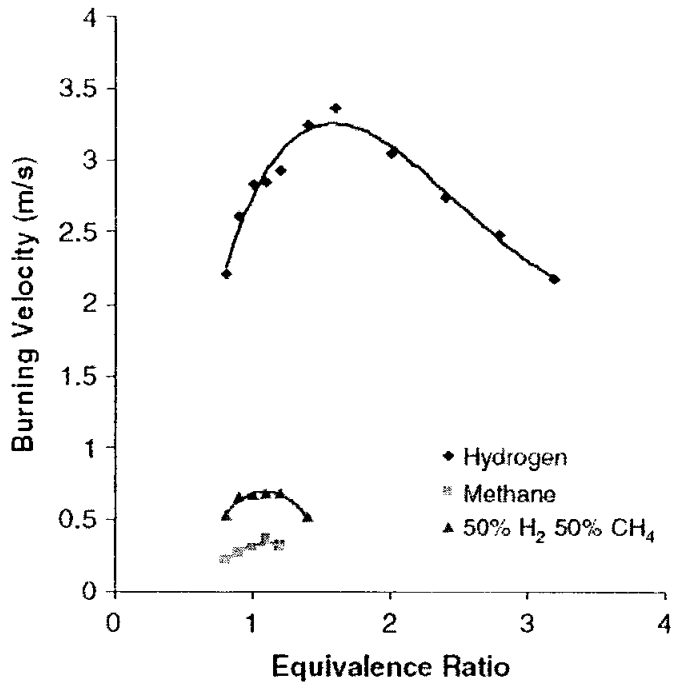

Figure 3-2 The laminar burning velocities for hydrogen and methane at different air fuel ratios [86]

In the previous section, it was shown in Figure 2-1, the ignition energy required to start the combustion of hydrogen at various equivalence ratio is lower than that of natural gas. Therefore it is expected that operating an engine with hydrogen would result in easier ignition in comparison to natural gas. This is also true at engine operating regions where air motion and mixing is poor.

As given in Table 2-3, the flame speed of hydrogen is approximately 6 times faster than natural gas. The relationship of the laminar flame speed with air fuel ratio is as shown in Figure 3-2 [86]. Thus it is expected that the combustion of hydrogen in a given engine will be faster even when mixing is poor as in the case of low engine speed. These two arguments lead to the assumption that operating an engine with hydrogen would result in a more efficient combustion at lower speeds where natural gas is shown to have poor efficiency and lower performance.

It is the intent of this study to demonstrate this in which the engine performance parameters and the combustion characteristics will be compared between hydrogen and natural gas. The following sections describe the parameters of interest.

3.2 Basic Calculation of Performance Parameters for Internal Combustion Engines

The important parameters when discussing engine performance are the brake torque, power, brake mean effective pressure, brake specific fuel consumption and efficiency. The definitions of the parameters are discussed in this section.

Torque

Torque, T, is defined as the ability of the engine to do work. It depends on the engine capacity and the unit of measure is in Nm. Torque is measured using a dynamometer and usually varies with engine speed and volumetric efficiency of the engine.

Power

Power is defined as the rate at which the work is done. The unit of measure is in kW. It is calculated based on the engine speed and torque as follows:

$$\text{Power, } P = 2\pi NT \quad \text{kW} \tag{3-3}$$

where N is the engine speed in rev/s.

T is the torque in Nm

Brake Mean Effective Pressure

While torque is a valuable measure of the engine's ability to do work, it is dependent on the engine size. The Brake Mean Effective Pressure (*BMEP*) is a relative measure of engine performance that is obtained by dividing the work done by the cylinder volume displaced per cycle. As such, the unit of measure is in terms of pressure, kiloPascal (kPa).

$$\text{Work done per cycle} = \frac{power}{speed}$$

$$= \frac{2\pi NT}{N}$$

$$= 2\pi T \qquad (3\text{-}4)$$

$BMEP$ = work done per cycle/volume displaced per cycle

$$= \frac{2\pi T}{V_s} \text{ kPa} \qquad (3\text{-}5)$$

where V_s = swept volume in dm^3

T = brake torque in Nm

Brake Specific Fuel Consumption

The measure of the fuel consumption in an engine is best represented by the specific fuel consumption. It is the fuel flow rate per unit power output which is also a measure of the efficiency of the engine in consuming the fuel to produce work. It is usually expressed in g/kWhr.

$$\text{Brake specific fuel consumption, } BSFC = \frac{FC}{P} \text{ g/kWhr} \qquad (3\text{-}6)$$

where FC = fuel consumption in g/hr

P = power in kW

Volumetric efficiency

Volumetric efficiency is the measure of the amount of air inducted into the engine over the theoretical air flow rate. It is dependent on the design of the air intake system, the throttle position and the intake valves timing and design.

$$\text{Volumetric efficiency, } \eta_v = \frac{2m_a}{\rho V_d N} \qquad (3\text{-}7)$$

where η_v = volumetric efficiency

m_a = mass flow of air in g/sec

V_d = swept volume

ρ = density of air

N = engine speed in rev/s

In case of direct injection, the volumetric efficiency is higher due to less air displacement by the gaseous fuel. Unthrottled operation also allow for maximum volumetric efficiency.

3.3 Combustion Analysis for Internal Combustion Engines

For a four stroke spark ignition engine, the combustion begins with a spark discharge at the end of the compression stroke. The flame propagates outwards through the premixed fuel-air mixture until it reaches the combustion chamber walls where it is extinguished. The flame propagation depends on the local mixture motion and composition, which varies from cycle to cycle. For different types of fuels, the characteristics of the combustion also differ.

In general, the combustion process can be divided into 4 distinct phases: (1) spark ignition; (2) early flame development; (3) flame propagation and (4) flame termination [19].

The first stage corresponds to the initiation of the flame by the spark discharge. The spark provides a large amount of energy to the mixture in a short time. There exists an interval of time before a small but significant energy is released. This is sometimes called the ignition delay. The interval depends on the properties of the mixture especially in the vicinity of the spark plug.

The second stage of combustion is the early flame development. Early flame development is mainly due to the chemical process which depends on the nature of the fuel and the temperature and pressure of air/fuel mixture. This early stage of flame development is

also governed by the mixture motion and composition in the vicinity of the spark plug. Thus, the exact control to get favourable mixture conditions around the spark plug is critical. Injection parameters, combustion chamber shapes, and in-cylinder flow characteristics are the parameters that have been used to control and obtain intended behaviour of initial combustion. The initial combustion duration is defined as the beginning 0-10% of total combustion duration.

The subsequent stage is the rapid combustion phase. Rapid combustion is defined as the following 10-90% of total combustion duration which is the bulk of the mixture energy release. Here, the cylinder pressure steadily rises to the maximum which usually occurs at slightly after TDC. This stage is dependent on the degree of turbulence in the in-cylinder flow, prevailing temperatures, pressures and also fuel availability. It is important to note that the local mixture motion and composition governs the flame growth. As such, optimisation of the in cylinder flows and fuel delivery especially in late direct injection is key to achieve maximum performance.

Final stage or flame termination basically is the process where the remainder of the charge burns to completion and quenched at the combustion chamber walls. At this stage, the cylinder volume continues to increase during the expansion stroke. This stage will be limited by the time of exhaust valve open. The fuel that is still left unburned on the final stage will go through with the combustion product to the exhaust. End of combustion occur at the final 90-100% of total combustion duration.

Combustion rate is limited by the time available during the process. Total time available in crank angle degree depends on ignition timing, exhaust valve opening, and engine speed. In a well designed engine, the end of stage 2 combustion process is close to the point of maximum cylinder pressure. In practice, for optimum performance and efficiency the maximum pressure should occur between 5-20° ATDC.

The characteristics of the combustion processes can be analysed using the cylinder pressure readings from the engine. Cylinder pressure changes with the crank angle as a result of volume, heat and mass changes in the combustion chamber, thus, combustion rate analysis can be done.

3.3.1 Cylinder Pressure

There exist two major methods for analysis of combustion characteristics and determination of the combustion rate and duration.

1. Through observation of in cylinder events via transparent engine parts. This method requires extensive and complicated equipment and devices such as laser and high speed camera system which are costly and not readily available.
2. Through the use of in-cylinder pressure data. This is simpler in set up and requires accurate and fast response pressure transducer and data acquisition system. This method is the most commonly applied in the field.

In this study, the calculations based on cylinder pressure data method were preferred. Piezoelectric pressure transducers are usually used for obtaining the cylinder pressure data. This is coupled to the crank angle encoder to trigger the measurement such that the pressure rise with respect to the engine crank position can be plotted. Observation and detail analysis of pressure reading from pressure transducer can be used to determine heat release rate, indicated work done by the combustion process (*IMEP*), burn rate and combustion efficiency. In-cylinder pressure (kPa or bars) usually presented against crank angle (degree) or cylinder volume (m^3).

3.3.2 Mean Effective Pressure (MEP)

As shown in Figure 3-3 and Figure 3-4, the cylinder pressure gradually increases in the compression stroke, followed by rapid increase during the combustion of the intake charge. The maximum pressure rise usually occurs immediately after the TDC. This is followed by the expansion in which pressure drops due to the increase in the cylinder volume. The area of the P-V diagram enclosed by this process is the work transferred from the gas to the piston. This indicated work can be calculated by integrating the enclosed area of the P-V diagram.

$$W_c = \oint pdV \tag{3-8}$$

where W_c is the indicated work

p is the cylinder pressure

V is the instantaneous volume of the cylinder

In four-stroke engine, the addition of intake and exhaust strokes lead to two definitions of the indicated work,

1. gross indicated work per cycle, W_c, work delivered to the piston by compression and expansion stroke at the power cycle
2. net indicated work per cycle, $W_{c,n}$, is the work delivered to the piston over entire cycle.

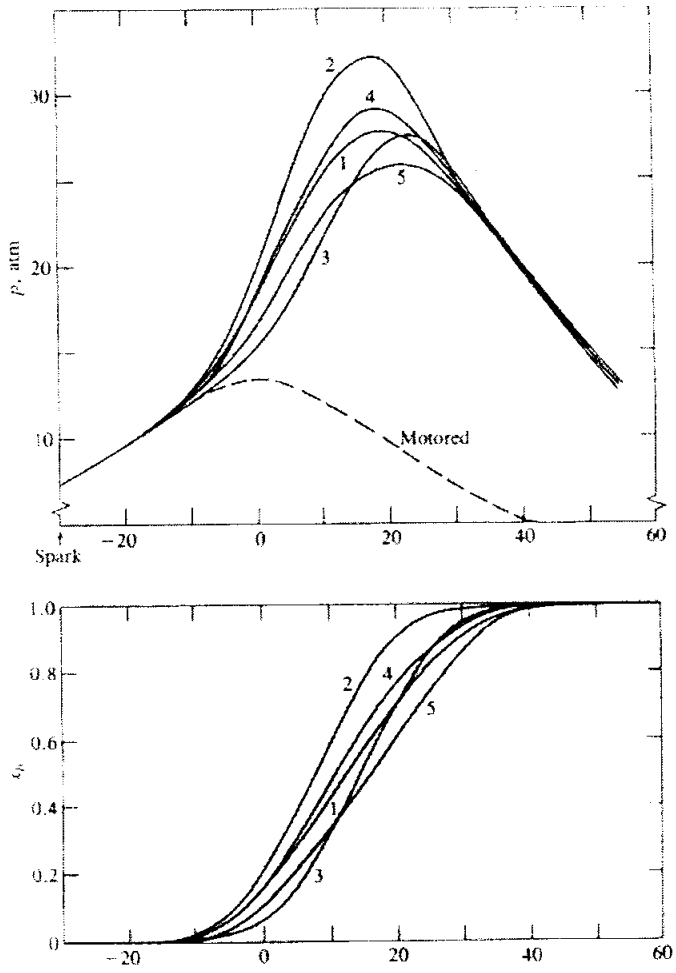

Figure 3-3 The typical cylinder pressure trace and the mass burn fraction of a spark ignition engine [19]

The gross indicated work is used as the definition of work in this thesis as this is the most commonly used term. Besides, indicated quantities are mostly used to identify the impact of the compression, combustion and expansion on the performance of the engine. To allow comparison with different sizes of engine, this indicated work is normalised by dividing with the engine capacity, or displacement volume. This is a relative engine performance measure and called the indicated mean effective pressure, *IMEP*.

$$IMEP = \frac{W_c}{V_d} \tag{3-9}$$

where W_c = indicated work

V_d= cylinder volume displacement (swept volume)

Direct injection gaseous fuelled engine is expected to have higher *IMEP* due to the higher volumetric efficiency. As hydrogen has higher stoichiometric heating value, it is expected that the *IMEP* of the engine will be higher than CNG.

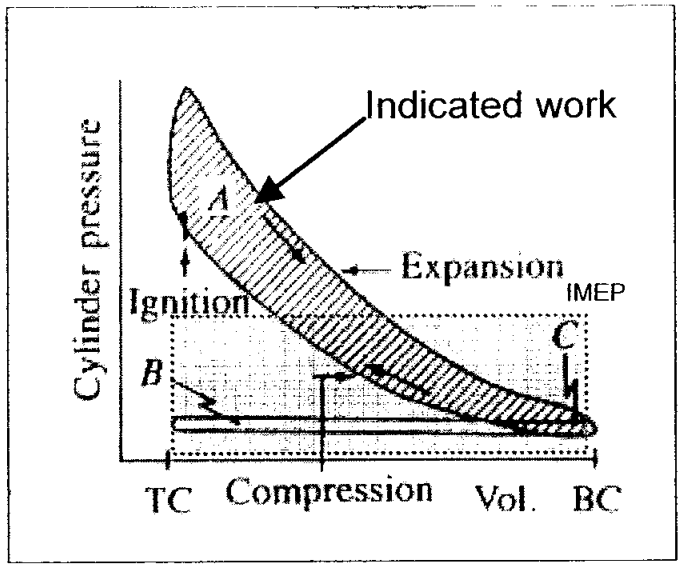

Figure 3-4 Indicated Work and Indicated Mean Effective Pressure [19]

3.3.3 Coefficient of Variation

As described in the preceding section, the combustion process depends on the local mixture composition and motion which varies from cycle to cycle. This leads to the cyclic variation in the combustion process and quality. One parameter that can indicate this variation is the coefficient of variation (*COV*) of the *IMEP*. It is defined as the standard deviation of *IMEP* divided by the average *IMEP*,

$$IMEP_{avg} = \frac{1}{n}\sum_{1}^{n} IMEP_i \tag{3-10}$$

Standard deviation of IMEP defined as:

$$\sigma_{IMEP} = \sqrt{\frac{\sum_{i=1}^{n}(IMEP_{avg} - IMEP_i)^2}{n}} \tag{3-11}$$

So, coefficient of variation of *IMEP* is:

$$COV = \frac{\sigma_{IMEP}}{IMEP_{avg}} \tag{3-12}$$

where n is the number of cycles.

COV is an indicator of the stability of the engine. In order to get a good drivability, *COV* value should not exceed 10% [19]. There are three factors that influence *COV*:

1. The variation in gas motion in the cylinder during the combustion, cycle-by-cycle
2. The variation in the amounts of fuel, air, and residual gas to a given cylinder each cycle.
3. Variation in mixture composition within the cylinder at each cycle-especially near the spark plug-due to variations of mixing.

Thus it is expected that the injection parameters can affect the *COV* in the direct injection engine as it influence the mixing and the mixture composition near spark plug. As

hydrogen has low ignition energy and fast flame speed it is expected that the COV will be low, even at low engine speed and lean ratios.

3.3.4 Heat Release Analysis

Two important parameters that need to be determined for the combustion analysis are the heat release rate and the mass burn fraction. These parameters are calculated from the P-V diagram of the combustion. The basis is that the cylinder pressure profile of the fired cycle is higher than the motored cycle. The pressure rise due to combustion can be determined by comparing the cylinder pressure to the expected pressure rise due to compression alone. This technique was described by Rassweiler and Withrow.

$$\Delta p = \Delta p_c + \Delta p_v \tag{3-13}$$

where Δp = change in cylinder pressure

Δp_c = change in pressure due to combustion

Δp_v = change in pressure due to volume change

Based on ideal gas law for adiabatic isentropic compression,

$$p_i V_i^n = p_j V_j^n \tag{3-14}$$

where i and j are the start and end of crank angle interval, $\Delta\theta$

For motored cycle, the pressure rise due to volume change is

$$\Delta p_v = p_i - p_j = p_i \left[\left(\frac{V_i}{V_j} \right)^n - 1 \right] \tag{3-15}$$

Hence, pressure rise due to combustion can be calculated

$$\begin{aligned} \Delta p_c &= \Delta_p - \Delta p_v \\ &= p_j - p_i \left[\left(\frac{V_i}{V_j} \right)^n \right] \end{aligned} \tag{3-16}$$

With the assumption that the mass fraction of the fuel burned is proportional to the pressure rise due to the combustion, the mass fraction burned is then

$$\frac{m_{b(i)}}{m_{b(total)}} = \frac{\sum_0^i p_c}{\sum_0^N p_c} \tag{3-17}$$

where N is the total number of crank angle interval

From the mass burn fraction curve, the start and the end of combustion can be determined based on the definitions as discussed previously.

This method is dependent on the polytropic index chosen for the calculation. In this method, several approximations are made. The effect of crevices and the heat transfer are not incorporated into the equation; however, due its simplicity and less computational requirements, this method is widely used. In this case, since all tests were done on the same engine set up, this method is adequate.

The Krieger and Borman method for the apparent heat release is widely used for their simplicity. Similar to the Rassweiler and Withrow, the crevices and heat transfer effects are not considered. The apparent heat release, dQ is given by

$$dQ = \frac{1}{\gamma - 1} V dp + \frac{\gamma}{\gamma - 1} p dV \tag{3-18}$$

In this test programme, the value for γ is taken as 1.33 based on data from motored cycle.

3.3.5 Combustion Efficiency

Combustion efficiency is the total heat released by combustion divided by the available energy of the fuel delivered to the cylinder for that cycle.

$$\eta_c = \frac{Q_{out}}{Q_{in}} = \frac{\sum Q_{ch}}{m_f q_{HV}} \tag{3-19}$$

where $\sum Q_{ch}$ is the total heat released by the combustion process, m_f is fuel mass, and q_{HV} is the specific heating value of fuel.

3.3.6 Indicated Thermal Efficiency

Indicated thermal efficiency is the indicated work per cycle over the energy available from the fuel per cycle. This is a measure of the engine efficiency to convert the combustion to useful work. The indicated efficiency can be determined from the *IMEP*, brake power and the *BMEP*.

$$P_i = \frac{IMEP}{BMEP} \times P_b \tag{3-20}$$

where P_i is the indicated power and P_b is the brake power

The indicated thermal efficiency is thus

$$\eta_{ind} = \frac{P_i}{\dot{m}_f \cdot q_{HV}} \times 100 \tag{3-21}$$

where $\dot{m}_f$ is the fuel mass flow rate and q_{HV} is the lower heating value of the fuel.

CHAPTER IV

EXPERIMENTAL WORKS

In this chapter, the experimental setup, preparation and process are described. The procedures adopted for the test and the calculation used are also highlighted.

4.1 The Experimental Set Up

Figure 4-1 shows the schematic of the experimental setup. A single cylinder engine was coupled to a direct current dynamometer that allowed the engine braking and motoring while the performance parameters were measured.

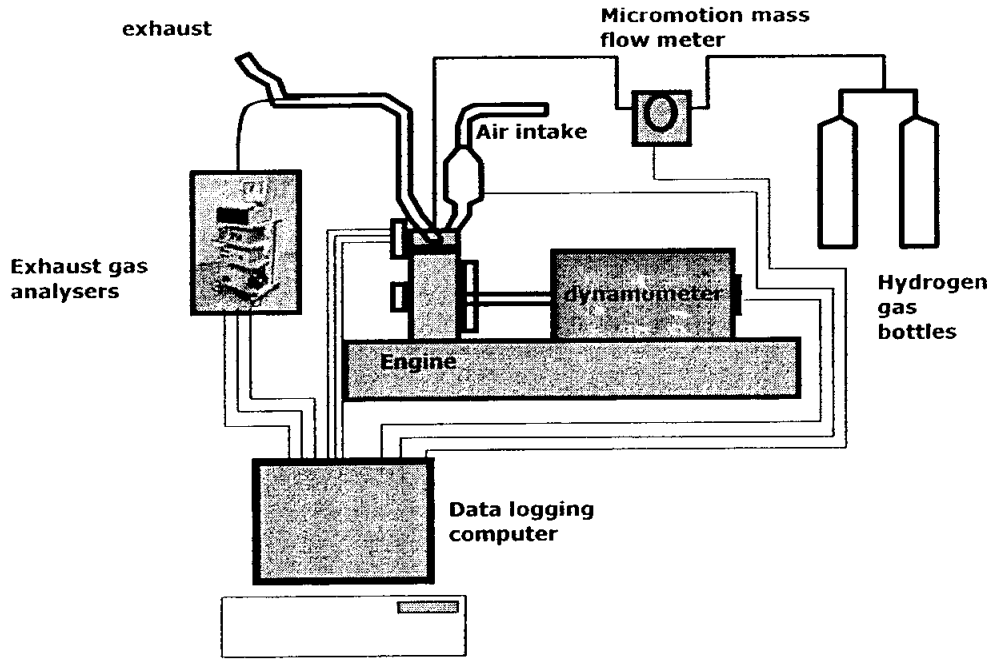

Figure 4-1 The schematics of the experimental set up

4.1.1 The Test Engine

The single cylinder engine was based on a PROTON CAMPRO engine with modifications to its cylinder head to enable direct injection of gaseous fuel (Figure 4-2). Originally, the engine was designed for natural gas application. To demonstrate practicality and easy adoption of hydrogen, no modification to the engine was made for this study. The specification of the engine is as given in Table 4-1. It was a 4 stroke spark ignition engine with a compression ratio of 14:1 to take advantage of the high octane of natural gas. Since hydrogen autoignition temperature is higher than natural gas, this compression ratio was maintained.

A programmable ECU connected to a computer was used to control the engine. Among others, the engine parameters that could be controlled from the computer were the injection timing and duration, the spark timing and throttle position. Real time data was available from the engine ECU and could be viewed and recorded accordingly.

The original natural gas direct injector was used for the study without any modification (Table 4-2). Due to hydrogen's low density and viscosity, narrow angle injector (30°) was chosen to allow maximum fuel spray penetration. Figure 4-3 shows the schlieren photographs for the comparison of the fuel spray penetration between hydrogen and natural gas. The spray was executed with 18 bar injection pressure in air at atmospheric conditions. It shows that although the penetration of hydrogen was quite similar to natural gas, the distribution of hydrogen was wider. This suggests that the mixing of hydrogen was better than natural gas.

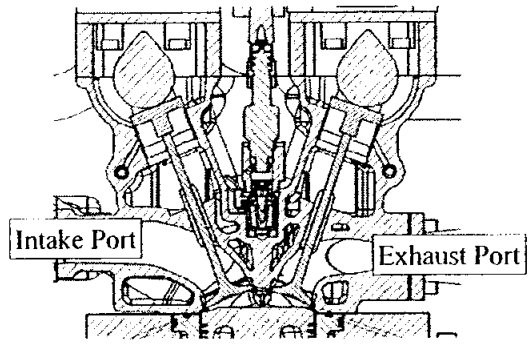

(a) Intake and exhaust port position

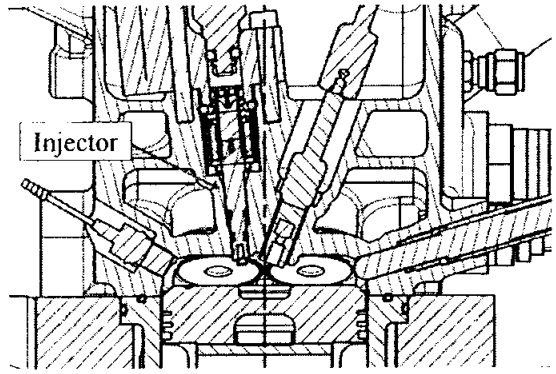

(b) Injector and sparkplug position

Figure 4-2 The cut off view of the engine showing the injector and sparkplug position

Table 4-1 The Specifications of the Single Cylinder Engine

Engine Specifications	
Displacement Volume	399.25 cm^3
Cylinder Bore	76 mm
Cylinder stroke	88 mm
Compression ratio	14
Exhaust Valve Open	ATDC 10°
Exhaust Valve Closed	BBDC 45°
Inlet Valve Open	BTDC 12°
Inlet Valve Closed	ABDC 48°
Injection type	Direct injection, spray guided, central injector, 30° spray angle.
ECU	Orbital Inc.
Positive Crankcase Ventilation	No
Injection pressure	18 bar

Table 4-2 The Specifications of the Fuel Injector

Manufacturer	Synerject
Part number/designation	37-152CNG
Nozzle spray angle	30°
Spring	33.0N
Stroke	0.135mm
Maximum operating pressure	2.0 Mpa (high pressure)
Turn on time	1.05ms
Turn off time	0.95 ms
Operating voltage	14.0 VDC
Coil resistance	1.3 ohm

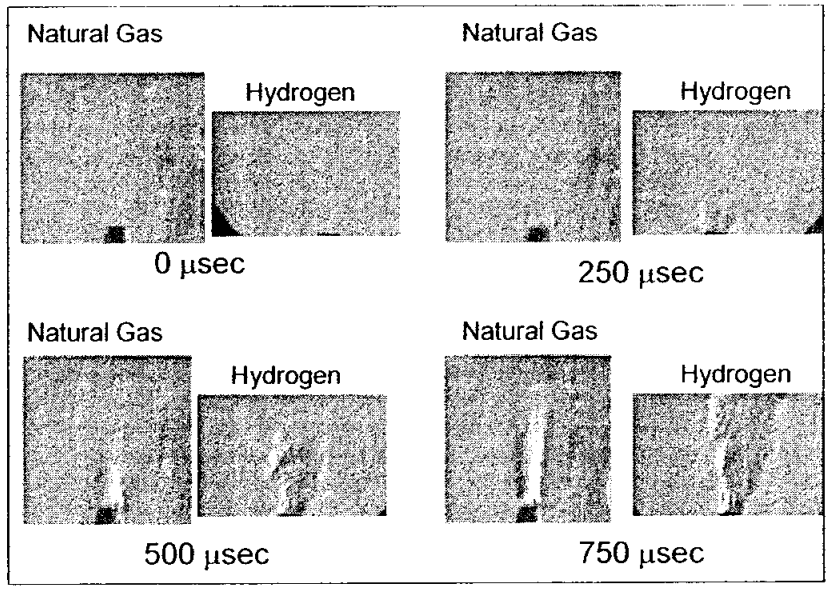

Figure 4-3 The schlieren image of the spray pattern and penetration of hydrogen in comparison to natural gas at atmospheric conditions (18 bar injection pressure).

4.1.2 The Dynamometer

Table 4-2 shows the specification of the direct current dynamometer. Being a DC dynamometer, it has the capability to motor the engine. This was useful to obtain the unfired cycle data for the cylinder pressure such that the combustion analysis can be carried out.

The data such as the torque, speed, engine oil temperature, coolant temperature and intake air temperature were recorded manually from the dynamometer panel.

Table 4-3 The Dynamometer Specifications [87]

Dynamometer Specifications	
Make and Model	David McClure DC30
Type	Direct Current
Capacity	30kW
Maximum Speed	5000rpm

4.1.3 The Fuel System

The fuel system used for the study is as shown in Figure 4-4. The hydrogen was supplied in gas bottles with 200 bar pressure. Pressure regulators were used to regulate the pressure delivered to the engine. A Micromotion™ CMF010 ELITE Series fuel flow meter was used to measure the fuel flow. The specification of the flow meter is as given in Table 4-3.

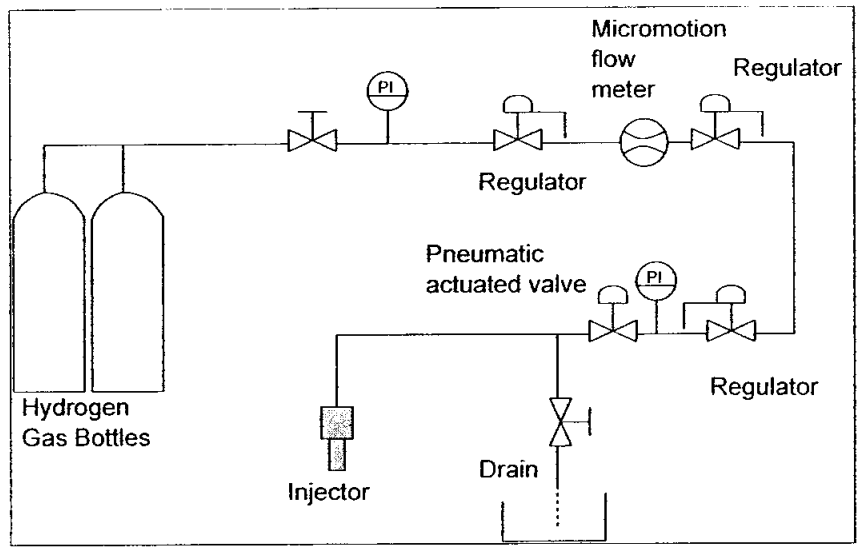

Figure 4-4 The fuel supply system

4.1.4 Gas Analysers

A GASMET CX Series Fourier Transformed InfraRed (FTIR) exhaust gas analysis systems was used to measure the concentration of the exhaust gas constituents (Figure 4-5). The system consisted of three main components. A heated sampling system complete with heated lines were used to sample the exhaust gas. An industrial computer automated the sampling process and logged the data. An FTIR analyser works on the principle of infrared spectroscopy measuring the concentration of each constituent. As the infra red light is passed through the gas sample, some of the light is absorbed giving an infra red spectrum. Fourier transform analysis identifies the gas constituents and their concentration.

For oxygen concentration measurement, a GASMET Oxygen Analyser was used. It utilised a zirconia measurement cell that gave out voltage in proportion to the oxygen concentration. The analyser was also able to calculate the lambda values based on the oxygen concentration. Table 4-4 shows the specifications of the GASMET analyser and the oxygen analyser.

Table 4-4 The specifications of the fuel flow meter [88]

Flow accuracy:	+/-0.05% of flow rate
Gas accuracy:	+/-0.35% of flow rate
Density accuracy:	+/-0.0002 g/cc
Wetted materials:	304L, 316L Stainless Steel or Nickel Alloy
Temperature rating:	-400 to 800°F (-240 to 427°C)
Pressure rating:	1450 - 6000** psi (100 to 413** bar)

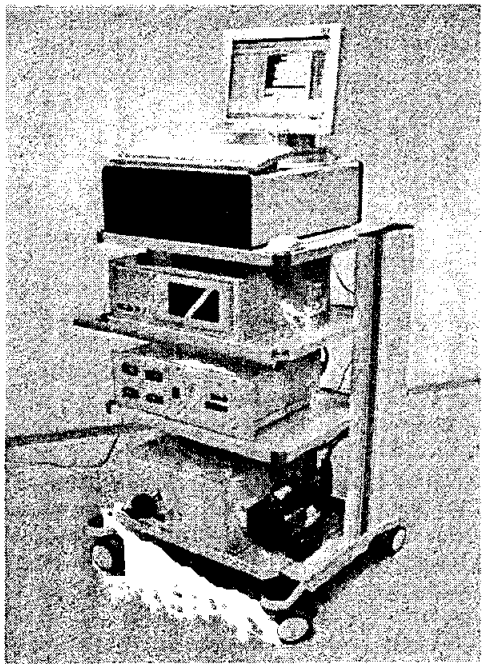

Figure 4-5 The GASMET Gas Analysers System. The second uppermost module is the oxygen analyser

Table 4-5 The Specifications of the Gas Analysers [89]

FTIR Analysers	
Measuring Principle:	Fourier Transform Infrared, FTIR
Performance:	simultaneous analysis of up to 50 gas compounds
Response time:	typically <<25s, depending on the gas flow and measurement
Operating temperature:	15-25°C non condensing
Storage temperature:	-20 - 60°C non condensing
Power supply	100-115 or 230V / 50-60 Hz
Power consumption:	300 W
Zero point calibration:	24 hours, calibration with nitrogen
Zero point drift:	<2 % of measuring range per zero point calibration interval
Sensitivity drift:	none
Linearity deviation:	<2 % of measuring range
Temperature drifts:	<2 % of measuring range per 10 K temperature change
Pressure Influence:	1 % change of measuring value for 1 % sample pressure change. Ambient pressure changes measured and compensated
Oxygen Analyser	
Measuring principle:	ZrO2 measuring cell
Detection limit:	< 1 ppm O2
Response time:	< 1 second
Sample Gas temp.:	120 °C to 300 °C, non condensing
Environm. Temp.: -	20 °C to +40 °C
Reference gas:	instruments air, dew point less than –40 °C, no oil, about 30 l/h
Measuring gas:	dry or wet, no combustibles
Calibration gas:	instrument air as above or test gas from bottles

4.1.5 Pressure Sensor and Cylinder Pressure Data Acquisition

For combustion analysis, the in-cylinder pressure transducer was the most important component. In this study, Kistler piezoelectric pressure transducer was used. A piezoelectric pressure transducer generated electric charge proportional to the pressure. It was then amplified using a charge amplifier that gives output in terms of voltage which was proportional to this charge.

Transducer temperature variation can affect the calibration of the sensor. This is due to expansion of the casing that results in decompression of the crystal. Thus, the piezoelectric transducer had water cooling passage for maintaining its temperature in order to ensure correct pressure readings. Table 4-5 shows the specification of the transducer.

A Hall Effect crank angle encoder was used to determine the angular position of the engine. It also served as the trigger for synchronising the data capture of the cylinder pressure. The data rate was at 10kHz. Typical set up for the cylinder pressure data capture system is as shown in Figure 4-6.

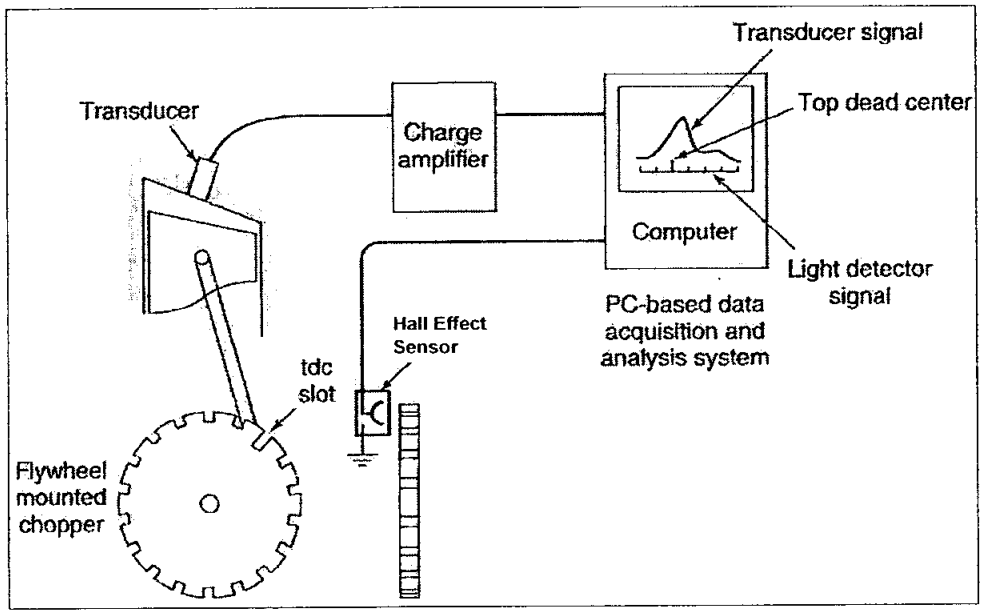

Figure 4-6 Typical set up for cylinder pressure measurement [90]

Table 4-6 The specifications of the pressure transducer

Make and model	Kistler ThermoCOMP®
Range	0-250bar
Linearity all ranges	<±0.5%FSO
Sensitivity shift, cooled 50±35°C	<±0.5%

4.2 Device Calibration

4.2.1 Dynamometer Calibration

The dynamometer described in section 4.1.2 was calibrated using standard weights. The weights were attached to the extension arm on the dynamometer and the torque readings were recorded. Table 4-6 shows the calibration weights and the corresponding torque readings. Readings for loading and unloading of weights were made for both sides of the dynamometer. The error of the readings was within 0.3 Nm.

Table 4-7 The Calibration of the Dynamometer

No	Weight (kg)	Torque (Nm)
1	1	4
2	2	8
3	5	20
4	10	40
5	12	48

4.2.2 Pressure Data Acquisition Systems Calibration Check

The pressure readings calibration was checked against the ABW Master Compression Tester. The compression tester was accurate to 2.5psi (0.2bar). The sparkplug was removed from the engine and the compression tester was installed in its place. By motoring the engine at low speed, 300 rpm, the maximum cylinder pressure was recorded. This was compared to the readings given by the pressure sensor.

4.2.3 Exhaust Gas Analyser Calibration

Zero calibration of the exhaust gas analysers was carried out daily before every test. This allowed the analyser to measure the background spectrum before exhaust gas was sampled. The zero gas used for this purpose must be a pure substance and in this study nitrogen was used. The spectrum obtained was be used by the analyser as a

baseline for the measurement. The analyser was considered fit for use if the background spectrum resembles the typical as is shown in Figure 4-7.

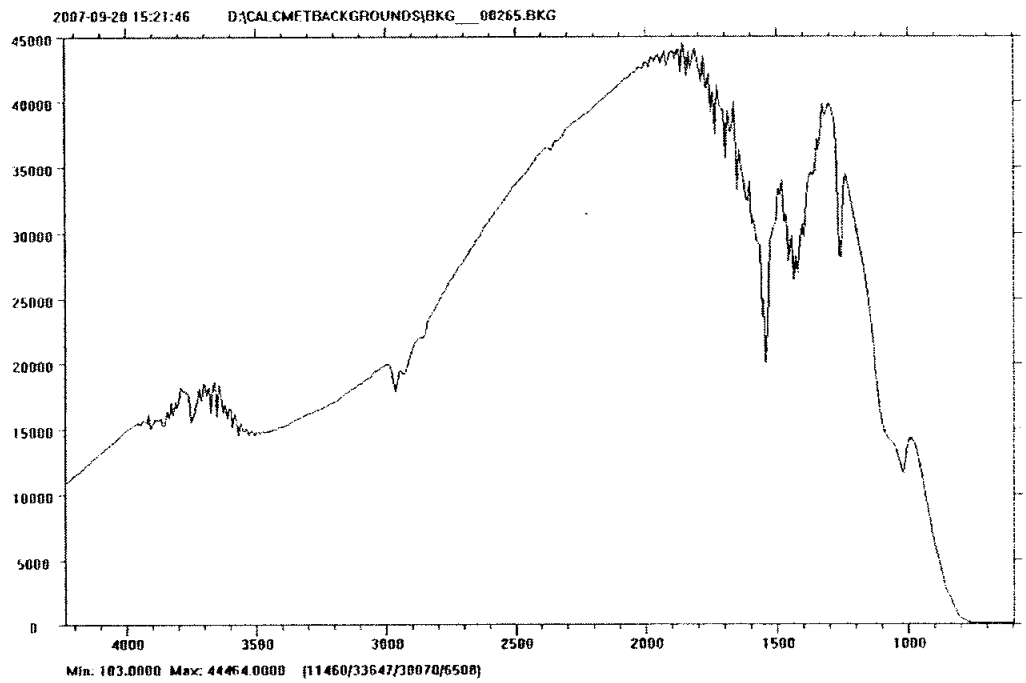

Figure 4-7 The background spectrum for the FTIR analyser. The x-axis is the wavenumber representing different wavelengths and the y-axis is the intensity

4.2.4 Injector Calibration

As the injector and the ECU were calibrated for natural gas, it was necessary to recalibrate for hydrogen use. This was to correct for the mass flow of fuel in relation to the injection duration. As the injector was designed to operate on the choked flow, the calibration can be done with outlet pressure in atmospheric conditions. Water displacement method as shown in Figure 4-8 was employed. 10 injections were made at several injection durations. The mass of the water displaced was weighed and the volume was calculated with the density of water assumed to be unity. This volume was equal to the hydrogen volume. Hence, the mass of hydrogen per injection duration was known. Appendix 1 gives the calibration curve of the hydrogen injection.

Although the injector calibration corrected the amount of fuel delivered per injection as given by the ECU, more accurate measure of fuel flow was given by the micromotion fuel flow meter. Thus, while this calibration helped the running of the test by having 'feed forward' value of air fuel ratio and fuel delivery, the more accurate readings for analysis would be from mass flow meters of fuel and air Another source of air fuel ratio measurement was from the oxygen gas analyser.

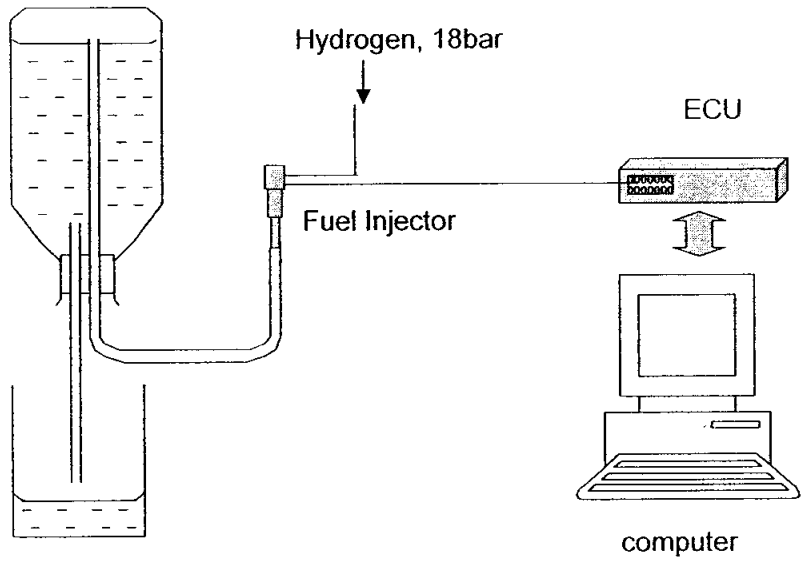

Figure 4-8 The set up for the injector flow calibration

4.3 The Test Fuel

In this study, industrial grade of hydrogen typical for electronics industry was used. It had high purity, up to 99.999%. The hydrogen was supplied by MOX Sdn. Bhd. in gas bottles with 200 bar pressure. Table 4-7 gives the specification of the hydrogen gas used in this study.

Natural gas from NGV station was used for engine performance and combustion comparison. Table 4-8 shows the typical properties of natural gas a supplied by Gas Malaysia Sdn. Bhd.

Table 4-8 The Specifications of Hydrogen

Purity	99.999%
Moisture	<3 vpm
Oxygen	<3 vpm
Hydrocarbon	<1 ppm
CO	<1 ppm
CO_2	<1ppm

Table 4-9 The Properties of the Natural Gas Used in the Study

Component	Unit	Leanest	Richest
Methane	%	96.42	89.04
Ethane	%	2.29	5.85
Propane	%	0.23	1.28
Iso-Butane	%	0.03	0.14
N-Butane	%	0.02	0.10
Iso-Pentane	%	N/A	N/A
N-Pentane	%	N/A	N/A
N-Hexane	%	N/A	N/A
Condensate	%	0.00	0.02
Nitrogen	%	0.44	0.47
CO_2	%	0.57	3.09
Gross Heating Value	kJ/kg	38130	38960

4.4 Test Procedures

This study aims at investigating the hydrogen combustion in the direct injection engine in comparison to natural gas, demonstrating its potential to improve the engine performance at low end speeds. As no modification was made to the engine, the parameters of interest were the injection and the air fuel ratio.

Since hydrogen is known to have abnormal combustion in the form of preignition, the operating envelop of this engine on hydrogen should be bounded by it. As for the engine speed, a range of 1800 rpm to 4000 rpm was selected. The minimum 1800 rpm was chosen as a safety precaution to avoid lower speed resonance frequency of the engine and dynamometer set up. The upper limit of 4000 rpm was chosen as the speed where the late partial direct injection is still achievable.

4.4.1 Injection Parameters

The injector type chosen was the narrow angle, with 30° outward opening injector. This was to maximise the spray penetration as hydrogen has very low density and viscosity. The injection pressure was fixed at 18 bar to allow maximum fuel delivery.

The injection timing was varied to cover the full direct injection, partial direct injection and simulated port injection. Injection after 132°BTDC (intake valve closed) was taken as full direct injection. SOI of 300° BTDC was chosen as the simulated port injection in which the injection duration was within the time when the intake valves were open. Partial direct injection was when the injection duration spanned across the time when intake valve was opened and closed.

The duration of the injection was set such that the air fuel ratio was close to stoichiometric. For leaner ratios, the injection duration was further reduced.

4.4.2 Abnormal Combustion Detection

Hydrogen burns with high flame speed that the pressure rise is almost instantaneous and gives out 'borderline knock' like sound. However, this combustion should not be regarded as abnormal combustion. Since the cylinder pressure can be monitored, it forms the basis for the detection of the preigintion. Figure 4-9 shows typical knocking phenomenon recorded in cylinder pressure readings. The trademark pressure ripple is the tell tale sign of knocking. Besides, such abnormal combustion was also detectable by loud knocking sound.

The ignition timing was adjusted such that the abnormal combustion did not occur. Careful adjustments were made for each operating point to detect and avoid the abnormal combustion by retarding the ignition timing. As such, for this test program, MBT timing was not achieved for every test points. With the presence of abnormal combustion, the timing was retarded away from MBT.

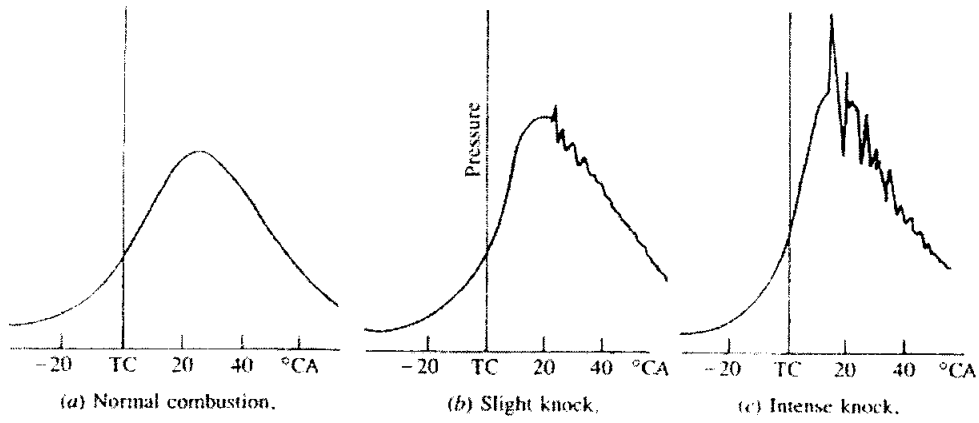

Figure 4-9 The knocking phenomenon as captured by cylinder pressure data [19]

4.4.3 Engine Warm Up and Fuel Flushing

Prior to the start of test, the engine needed to be warmed up. This was to ensure that the engine had reached operating temperatures and had stabilised. As hydrogen cost was substantially higher than other fuels, the engine warm up was done on natural gas. Since a common fuel line was used, this process would result in potential cross contamination of the fuel being tested.

In order to avoid contamination of natural gas in the hydrogen, the fuel line needed to be flushed with hydrogen prior to the data collection. Once the engine had reached stabilised temperatures, the engine was stopped and the fuel line purged. The engine was then re-started with hydrogen. A duration of 5 minutes was specified after the fuel switchover before any data can be recorded. This would allow the fuel line to be flushed while the temperature of the engine re-stabilised. This duration was deemed adequate based on the observation of the CO and CO_2 emissions data. For hydrogen, these emissions were almost non-existent in comparison to natural gas.

4.4.4 Engine Performance and Combustion Parameters

Engine performance

ISO1585 procedure "Road Vehicle – Engine Test Code – Net Power" [91] formed the basis of the test procedure adopted for the study. The test procedure specifies the method for measuring the power and torque output of an engine on a dynamometer.

Data such as torque, engine speed, engine temperatures and exhaust gas temperature were manually recorded from the dynamometer control panel. Automatic data recording was available for the real time data from the ECU as well as for the emissions. For this engine test program, the dynamometer was capable of maintaining the speed to ±0.1 rev/sec, or ±6 rpm. For each operating point, data were recorded once the engine had stabilised, after 3 minutes.

The power, *BMEP*, *BSFC* and the volumetric efficiency were calculated based on the following equations.

$$\text{Power, } P = \frac{2\pi NT}{60} \qquad \text{[kW]} \qquad (4\text{-}1)$$

$$BMEP = \frac{2\pi T}{V_d} \qquad \text{[kPa]} \qquad (4\text{-}2)$$

$$BSFC = \frac{FC \times 3600}{P} \qquad \text{[g/kWhr]} \qquad (4\text{-}3)$$

$$\text{Volumetric efficiency, } \eta_v = \frac{2m_a}{\rho V_d N} \qquad (4\text{-}4)$$

where N = engine speed, rpm

V_d = swept volume, m^3

T = torque,Nm

FC = fuel consumption, g/sec

m_a = mass flow of air, g/sec

ρ = density of air, kg/m^3

The motored cycle volumetric efficiency measurements were used as a basis for determination of volumetric efficiency loss when using gaseous fuel.

The air fuel ratio was calculated from the mass flows of both intake air and fuel. Another source of air fuel ratio measurement was from the lambda values given by the oxygen analyser. It should be noted however, for rich air fuel ratio, oxygen analyser lambda values were not accurate. In this condition, only the former air fuel ratio measurement was used.

Analysis of combustion characteristics

The cylinder pressure data and the corresponding crank angle position were captured via a high speed data acquisition system. Cylinder pressure data was used to determine the *IMEP*, *COV*, heat release rate and the mass burn fraction. The calculations of the combustion parameters were done in an Excel spreadsheet. A special MACRO code was developed in Microsoft Excel to analyse the data. This code selects the data relevant to the calculations, analyses and summarises it.

Brake specific emissions calculation

Since hydrogen and natural gas has different heating values and air fuel ratios, the emissions cannot be compared based on the concentration. A more suitable measure is

the brake specific emissions which normalises the emissions based on the power output. It gives the mass emissions in g/kWhr.

The following assumptions are important for the calculation of the mass flow of the emissions constituents.

1. By conservation of mass, the mass of exhaust is the same as the mass input into the engine.
2. Since engine exhaust consist mainly of air, the molecular weight of the exhaust is taken as the same as air, i.e, 29g/mole
3. The emission was measured in volumetric concentration, thus, this is equal to mole fraction.

Thus, it follows that the mass flow rate of exhaust is equal to the sum of the air and fuel mass flow rate.

$$\dot{m}_{exh} = \dot{m}_a + \dot{m}_f \tag{4-5}$$

where $\dot{m}_{exh}$ is the exhaust mass flow, in g/hr

$\dot{m}_a$ is the air mass flow, in g/hr

$\dot{m}_f$ is the fuel mass flow, in g/hr

No. of moles of exhaust, $\dot{n}_{exh} = \dfrac{\dot{m}_{exh}}{mw_{exh}}$ (4-6)

where mw_{exh} is the molecular weight of exhaust, which is the same as air, 29g/mole.

Note that the exhaust gases contain all the emissions constituents such as CO, CO_2, HC, NO_x, etc. Since these gaseous emissions measurements are given in volumetric concentration, it is also the molar fraction of the gas in the exhaust.

No. of moles of emission constituent, $\dot{n}_e = \dfrac{conc_e \times \dot{n}_{exh}}{1 \times 10^6}$ (4-7)

where $conc_e$ is the concentration of the emission constituent in ppm

$\dot{n}_e$ is the moles of the emission constituent, in mole/hr.

Thus, the mass flow of emissions, $\dot{m}_e = \dot{n}_e \times mw_e$ g/hr (4-8)

The brake specific emissions is thus,

$$S_e = \frac{\dot{m}_e}{P} \tag{4-9}$$

where S_e is the specific emissions and P is the brake power output

The FTIR analyser measured the hydrocarbons species such as methane, ethane, toluene, alcohols etc in ppms. The specific emissions of each species was calculated and summed together for THC. For NO_x, both the NO and NO2 specific emissions were calculated and added together. It should be noted that for analysis of emissions when operating on hydrogen alone, only the emissions concentration was used as comparison.

CHAPTER V

RESULTS and ANALYSIS

5.1 Abnormal Combustion of Hydrogen and Effects of Ignition Timing and Air Fuel Ratio

The tests were conducted on a single cylinder engine designed for CNG with a compression ratio of 14:1. The high compression ratio was intended to take advantage of the high auto ignition temperature of natural gas. It is thought that due to the high autoignition temperature of hydrogen, this high compression ratio was maintained to maximise the thermal efficiency. As such, no modification to the engine was carried out. The same direct injection fuel system was also used for both fuels.

The autoignition temperature of hydrogen is 574°C, which is higher than that of natural gas (540°C). However, abnormal combustion in the form of 'knocking' was observed during the tests with hydrogen. When the engine was operated under certain conditions, pinging noise was detected accompanied by a sharp rise in cylinder pressure and the corresponding pressure ripple (Figure 5-1). These were characteristics of engine knocking.

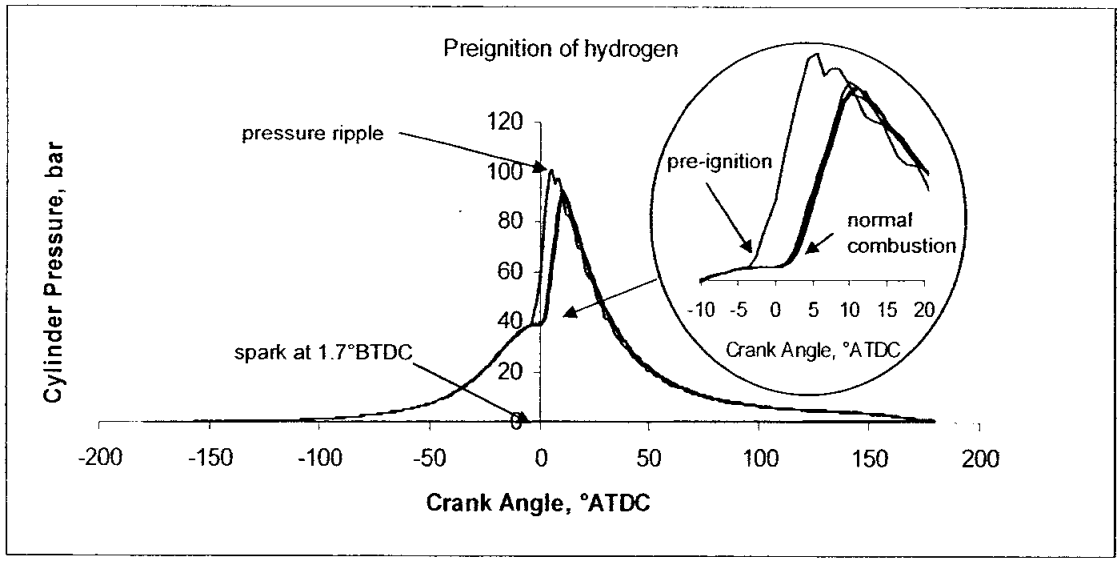

Figure 5-1 Engine knocking caused by preignition.

As shown in the figure, combustion started prior to the spark, thus the knocking observed was thought to be due to preignition caused by hot spots in the engine. As the engine was cleaned prior to the test program, and the engine was inspected to be clean after the tests, the existence of hot spots from engine deposits was ruled out. Other possible sources were spark plug tip, sharp edges in the combustion chamber or as a result of pyrolysis of engine oil.

At early injection timing and air fuel ratio close to stoichiometric, there was a tendency for the preignition to start before the intake valve closed, giving rise to the "backfire" condition. This is shown in Figure 5-2. If the engine continues to operate with this abnormal combustion, damage to the engine intake systems would ensue.

These abnormal combustions led to the need to retard the ignition timing during the tests, especially at air fuel ratios close to stoichiometric. Figure 5-3 shows the ignition timing for various speeds at different start of fuel injection (SOI). It was evident that for SOI of 300°BTDC, the ignition retard needed to avoid preignition was less. This was due to the low volumetric efficiency and the subsequent lower combustion temperatures. The ignition retard was maximum at speed 3000 rpm, i.e. the speed at which the volumetric efficiency was highest.

Figure 5-4 shows the variation of the ignition timing with respect to changes in air fuel ratio. As the air-fuel ratio approached stoichiometric, the combustion was more prone to preignite. In general, depending on speed, there was approximately 3 to 6 degree ignition retard needed for every 0.1 lambda as it was approaching stoichiometric.

Figure 5-5 shows the corresponding cylinder pressures for different air fuel ratios. It is evident that as a result of the retarded timing, the peak pressures were moving away from the typical optimum of about 15 °ATDC as the air fuel ratio was approaching stoichiometric. Thus, the maximum brake torque (MBT) timing was only possible on hydrogen operation at leaner mixtures. At close to stoichiometric, ignition timing was much retarded with consequent penalty on the engine performance, as shown by the curve for lambda 1.16 which indicates that combustion starts very late in the

expansion stroke. Thus, it is of interest to investigate whether operating at slightly leaner ratios with MBT timing would offset the performance deficit at stoichiometric.

It is important that for future efforts to adopt hydrogen for this engine, this abnormal combustion issue is addressed. It is even more important should higher engine speeds are intended as the engine is expected to be running hotter and the risk of melting the engine is higher.

For all the tests conducted in this study, the best possible ignition timing without abnormal combustion was used throughout.

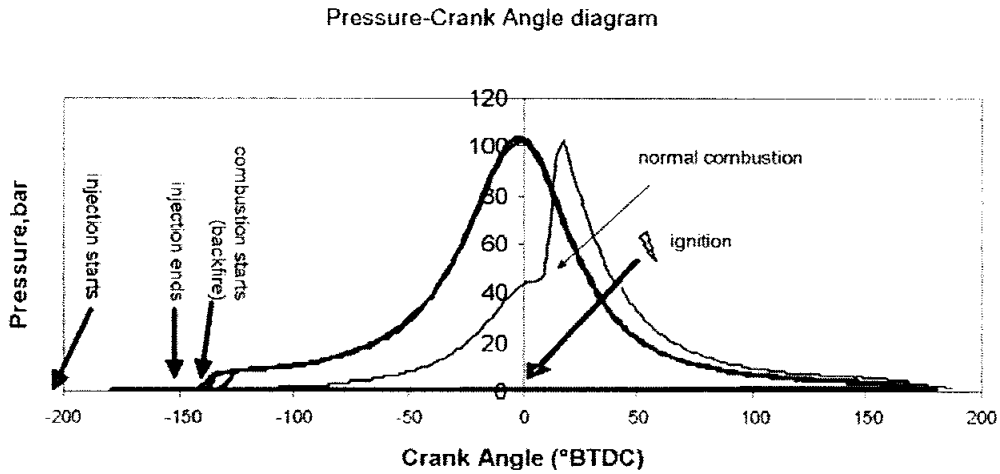

Figure 5-2 Engine backfire due to early preignition

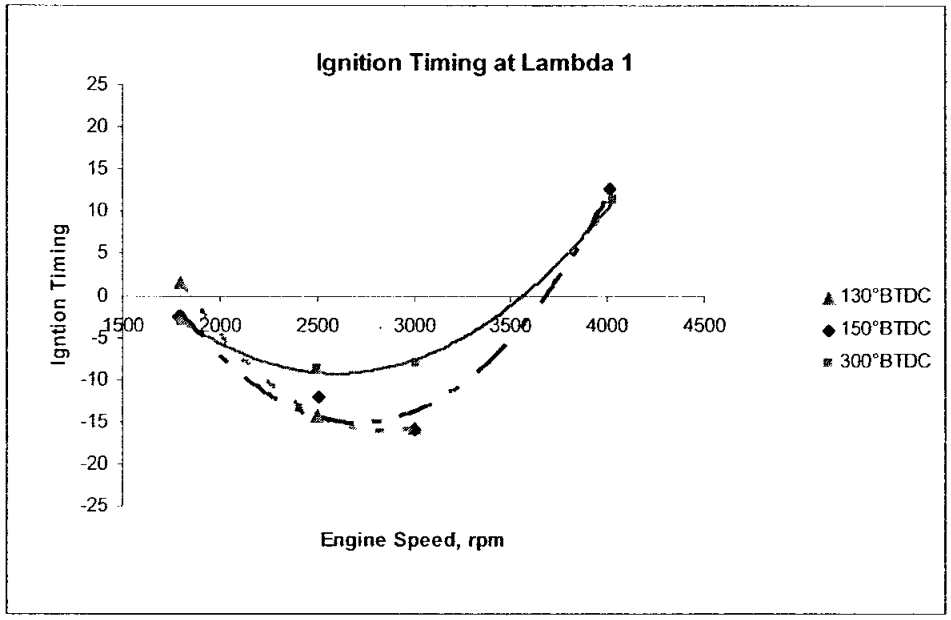

Figure 5-3 The ignition timing for start of fuel injection of 130, 150 and 300°BTDC

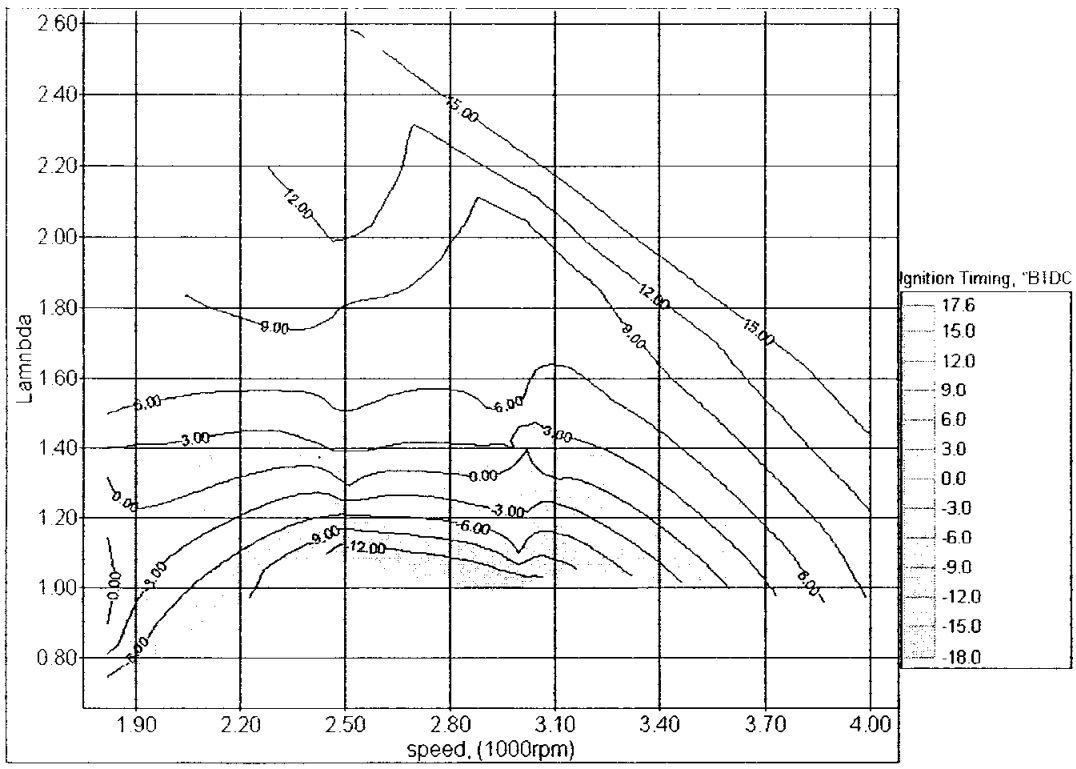

Figure 5-4 Ignition timing map for stoichiometric air fuel ratio of hydrogen

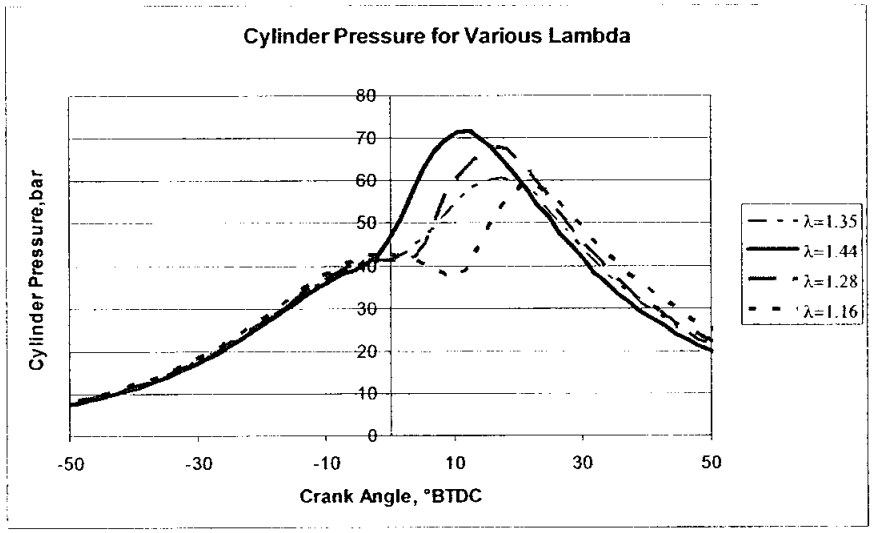

Figure 5-5 Cylinder pressure showing the effect of retarding the ignition to avoid preignition at speed 3000rpm

5.2 Effects of Injection Timing to the Performance and Combustion of Hydrogen DI engine.

In this study, the tests were carried out for start of injection (SOI) from 130° to 300°BTDC. Figure 5-6 shows the relationship between the start of injection and the end of injection for different speeds at stoichiometric. At SOI 300°BTDC, fuel was injected during the intake stroke, thus assumed to have the same mixture properties as port injection. Note also that at speed higher than 3000 rpm, direct injection was not possible for stoichiometric air fuel ratio.

As the aim of the study is to investigate the potential to improve the engine performance, full load operation was assessed. Thus, the analysis made in this section deals with stoichiometic air fuel mixture. The ignition timing was set at the optimum possible without occurrence of preignition.

The purpose of this experiment is to optimise the hydrogen injection timing for best performance of the engine. The effect of varying injection timing is discussed in terms of combustion characteristics, engine performance and emissions.

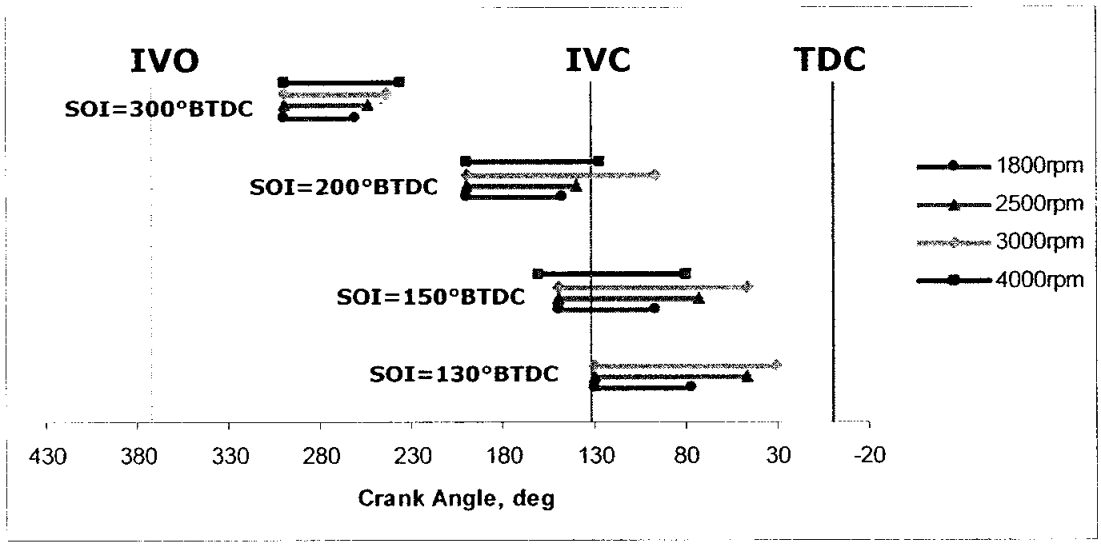

Figure 5-6 Injection timing and duration for stoichiometric operation of hydrogen

5.2.1 Engine Combustion

Figure 5-7 shows the *IMEP* of the engine at stoichiometric against the engine speeds. For direct and partial direct injection, *IMEP* shows a reducing trend with speed, despite the engine breathing characteristics that suggests maximum intake charge at 3000rpm (Figure 5-8). This discrepancy was due to the need for significant ignition retard at this speed. For early injection (300°BTDC), the ignition retard was somewhat smaller; hence the *IMEP* was relatively unchanged with speed. Also, with early injection, the mixing is more complete, allowing better combustion than late injection at higher engine speed.

It is also shown that at SOI of 130° and 150°BTDC, the differences in *IMEP* was small suggesting that the volumetric efficiency loss was not evident. At earlier

injections (300°BTDC) however, the *IMEP* was approximately 34% lower at speed below 3000 rpm.

Figure 5-9 shows the volumetric efficiency variation with respect to the injection timing. The volumetric efficiency drops from 86% to 55% as the SOI is advanced from 130° to 300° BTDC. At SOI of 130°BTDC and 150° BTDC, the curve appears flat, suggesting that at those SOIs, volumetric efficiency loss was not significant, possibly due to intake charge cooling effect of the hydrogen expansion. This explains the small difference in *IMEP* for both SOIs.

The combustion's coefficient of variation (*COV*) is as shown in Figure 5-10. The *COV* was well below 10% suggesting that the combustion was stable and the resultant driveability would be acceptable. Although it was shown that at 3000 rpm the *COV* was highest, the magnitude was still small, at 2.5% variation. This is expected as hydrogen is known to have low ignition energy and has wide combustibility limits, leading to consistent and stable combustion.

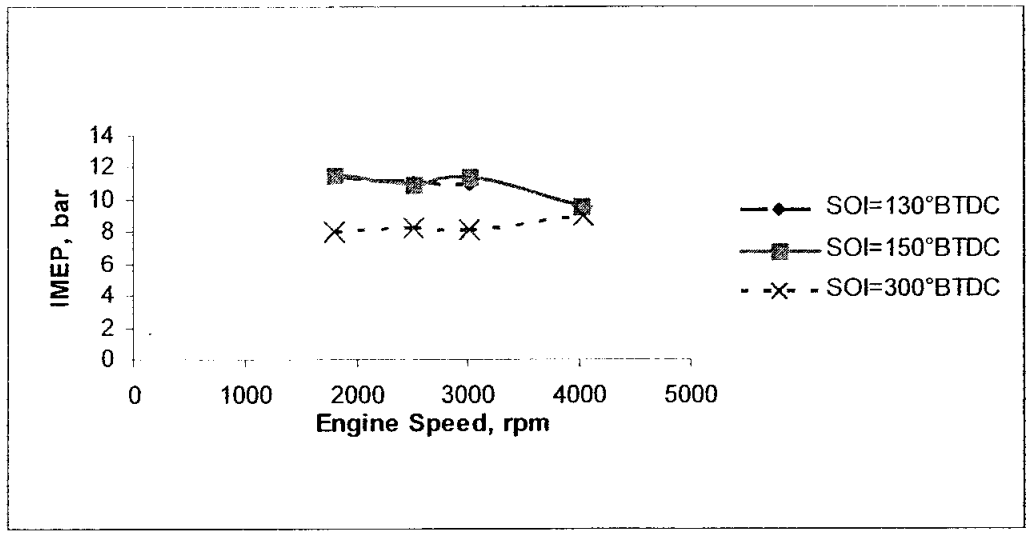

Figure 5-7 The *IMEP* of the engine with hydrogen as fuel

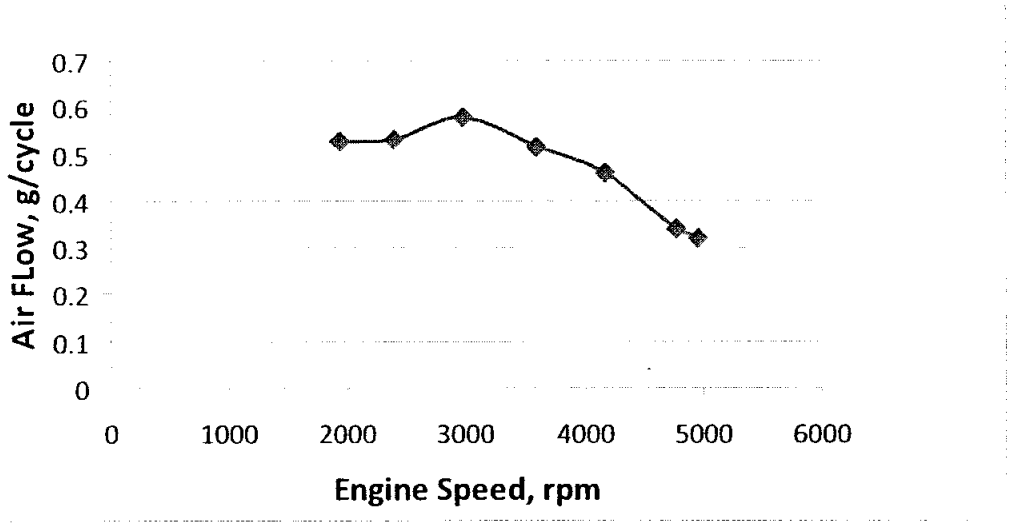

Figure 5-8 The airflow rate of the engine during motoring across various speeds

The rate of heat release for hydrogen combustion for various SOI is as depicted in Figure 5-11(a) and (b). At SOI 130° and 150° BTDC the difference was small especially at low speed, 1800 rpm. However, as the SOI was advanced to 300°BTDC, the rate of heat release was reduced. This was more evident at 3000 rpm than at 1800 rpm. It appears that the highest rate of heat release was at SOI 200°BTDC. Similar trend was reported earlier when using CNG on this engine [10]. It was thought that at this injection timing, the mixing was optimum in comparison to later injection which yielded maximum heat release.

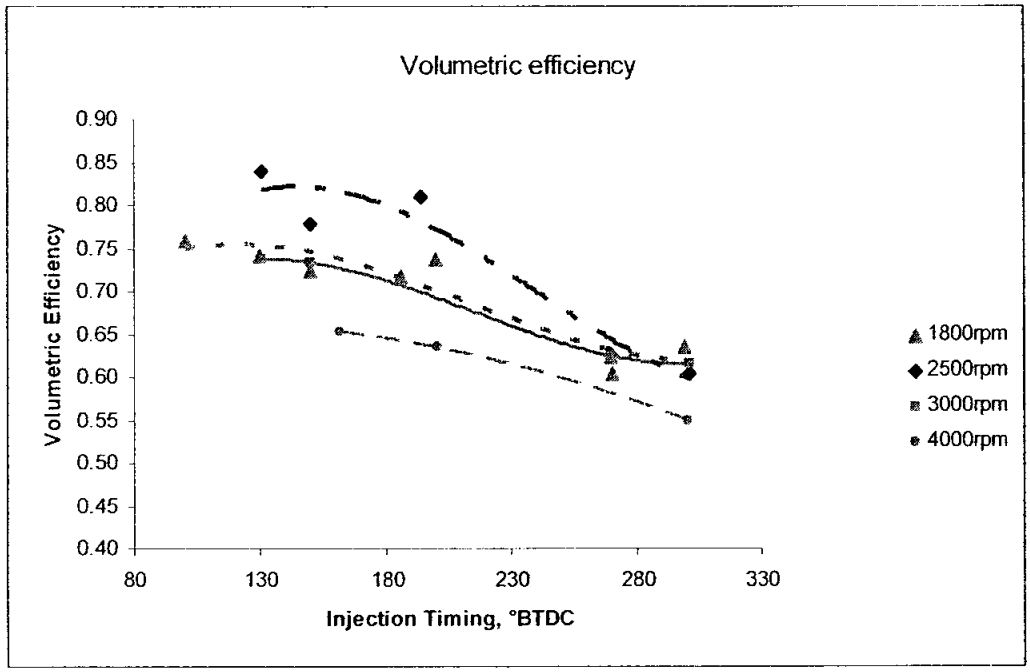

Figure 5-9 The volumetric efficiency of the engine when operating with hydrogen at different fuel injection timing

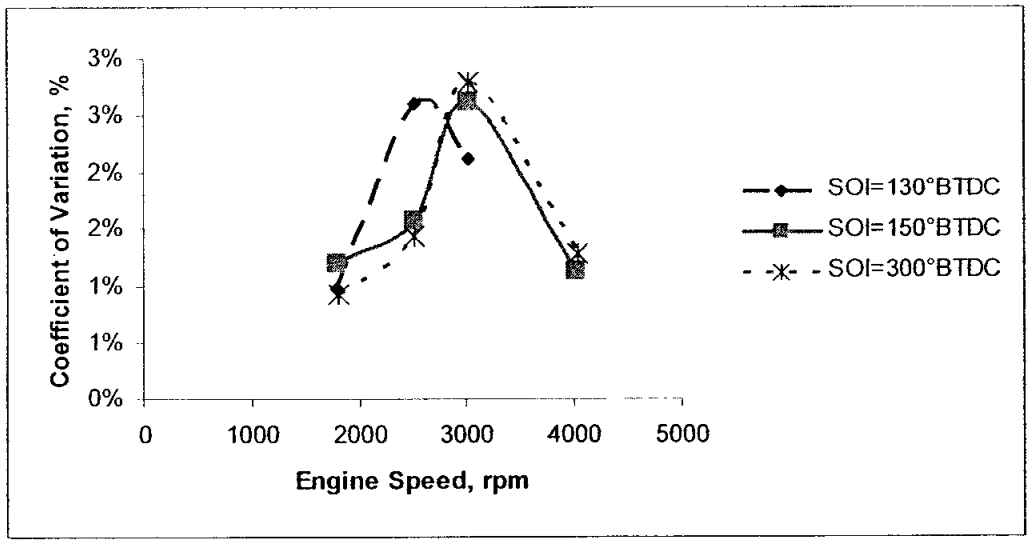

Figure 5-10 The coefficient of variation of the hydrogen combustion at lambda 1

The mass burn fraction is as shown in Figure 5-11(c) and (d). At 1800 rpm, the difference in the combustion duration and the ignition delay with respect to the SOI was small, with only a maximum of about 1°CA difference. At 3000rpm, the combustion appeared to have longer delay as SOI was advanced. This may be due to the lower volumetric efficiency that led to less heat and thus affected the flame speed.

Figure 5-12 shows the combustion efficiency for the engine at stoichiometric against speed. It was shown that the combustion efficiency were between 65% to 85% with a slightly increasing trend with speed. At low speed, 1800 rpm, it was shown that the simulated port injection (SOI 300°BTDC) had slightly higher efficiency, 76% in comparison to 70% at SOI 130°BTDC. This was due to the less ignition retard for early fuel injection that leads to more work by the piston. Also, at low speed, the mixing for direct injection may be relatively poor due to less turbulence.

On the other hand, at higher speed, the effects of varying the SOI was small, there was only 2% difference in combustion efficiency between DI and simulated port injection. This may be attributed to the better mixture formation at higher speed for DI operation, leading to better combustion.

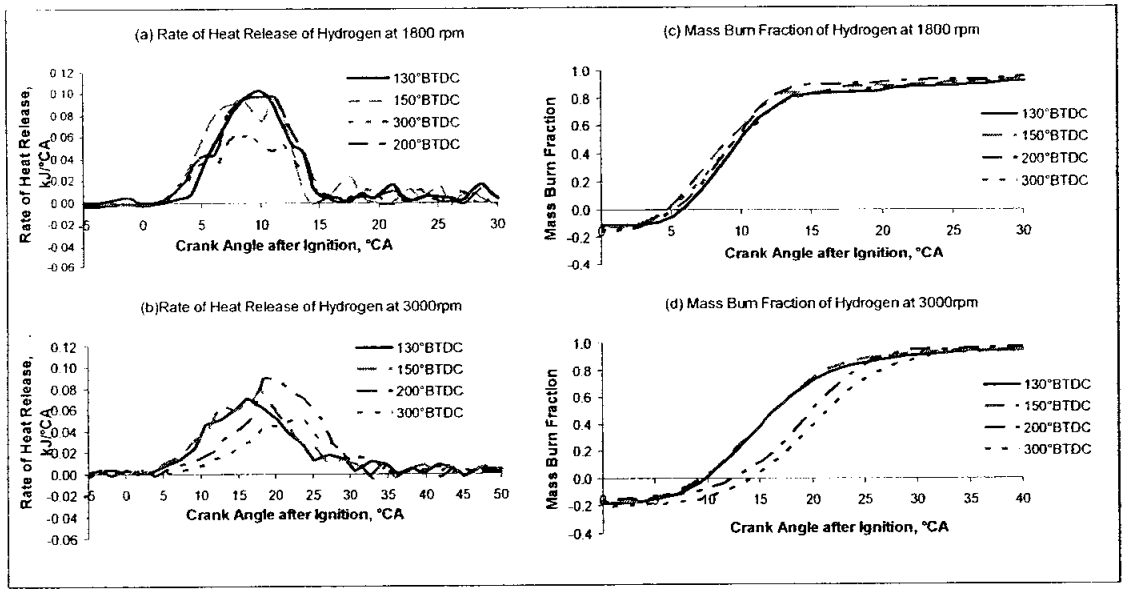

Figure 5-11 The combustion characteristics of hydrogen for various start of fuel injection timing

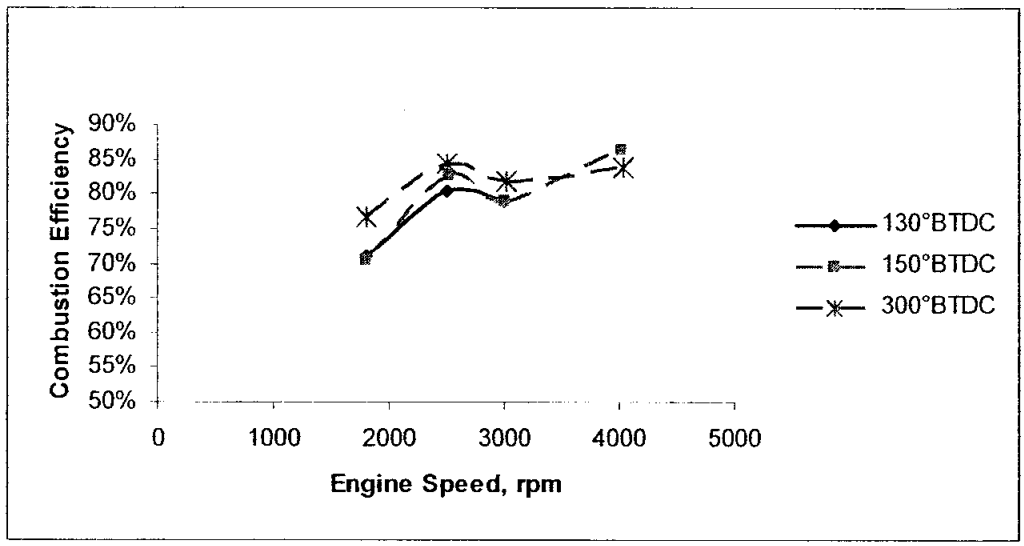

Figure 5-12 The combustion efficiency of hydrogen at various start of fuel injection

5.2.2 Engine Performance

Figure 5-13 shows the effect of variation in injection timing to the engine performance. The maximum torque of the engine was recorded to be 29.6 Nm at 1800rpm. As indicated by the *IMEP* (see section 5.2.1), for direct and partial direct injection, the torque curve shows a decreasing trend with the engine speed, although the engine breathing (Figure 5-8) shows that the maximum intake charge should occur at 3000rpm. This was due to the ignition retard required to avoid preignition. Thus, at higher speed, the maximum torque was not achieved.

At speed above 3000rpm, direct injection (SOI 130°BTDC) was not achievable due to the long injection duration requirement (limitation by ignition event as well as cylinder pressure). As is shown, injection timing earlier than 150° BTDC resulted in lower torque and power. At 300°BTDC, the loss was about 34% in comparison to injection at 130° BTDC. This was due to the loss in volumetric efficiency as the air is

being replaced by hydrogen (Figure 5-9). This result compares well with the *IMEP* data.

It was also evident that, the injection timing of 130° and 150° BTDC gave the highest torque and power. Although 150°BTDC is a partial direct injection, the volumetric efficiency loss was not evident, probably due to the charge cooling effect of hydrogen expansion. This resulted in more fuel-air mixture being drawn into the combustion chamber.

Figure 5-13(c) shows the brake specific fuel consumption (*BSFC*) of the engine across the speed for various start of fuel injection which ranged between 103 to 113g/kWhr. At lower speeds, the change of *BSFC* with respect to SOI was small, around 4 g/kWhr or 3.7%. At 4000rpm however, early injection (300° BTDC) showed 9% lower *BSFC* in comparison to partial direct injection. This is probably due to improved mixing with early injection.

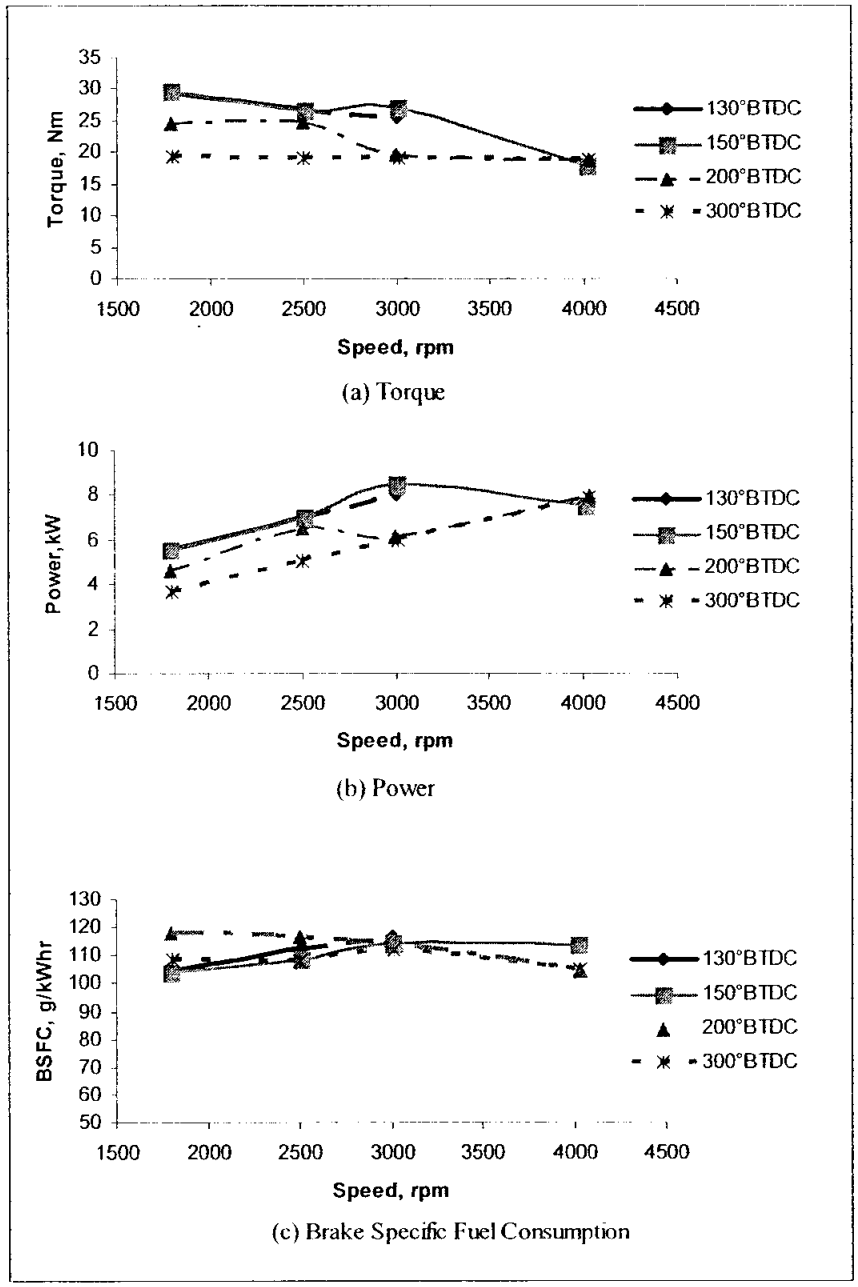

Figure 5-13 The performance of the engine when operating on hydrogen at various start of fuel injection

In summary, it can be concluded that the effect of volumetric efficiency loss was the dominant factor after the ignition retard requirement. At partial direct injection, SOI of 150° BTDC, the performance compared well with direct injection. This helped to

extend the operating range on hydrogen without significantly reducing the volumetric efficiency. However, at SOI earlier than 200° BTDC, the performance drop was significant (more than 17%) due to the volumetric efficiency loss. In all cases, it should be noted however, that the performance also depends very much on ignition timing. Thus it is essential that the issue of hot spots be resolved in the future.

5.2.3 Engine Out Emissions

As hydrogen is a carbon free fuel, the fuel originated emissions of total hydrocarbons (THC), carbon monoxide (CO) and carbon dioxide (CO_2) is non existent. However, as shown in Figure 5-14, although very small, the carbon emissions of hydrogen DI engine was not zero. These carbon emissions were thought to be originating from the engine oil. The other possible source is the hydrocarbons in the intake air. In general, under full direct injection, the emissions of hydrocarbon seemed to decrease as the speed was increased. As shown in Figure 5-15, the THC emissions concentration scattered across the injection timing tested. As such, no definite trend can be observed with respect to injection timing. Note also that the emission was very low (approximately 10-15 times normally recorded on natural gas).

The general understanding of the effects of the lubricant film in hydrocarbon emissions of spark ignition engine is through the adsorption and desorption of liquid fuel in the film [92]. However, as there was absence of liquid fuel, the emission of hydrocarbon from the lubricant in this engine was related to the quenching distance of the hydrogen flame [93]. The smaller the quenching distance, the hydrocarbons emission is expected to be higher.

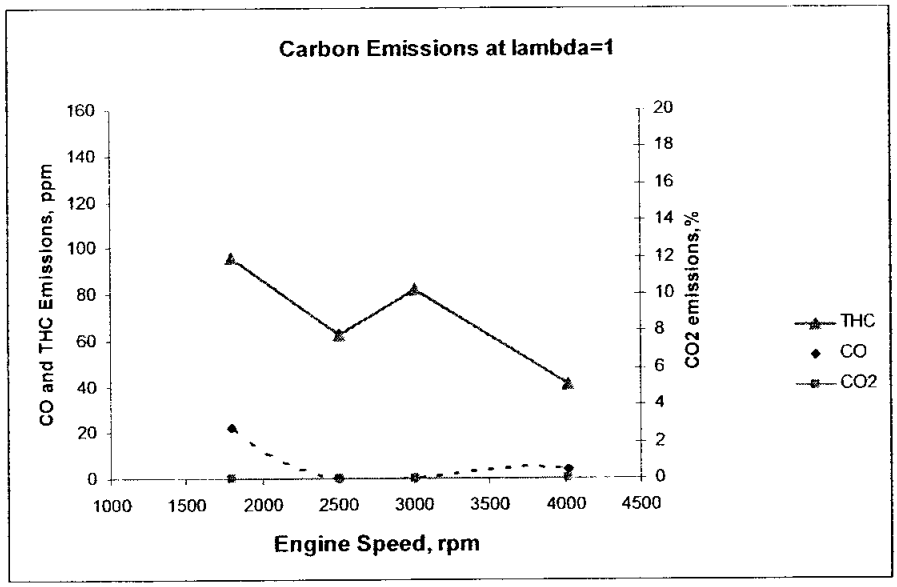

Figure 5-14 The engine out emissions on hydrogen at stoichiometric (SOI=130°BTDC)

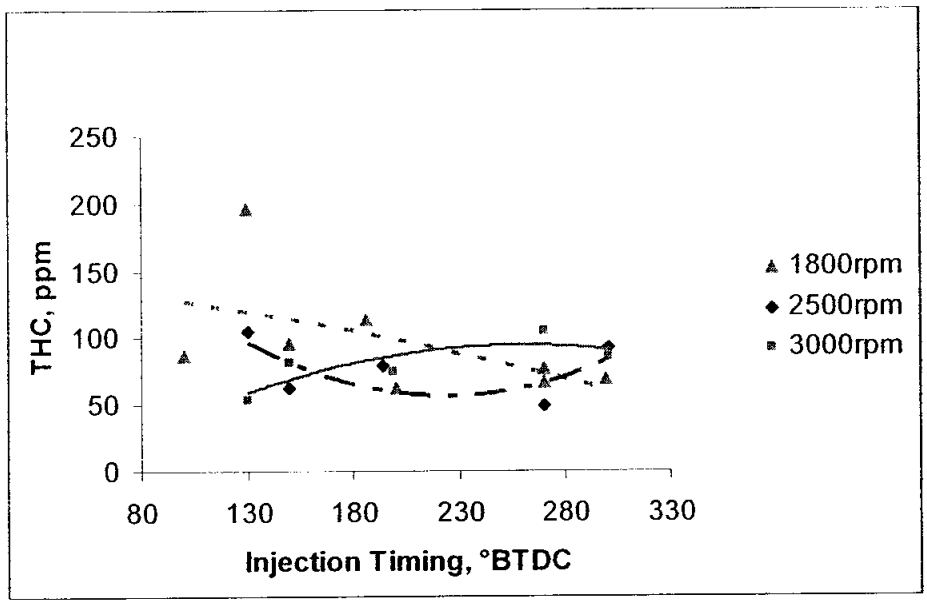

Figure 5-15 The Total Hydrocarbons emissions of the engine for various start of fuel injection for hydrogen

The CO emission of the engine is as shown in Figure 5-16. CO emission at close to stoichiometric and late SOI was almost non existent, indicating that there was insignificant amount of engine oil burned in the hydrogen combustion process. It thus follows that the hydrocarbons emissions discussed above was a result of other chemical or physical process other than combustion. Similar observation as in hydrocarbon emissions was noted, i.e. the emission was low and relationship to SOI was not strongly demonstrated.

As is shown in Figure 5-14, the CO_2 emission was not detected by the analysers, due to the very low concentration. Note that the equipment unit of measure for CO_2 was in percentage values which means that the readings were smaller than the 2% full scale error of the equipment.

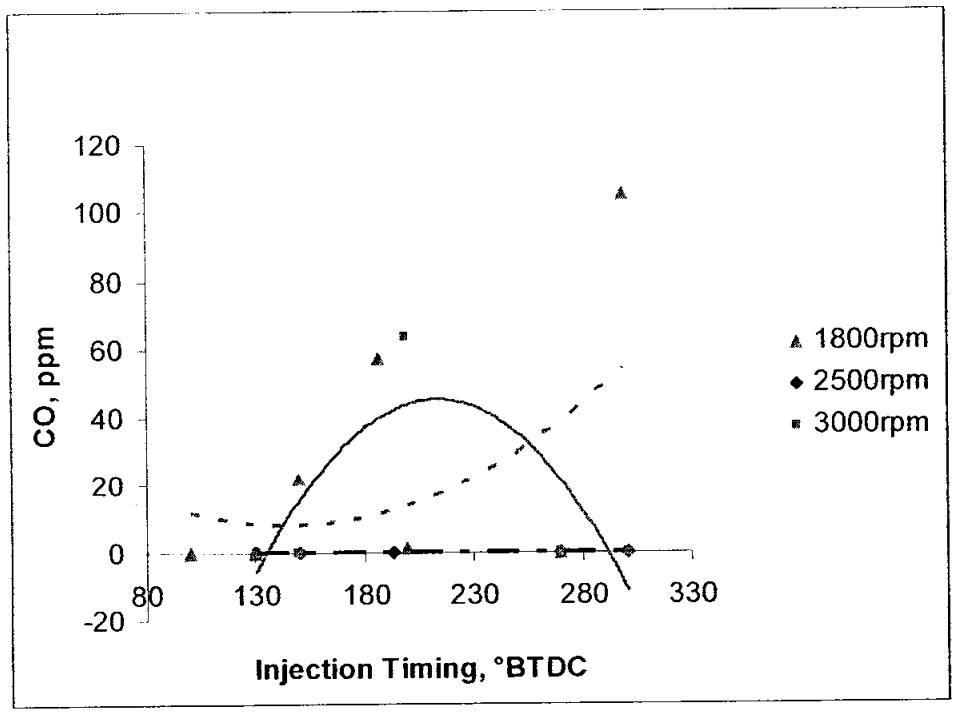

Figure 5-16 The emissions of carbon monoxide for various start of hydrogen injection

Of prime importance is the emission of oxides of nitrogen (NO_x). It was expected that with hydrogen, the peak cylinder pressure and the accompanying temperature is high that NO_x emissions could be an issue. Figure 5-17 shows the NO_x emissions from the engine with respect to changes in the fuel injection timing. In general, the NO_x emission increased as the injection timing was advanced.

Figure 5-18 shows the peak cylinder pressure against the injection timing which shows a reducing trend. It was evident that the NO_x emission did not correspond to the peak cylinder pressures. Therefore the increase in NO_x emission with respect to the SOI maybe attributed to the mixing of the fuel. At later SOIs, there was some degree of stratification occurred which resulted in smaller localised stoichiometric mixtures regions [31]. At earlier SOIs the mixture is more homogenous and stoichiometric resulting in higher NO_x emission.

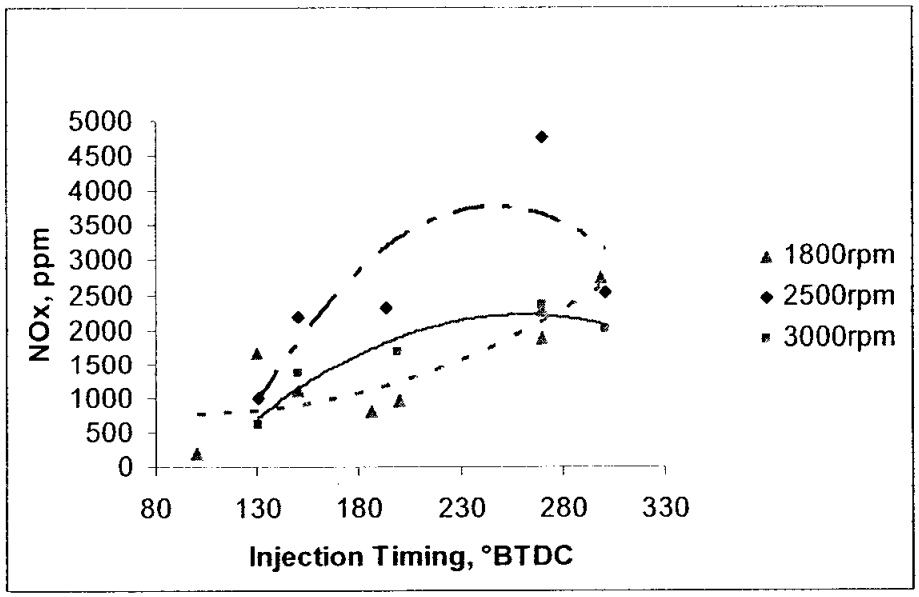

Figure 5-17 The NO_x emissions for various start of fuel injection

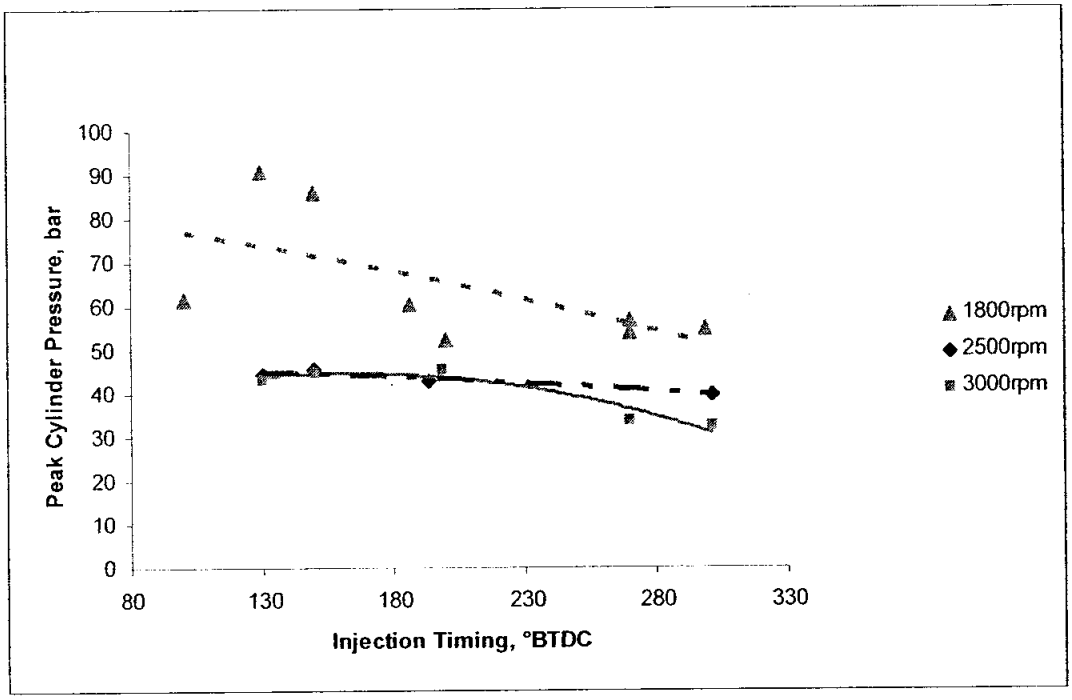

Figure 5-18 The Peak Cylinder Pressure for various SOIs

Summary

The presence of abnormal combustion limits the operation of the engine on hydrogen. At low speed, below 2000rpm, the engine was able to produce high torque and power. At higher speed, however, the ignition retard required to suppress the preigntion resulted in substantial penalty to the engine performance.

Direct injection and late partial direct injection (SOI of 130° and 150° BTDC) proved to be able to maximise the performance of the engine. At earlier injections, the volumetric efficiency loss was significant, with only 55% at 300° BTDC in comparison to 86% at 130°BTDC. This resulted in performance deficit as high as 34%.

In terms of emissions, hydrogen produced very little hydrocarbons and carbon emissions. The emissions were expected to be as a result of the small quenching distance of hydrogen flame. Nonetheless, the magnitude of the THC and CO

emissions was low in comparison to hydrocarbon based fuels by 1 order of magnitude. In terms of NO_x emissions, the more homogenous mixture of advanced injection timing produced more NO_x.

Overall, for hydrogen, the injection timing covering direct and late partial direct injection was required for maximising performance. This was due to the low density of hydrogen that early injection would reduce the volumetric efficiency significantly as it displaces the intake air.

5.3 Effects of Air Fuel Ratio on the Performance and Combustion of Hydrogen DI Engine

As was discussed in section 5.2, for operation on hydrogen, the ignition timing needed to be retarded to avoid abnormal combustion. This had led to the inability to operate at MBT timing for air fuel ratios close to stoichiometric. It is thus important to investigate whether operating at slightly lean mixture that allows the ignition to be advanced to MBT would consequently offset the performance deficit or an optimum operating mode can be found. The air fuel ratios evaluated were between lambda 1.5 and lambda 0.95. This was because the region of interest was at air fuel ratios not too far from stoichiometric, as the intent was to improve the performance of the engine at full load. In addition, this operating region was where test equipment can have all the measurements made, in particular the hydrogen mass flow rate. In addition, operation at too rich mixture would result in unburned hydrogen in the exhaust and could lead to explosion risks.

The aim of this experiment was to investigate whether operating the engine at slightly lean ratio would allow for optimised engine operation while improving the performance. The effects of varying the air fuel ratio on the engine performance, emissions and combustion characteristics are discussed in this section.

5.3.1 Engine Combustion

The *IMEP* of the engine with respect to changes in the air fuel ratio is as shown in Figure 5-19. At 1800 rpm, it is shown that as the air fuel ratio becomes leaner, the *IMEP* dropped from 12 bar at lambda 1, to 8 bar at lambda 1.3. As the injection timing is advanced, the *IMEP* curve appears flatter and converges at lambda value of approximately 1.3. This maybe explained by more air displacement by hydrogen as the injection was advanced beyond direct injection. Thus, small change in hydrogen input would result in a significant change in the lambda values. This is further illustrated by Figure 5-20 which shows the mass flow rate of hydrogen with respect to

air fuel ratio. At 300° BTDC, the mass flow rate was flatter across the air fuel ratio tested, with small change in fuel flow. Hence the change in energy and power delivered across the variation in air fuel ratio was also small, resulting in the flat trend in the *IMEP* Figure.

The curve also shows that the spread of *IMEP* with respect to SOI was larger at lambda less than 1.3 for 1800 rpm. The *IMEP* was sensitive towards changes in SOI for lambda less than 1.3 while for leaner mixtures above lambda 1.3, the sensitivity was less. This suggests that for lower load operations, where the air fuel ratio is leaner than 1.3, wide window for SOI is available for optimisation of efficiency and performance.

At higher speed, 3000rpm, the *IMEP* drop due to changes in lambda was less dramatic, from 12 bar to 10 bar for lambda 1 and lambda 1.3 respectively. The curve also appears flat up to lambda 1.2. This suggests that there is possibility to run the engine at slightly leaner ratio while maintaining the performance at this speed.

Similar to 1800 rpm, later injection also resulted in higher *IMEP* at 3000 rpm. However, the sensitivity of the *IMEP* towards the SOI was shown to be consistent throughout the air fuel ratio tested.

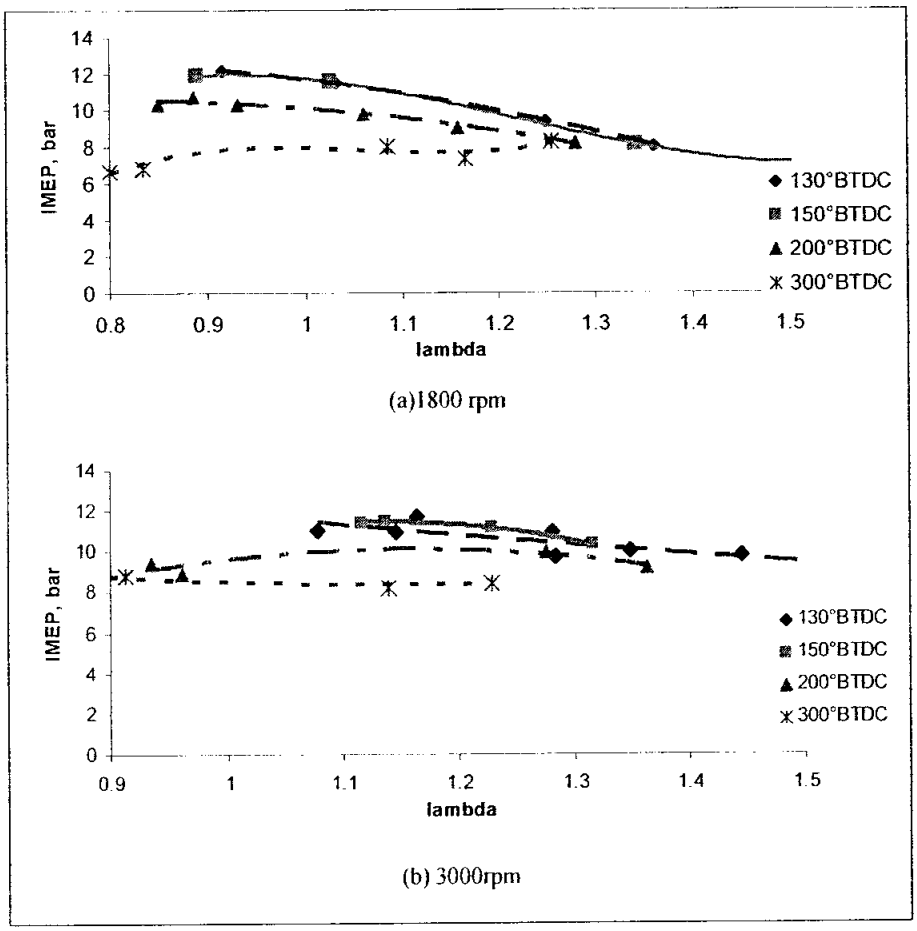

Figure 5-19 The *IMEP* of the across the air fuel ratio of hydrogen

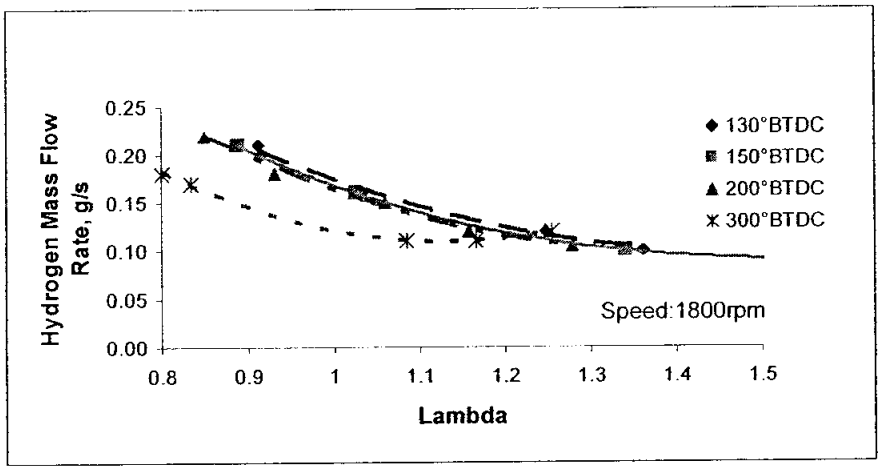

Figure 5-20 Hydrogen mass flow rate against air fuel ratio for various start of fuel injection

Figure 5-21 shows the *COV* of the combustion at various air fuel ratios. It is evident that the combustion was stable and repeatable with the variation at below 4%, indicating that the engine would result in good driveability.

Figure 5-22 shows the rate of heat release and mass fraction burned for hydrogen combustion at air fuel ratios of 1.08 and 1.25. It was evident that as the lambda increase from 1.08 to 1.25, the maximum rate of heat release was reduced from 0.1kJ/CA to 0.06kJ/CA due to less energy fed into the engine. The combustion duration also increased as the lambda was increased, implying that the combustion was slower. This is also depicted in the figure of mass fraction burn. Thus it follows that the combustion becomes slower with lower heat as the air fuel ratio is increased.

Figure 5-23 shows the effects of air fuel ratio to the ignition delay of the hydrogen combustion. It shows that the ignition delay increased slightly as the air fuel ratio became leaner, approximately 1 degree CA for every 0.2 increase in lambda. (1800rpm and 2500rpm)

The combustion efficiency with respect to changes in the air fuel ratio is depicted in Figure 5-24. It shows that the combustion efficiency increased with increase in air fuel ratio signifying that the combustion was more complete at slightly leaner than stoichiometric. At lambda 1 the combustion efficiency stood at 60% while at lambda 1.3 the efficiency was increased to 80%. This can be attributed to the lower heat generated and larger quenching distance for leaner ratios resulted in less heat loss to the combustion chamber walls.

The combustion efficiency peaks at around lambda 1.3 for 1800 rpm and 1.2 for 3000rpm and appears to flatten thereafter. Thus, it suggests that at 3000rpm, running the engine at lambda 1.2 would be optimum with the high *IMEP* and combustion efficiency. At 1800 rpm, a lambda trade off may be needed to operate the engine at high efficiency while avoiding significant *IMEP* loss.

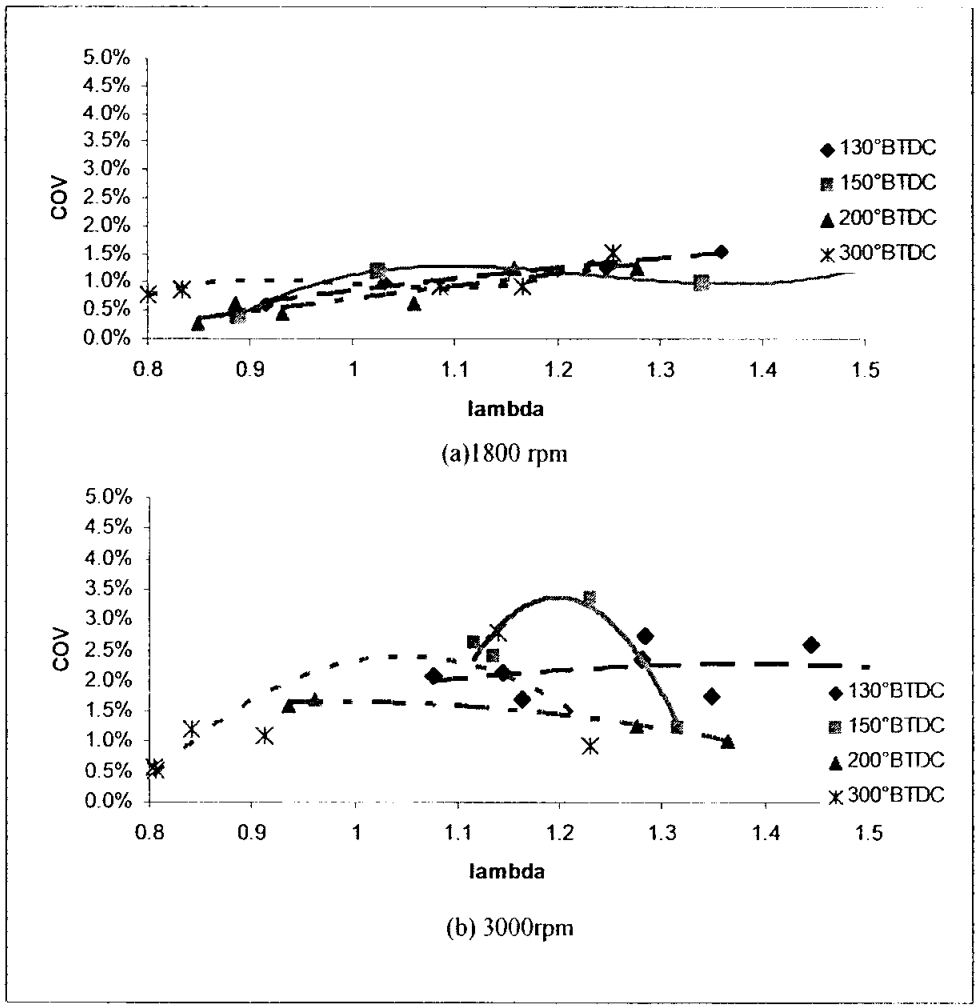

Figure 5-21 Coefficient of variation of hydrogen combustion with respect to air fuel ratio

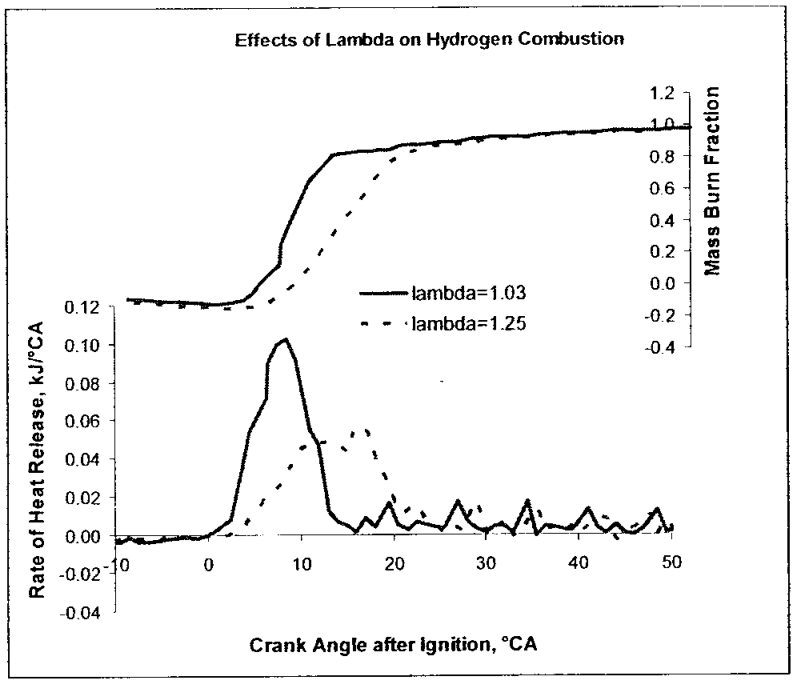

Figure 5-22 The combustion characteristics of hydrogen for different air fuel ratios

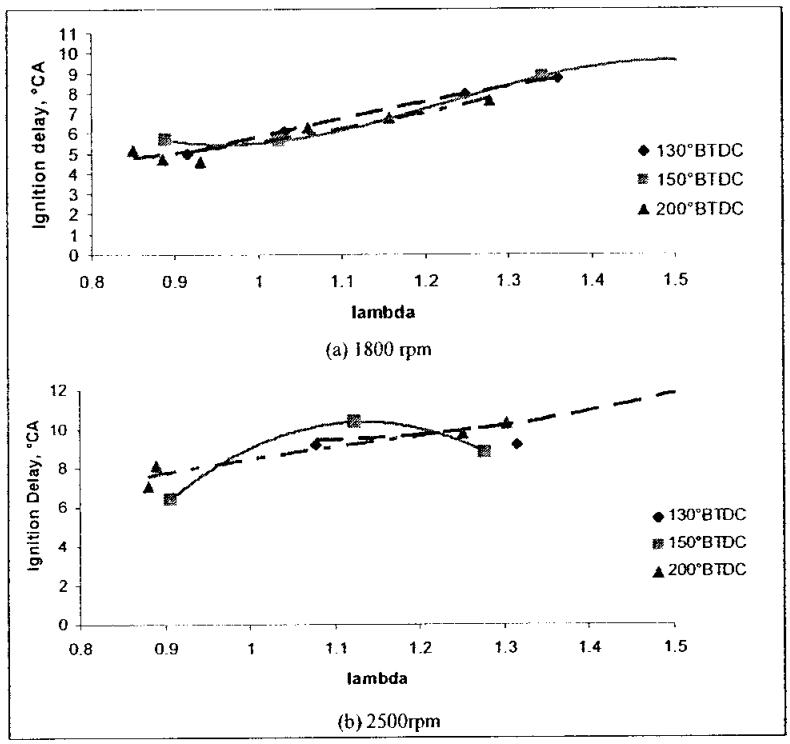

Figure 5-23 Ignition delay of hydrogen combustion with respect to air fuel ratio

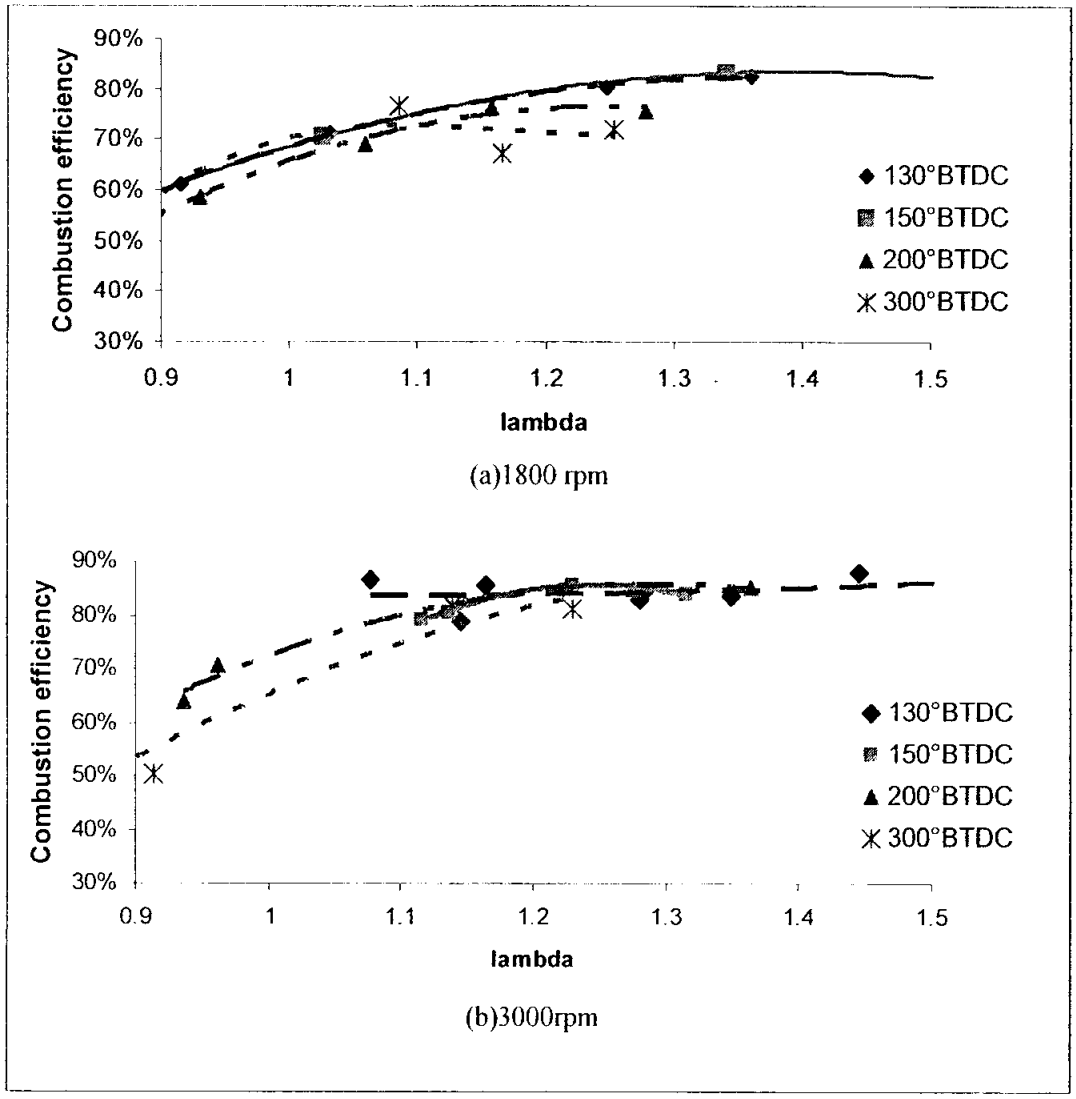

Figure 5-24 The combustion efficiency with respect to the air fuel ratio of hydrogen

5.3.2 Engine Performance

Figure 5-25 shows the engine performance with respect to variation in the air fuel ratios for various fuel injection timings. As expected from the *IMEP* results, the performance dropped as the lambda was increased. As the injection timing is advanced, the torque curve appears flatter and converges at lambda approximately 1.3 at 1800 rpm. This corresponds well to the *IMEP* curves. At this speed, for maximum torque and power, operation at stoichiometric is required.

At 3000 rpm, the sensitivity of the torque and power towards air fuel ratio was less. The torque was relatively constant up to lambda 1.2. Thus, there exists an opportunity to run the engine lean up to lambda 1.2 while maintaining the same performance.

The *BSFC* variation with respect to changes in the air fuel ratio is also depicted in Figure 5-25. *BSFC* reduced with increase in air fuel ratio, showing more efficient combustion at leaner ratios up to lambda 1.2 where the curve becomes flat. As was discussed in the preceding section, this suggests that at 3000 rpm, operating at lambda 1.2 would be optimum. For 1800 rpm, a trade off between maximum performance and efficiency need to be achieved.

Figure 5-26 shows the map of the engine torque across the various speed and the air fuel ratios. It is worth noting that at leaner ratios (lambda>1.2), the ignition timing can be advanced and MBT timing can be achieved (as shown in Figure 5-4). However, as is shown in the map, the increase in torque was not sufficient to offset the performance drop caused by the leaning of the intake charge.

The torque map also shows the potential of controlling the power of the engine through mixture quality control method at low loads with unthrottled operation. It was shown that the engine could be run at least to 60%-50% load without throttle. The advantage of running the engine lean unthrottled is the increased thermal efficiency.

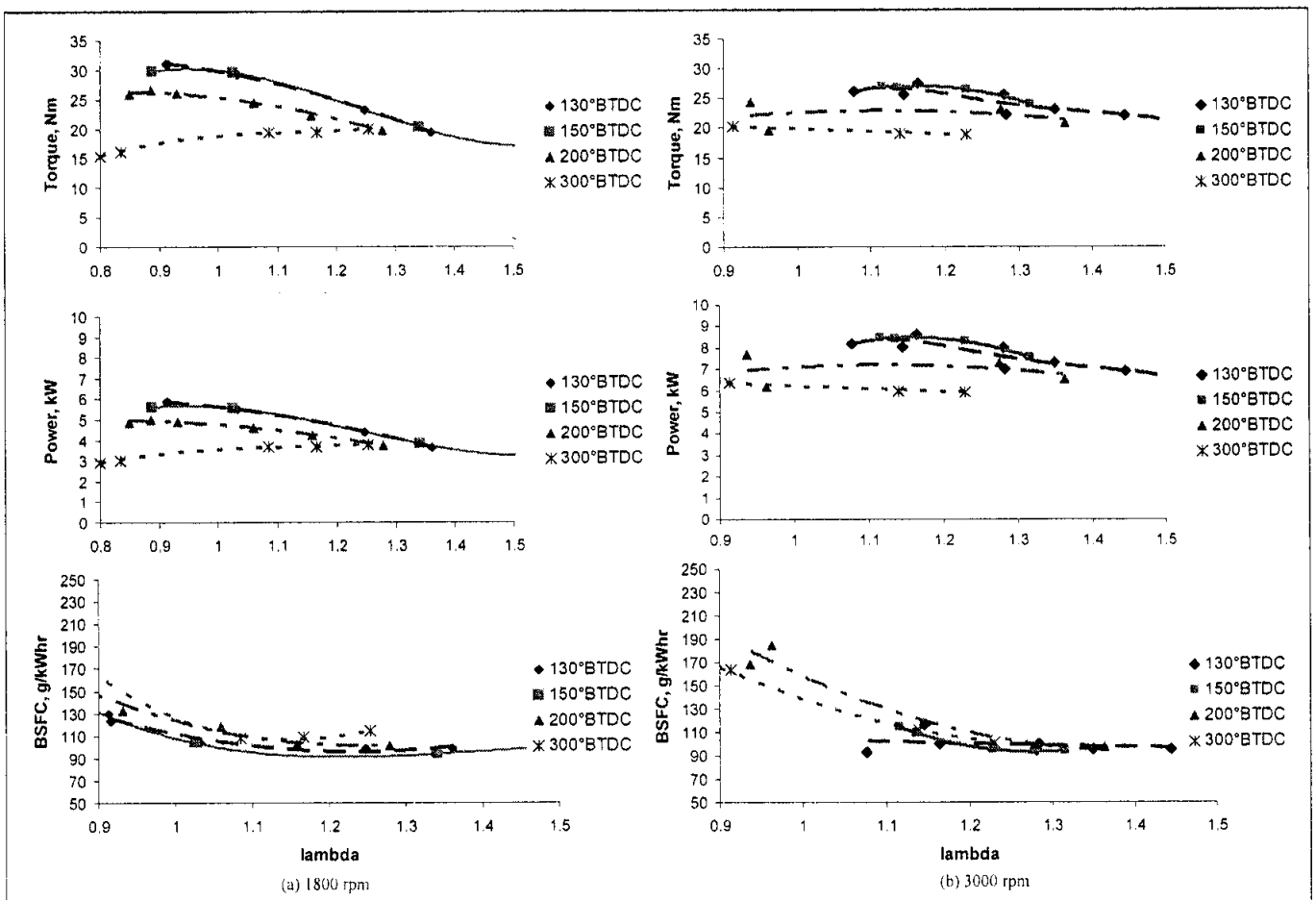

Figure 5-25 The engine performance when operating with hydrogen at different air fuel ratios

Map showing the indicated thermal efficiency across the engine speed and *BMEP* is depicted in Figure 5-27. Indicated thermal efficiency as high as 46% was achievable on this engine. Note, however, as the study objective is to improve the performance at full load, higher air fuel ratios were not tested. Thus, the possibility of unthrottled operation at much lower loads was not assessed.

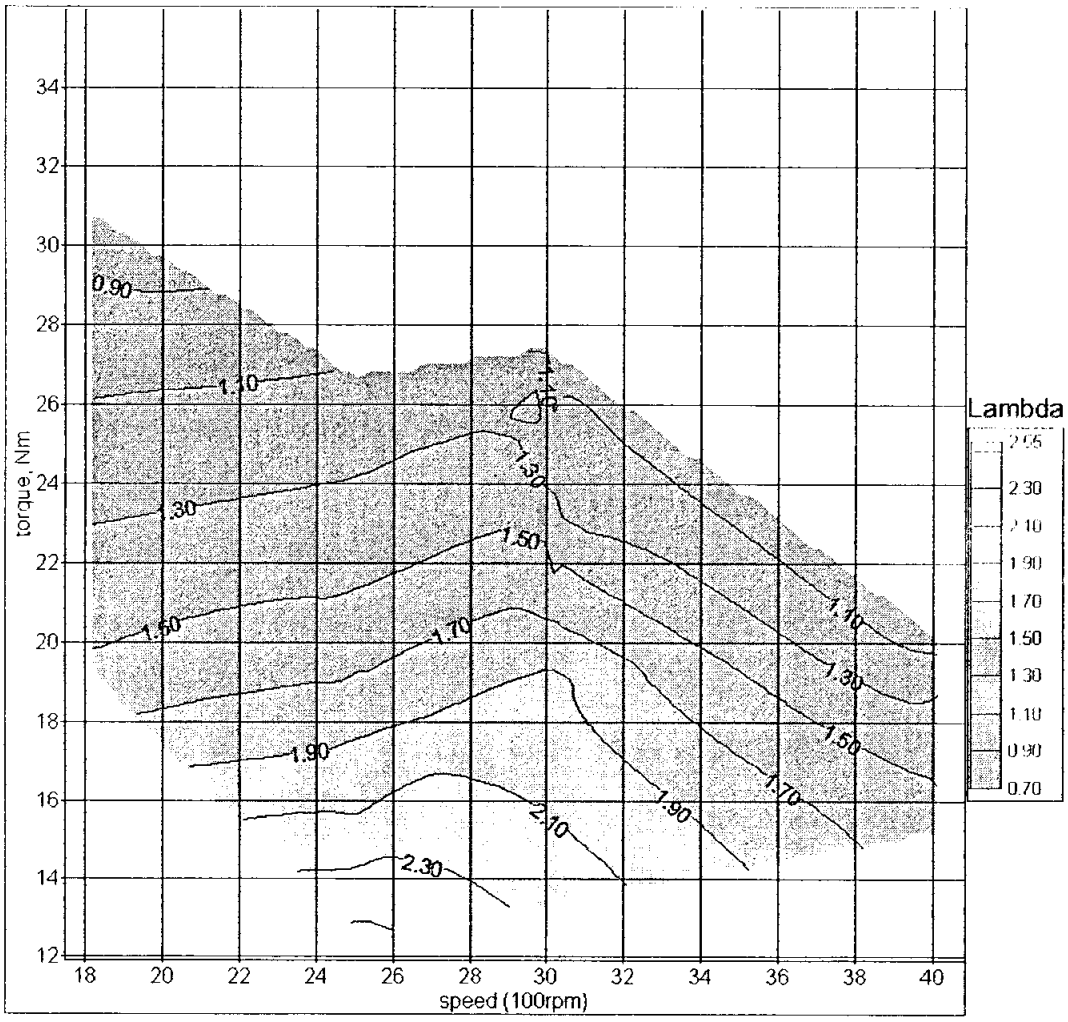

Figure 5-26 Contour map of engine torque with respect to speed and air fuel ratio (SOI=130°BTDC except at 4000rpm SOI=160°BTDC)

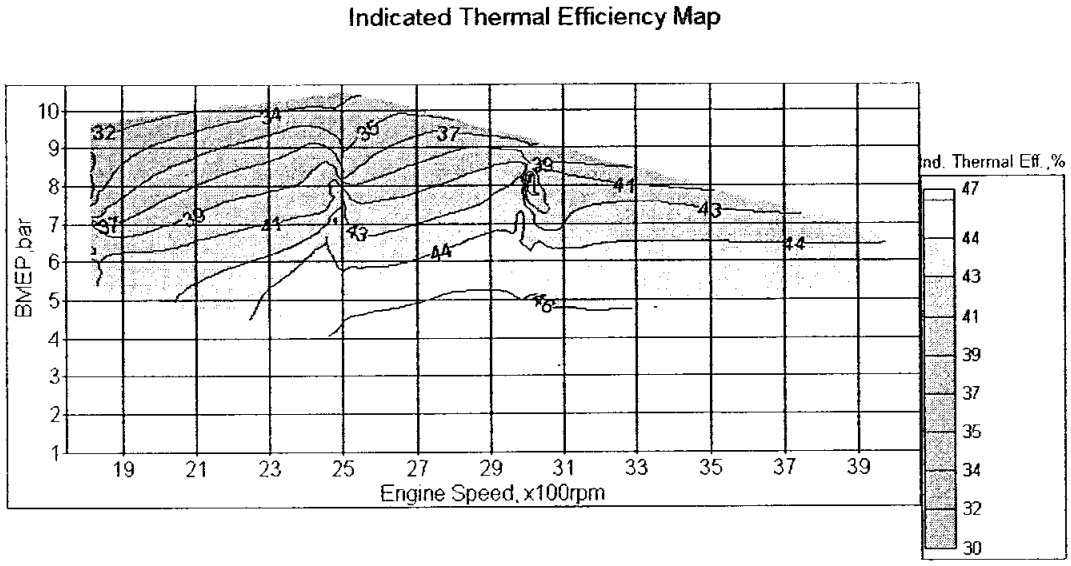

Figure 5-27 Contour map of the engine's indicated thermal efficiency

5.3.3 Engine Out Emissions

The emission of hydrocarbons is depicted in Figure 5-28. In general, the emissions concentration decreased as the air fuel ratio became leaner. As discussed in the previous section, the emission of hydrocarbon was probably originated from the lubricating oil and related to the quenching distance of the flame. As leaner ratios had slower speed and lower temperature flames, the quenching distance was higher. This explains the lower hydrocarbon emissions at leaner ratios.

As was discussed in the previous section, the emission of CO is not significant at air fuel ratio lean or close to stoichiometric. However, at slightly rich air fuel ratio, there was detectable CO emissions of up to 700 ppm. The possible explanation for this phenomenon is that rich air fuel ratio resulted in the flame to quench closer to the walls, resulting in oxidation of the engine oil film. This was more predominant at early injection timing, suggesting that the more homogenous is the mixture the shorter would be the quenching distance.

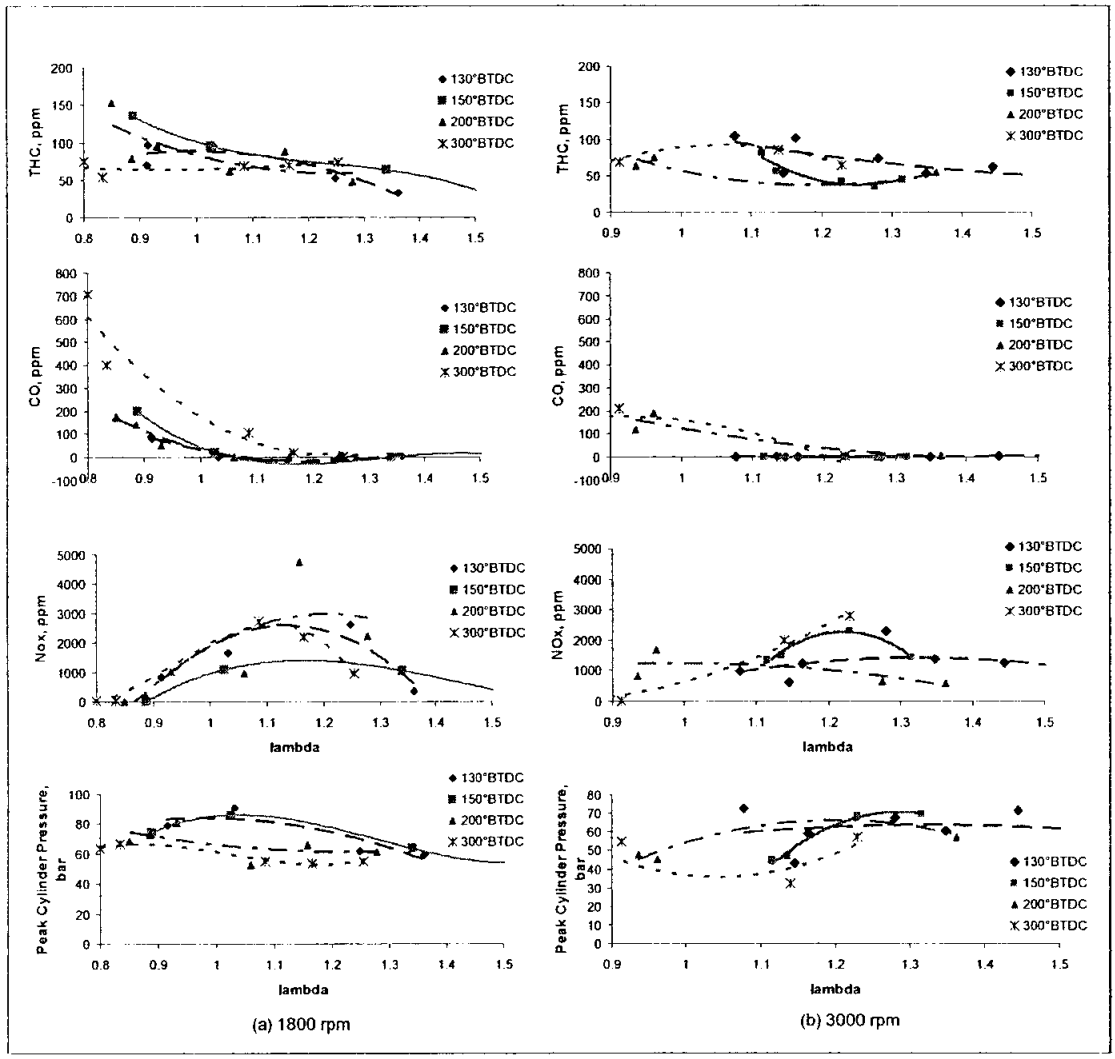

Figure 5-28 The engine out emissions when using hydrogen at different air fuel ratios

NO_x emission variation with changes in air fuel ratio is also shown in Figure 5-28. Overall, NO_x emission was highest at lambda of around 1.1, at 3000-4000ppm. At lambda ratios of more than 1.3, the NO_x emission were reduced as leaner ratios resulted in lower temperatures, which is also illustrated in the Figure showing the peak cylinder pressures. This agrees with the general understanding of NO_x emission trend with air fuel ratios of hydrogen as depicted in Figure 5-29 [26]. At stoichiometric air fuel ratio, the NO_x emission is similar to that at lambda 1.3, suggesting that for low NO_x operation, air fuel ratio higher than lambda 1.3 is desired.

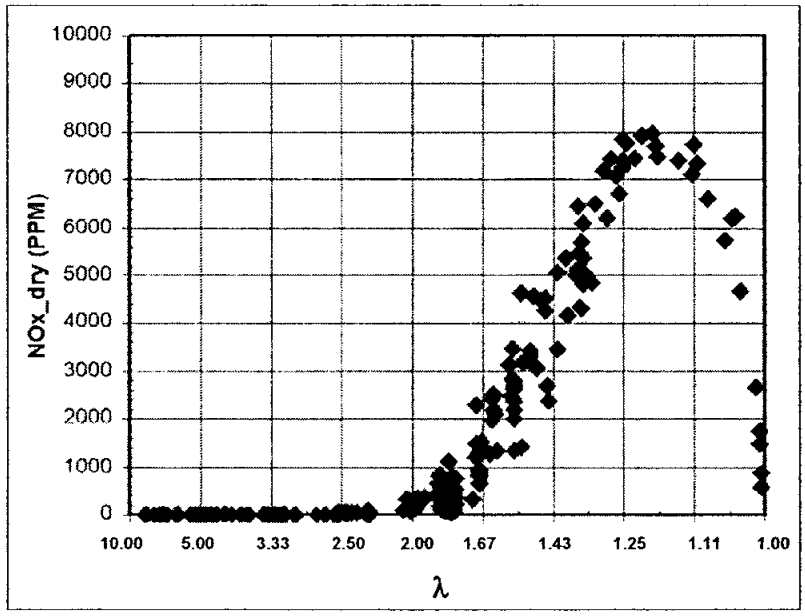

Figure 5-29 Typical NO_x emissions charateristics using hydrogen [26]

Summary

Generally, running the engine on hydrogen at leaner ratios resulted in lower performance. Despite the ignition timing could be advanced to MBT at leaner ratios, the expected torque increase could not offset the deficit due to the leaning of the intake charge. Thus, no torque or power increase was observed across the air fuel ratio tested.

For low engine speed, 1800 rpm, the performance sensitivity towards air fuel ratio was more evident. At lambda 1.2, the *BSFC* and efficiency was optimum, however, the torque deficit was as high as 5Nm. As such, there is a need to compromise between high performance, efficiency and emissions. For maximised performance purposes, operation and stoichiometric is thus preferred.

At 3000rpm however, the changes in performance against air fuel ratio was less dramatic. The torque was consistent while the *BSFC* and efficiency optimum at

lambda 1.2. Thus, the results suggest that the optimum engine operation at intermediate speed, 3000 rpm, is at lambda 1.2.

It is shown that there is a potential for running the engine with indicated thermal efficiency as high as 46% at lean air fuel ratios. This would allow for unthrottled operation with power control by fuel quantity means for loads down to at least 50%. It should be noted, however, that leaner ratios was not evaluated in this study. Thus potential for unthrottled operation for much lower loads was not assessed.

Based on results of *IMEP*, torque, power and efficiency, it was demonstrated that the engine was less sensitive to the SOI at air fuel ratio leaner than 1.3, particularly at low engine speed. Hence, for intermediate load operation, where mixture is lean, wide window of SOI is available for optimisation of engine performance and efficiency.

In terms of engine out emissions, NO_x was found to be maximum at lambda 1.1, at 3000-4000 ppm. At stoichiometric air fuel ratio, NO_x emission was similar to that at lambda 1.3. Thus, for low NO_x operation, operation leaner than lambda 1.3 is required. However, this would result in reduced performance, a 25% drop in torque. As such, no 'sweet spot' in terms of NO_x-performance trade off was found.

CO emissions was found to increase at airfuel ratio richer than stoichiometric due to the shorter flame quenching distance to the cylinder walls. However, it should be noted that running rich mixture for hydrogen engine is not desired from safety stand point.

5.4 Comparison of Engine Performance and Combustion between Hydrogen and Compressed Natural Gas.

In this section, the full load engine performance, emissions and combustion characteristics of hydrogen are compared to compressed natural gas. The engine was operated at the best setting for performance on each fuel type, based on the results as discussed in previous sections for hydrogen and Firmansyah [10] for CNG. This is summarised in Table 5-1.

Table 5-1 The optimum engine operating setting for hydrogen and natural gas for maximum power.

	CNG	Hydrogen
Air fuel ratio, lambda	~1	~1
Start of fuel Injection, °BTDC	180	130 - 150
Throttle position	WOT	WOT
Injection Pressure, bar	18	18

5.4.1 Engine Combustion

Figure 5-30 shows the comparison of the rate of heat release and mass fraction burn for hydrogen and CNG at speeds of 1800 and 3000rpm. It is evident that hydrogen had higher rate of heat release for both speeds, with a maximum rate of heat release of 0.8 and 0.01kJ/degCA in comparison of 0.04 and 0.03kJ/degCA for CNG. Also for CNG, the rate of heat release at 3000 rpm was slightly higher than at 1800rpm. This is the opposite for hydrogen, which showed that the combustion at 1800rpm has higher rate of heat release.

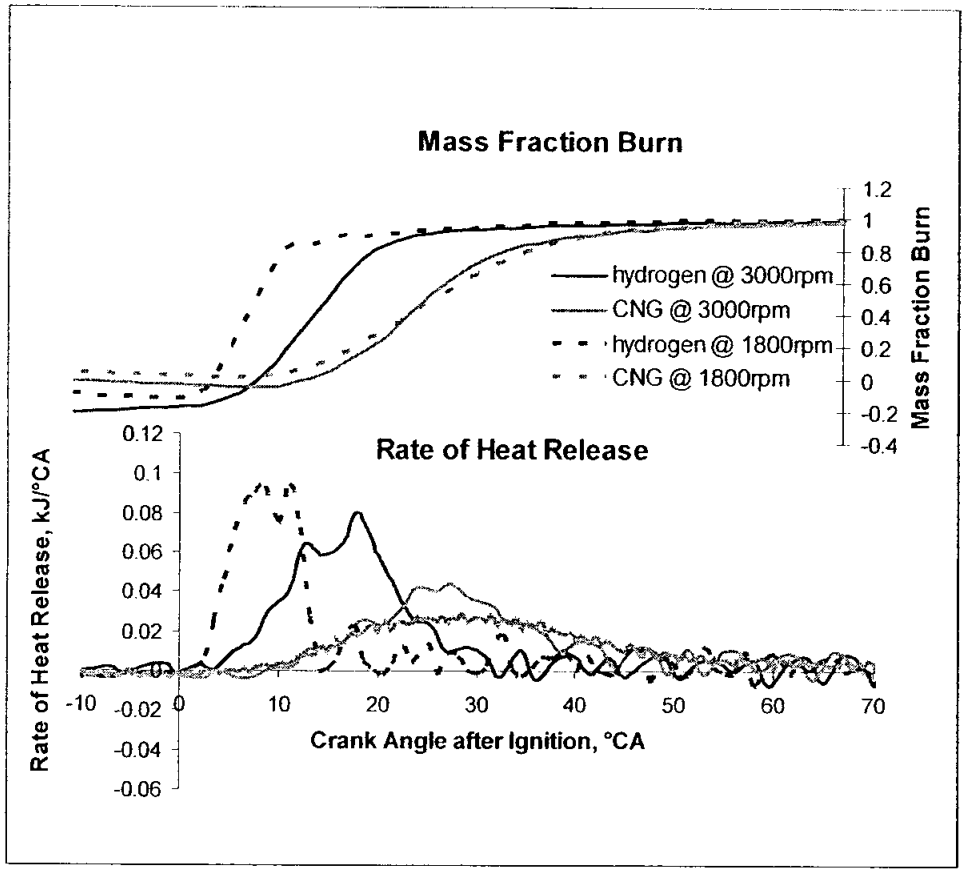

Figure 5-30 The combustion characteristics of hydrogen in comparison to CNG

It is also important to note that the ignition delay and the combustion duration of hydrogen was less than that of CNG, by about 50%. It is also shown that at low speed of 1800rpm, the combustion of hydrogen remained to be rapid even when there was less air motion and mixing. This is further illustrated in Figure 5-31 which shows the combustion duration and the ignition delay across the engine speed tested. This short delay and rapid combustion is expected to increase the performance of the engine at low speed where turbulence is less.

The lesser sensitivity of the hydrogen combustion towards mixing rate is further illustrated in Figure 5-32, which shows the ignition delay changes with respect to the start of injection. It was obvious that for hydrogen, the combustion began with shorter delay than CNG across the injection timing, although the mixing was expected to be reduced as the SOI was retarded.

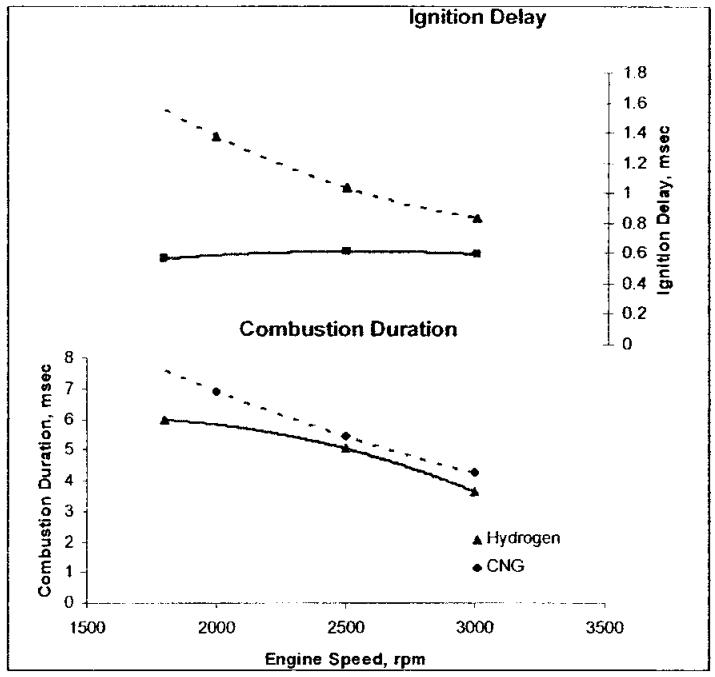

Figure 5-31 The combustion duration and ignition delay with respect to speed for hydrogen and CNG

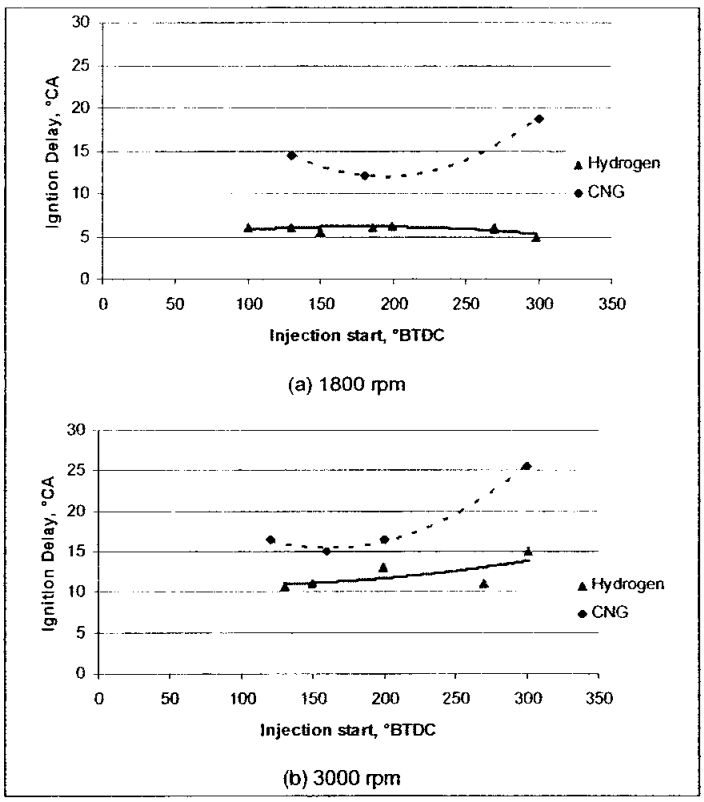

Figure 5-32 The ignition delay at 1800 and 3000 rpm at various start of fuel injection

The comparison of the *IMEP* for the engine when fuelled with hydrogen and natural gas is shown in Figure 5-33. At speeds of 2000rpm and lower, the *IMEP* for hydrogen was higher than that for CNG with the largest difference of 25% at 1800rpm. This demonstrates the potential of hydrogen to improve performance at these speeds.

At speeds higher than 2000rpm however, the *IMEP* of hydrogen was lower than CNG, with increasing gap as the speed was increased. This is attributed to the increasing ignition retard required at higher speed and power.

Figure 5-34 shows the comparison of *COV* of the combustion for both types of fuel. It is evident that the combustion was stable and repeatable as the *COV* was well below 10%. It was also showed that the *COV* of hydrogen was similar to CNG.

Figure 5-35 compares the combustion efficiency of hydrogen and CNG. At speeds lower than 2500 rpm, the combustion efficiency of hydrogen could be up to 10% higher than CNG. At higher speeds, the combustion efficiency was similar for both fuels. This suggests the hydrogen combustion efficiency was less affected by the lower turbulence at the low speeds.

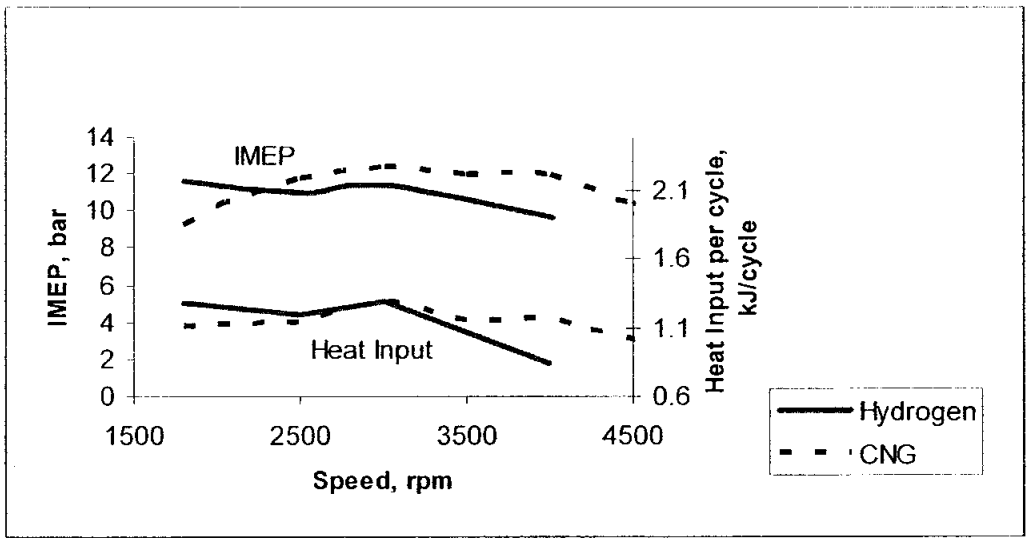

Figure 5-33 Comparison of *IMEP* between hydrogen and CNG operation

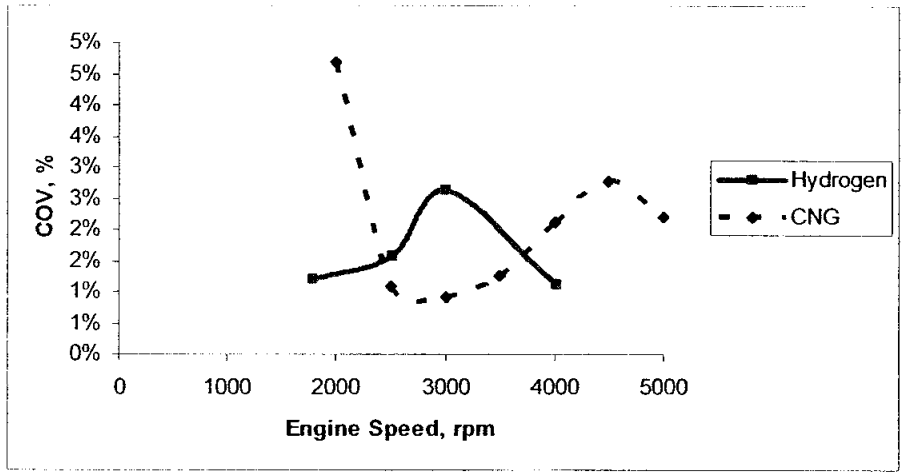

Figure 5-34 Comparison of Coefficient of Variation between hydrogen and CNG operation

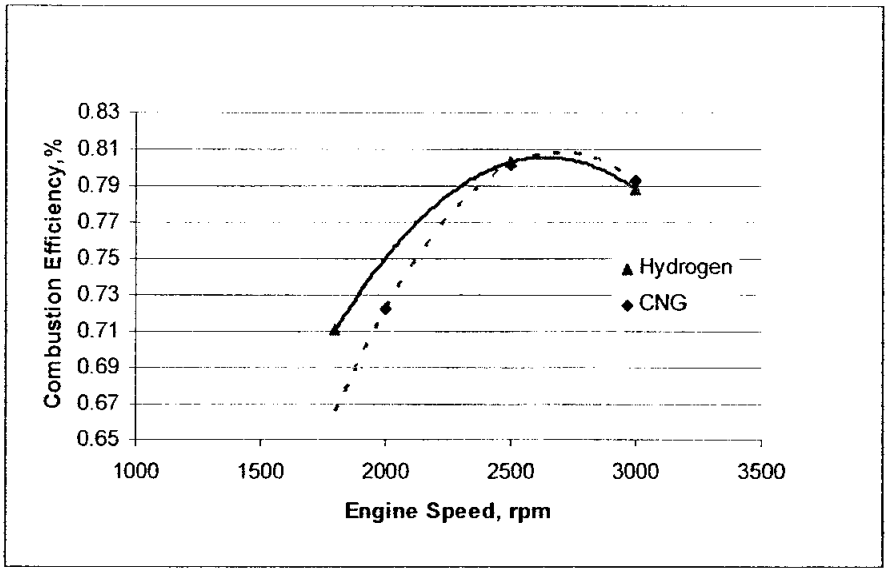

Figure 5-35 Comparison of the combustion efficiencies of hydrogen and CNG at different speeds.

5.4.2 Engine Performance

Figure 5-36 compares the engine torque and power output when operating on hydrogen and natural gas. At low speeds, 2000 rpm and below, the torque and power of the engine were higher when operating on hydrogen. At 1800rpm the torque and power of the engine was 10% higher than CNG.

Figure 5-37 superimposes the hydrogen torque-lambda map with torque curve of CNG. It shows that it was possible to run the engine on hydrogen at similar torque as CNG at low speed with leaner mixture or lambda around 1.1 to 1.2. In this case, a further 3% thermal efficiency gain was possible, as discussed in section 5.3.2

At higher speeds however, the performance when using hydrogen continued to lag behind CNG as the speed was increased. This is because of the ignition retard needed to avoid abnormal combustion on hydrogen. As higher rpm would produce more power and heat, the engine was more prone to preignite and hence more ignition retard was required with significant penalty on performance.

The comparison of *BSFC* when using hydrogen and CNG is depicted in Figure 5-38. In general, the *BSFC* on hydrogen was 60% lower than that for CNG, due to hydrogen having approximately 60-65% more heating value per unit mass. For CNG, the BFSC tend to increase at low speed, while for hydrogen, it maintained relatively constant throughout the speeds. This suggests that hydrogen maintained its efficiency at lower speeds.

Figure 5-39 shows the indicated thermal efficiency of the engine when operating on hydrogen and CNG. In general, the indicated thermal efficiency increased with the speed. For hydrogen the indicated thermal efficiency was between 36% to 46% while for CNG it was between 33% to 42%. At low speed (2000rpm and lower) the indicated thermal efficiency of hydrogen was higher than that of CNG. This shows that combustion on hydrogen remained efficient even at low speed where CNG suffered some losses due to less mixing.

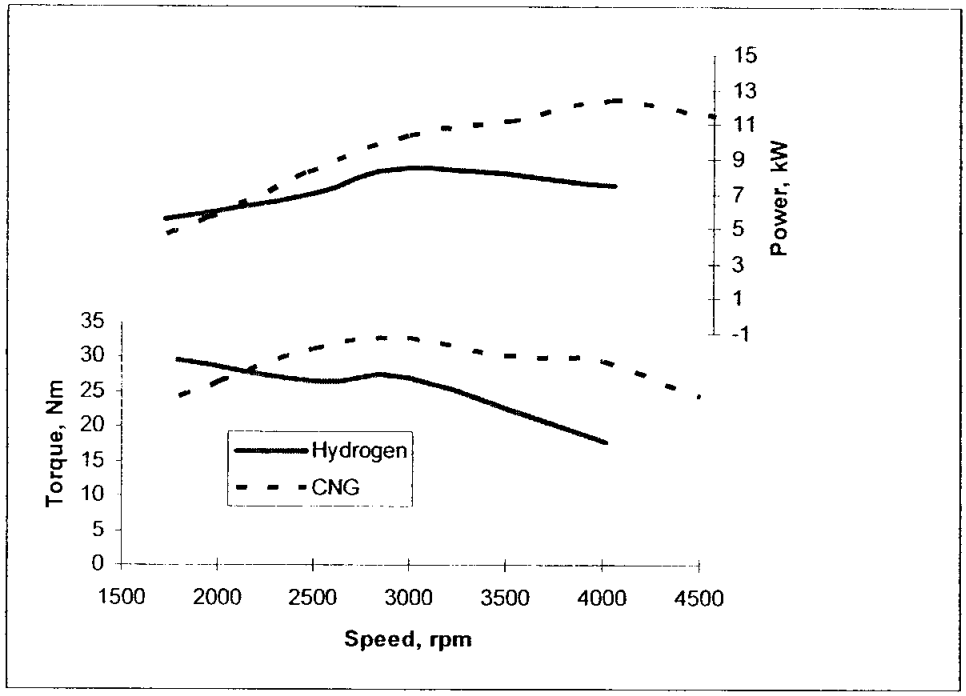

Figure 5-36 The comparison of engine performance between hydrogen and CNG

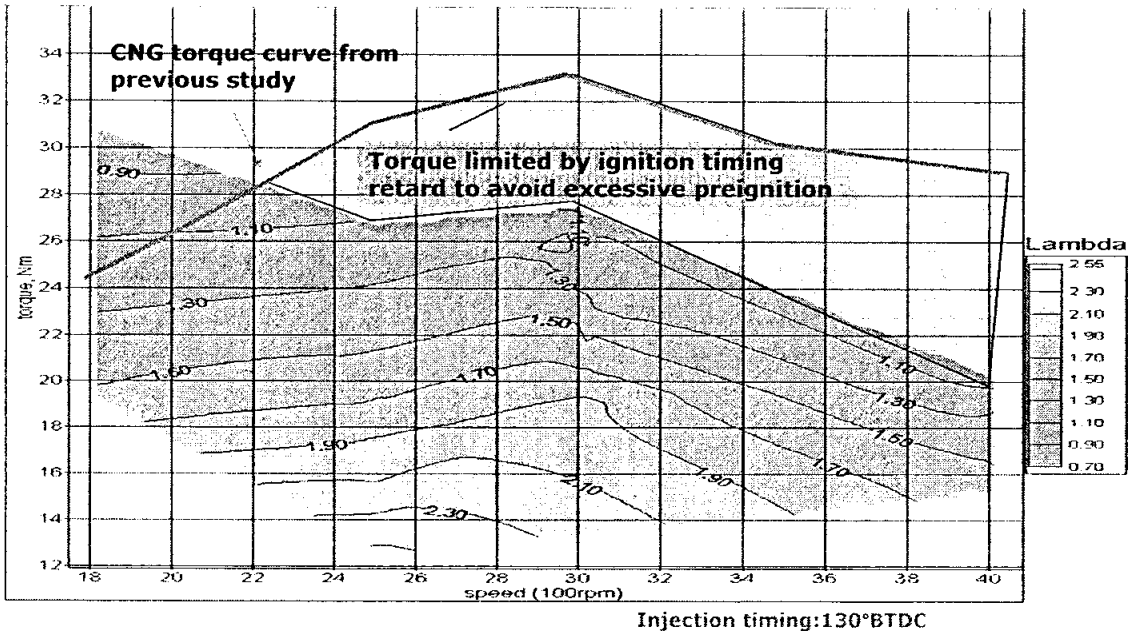

Figure 5-37 Torque map showing comparison with CNG full load performance

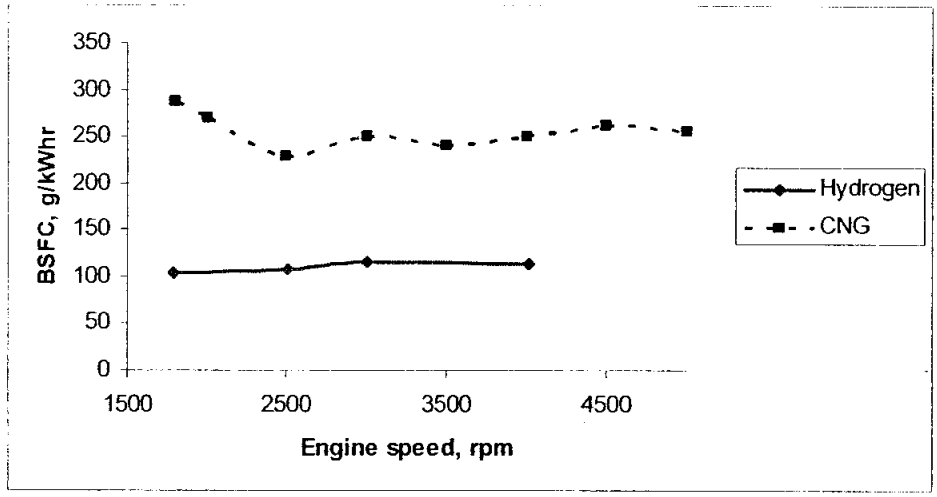

Figure 5-38 Comparison between hydrogen and CNG brake specific fuel consumption

At a high speed of 4000 rpm, the indicated thermal efficiency of hydrogen was 46% which was 10% higher than that of CNG. This can be attributed to the higher flame speed of hydrogen that enables the combustion to occur at near constant volume, which also raised the thermal efficiency [38]. However, at this speed (4000rpm), the start of injection was at 200° BTDC as later injection timing was not possible, and this resulted in volumetric efficiency loss and subsequent performance drop.

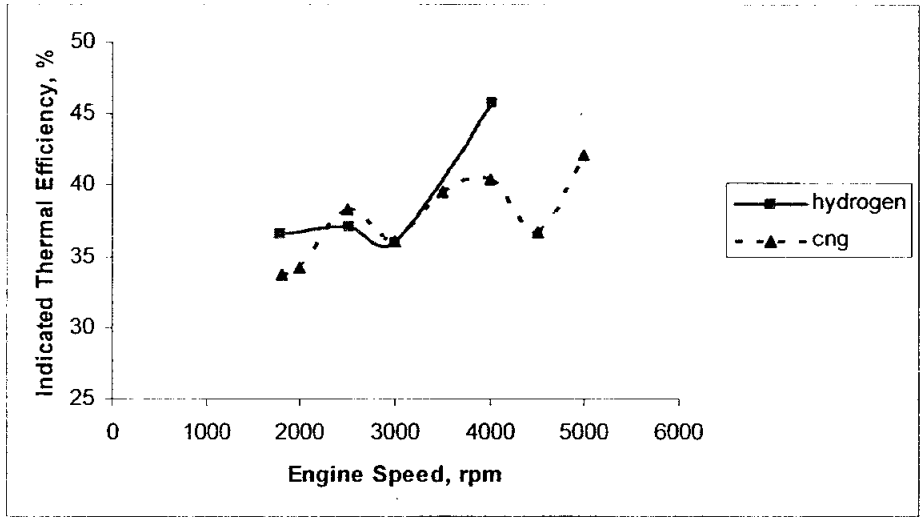

Figure 5-39 Comparison of the indicated efficiency of hydrogen and CNG

5.4.3 Engine Out Emissions

Since hydrogen air fuel ratio is at 33.4:1, which is significantly larger than CNG (16.9:1), direct comparison using concentration of its emissions is not possible. Hence the comparison is made in terms of its specific emissions, g/kWhr.

Figure 5-40 shows the comparison of brake specific emissions of the total hydrocarbons of the engine when using hydrogen and CNG. The specific emissions when using hydrogen (0.6g/kWhr) was found to be almost an order of magnitude lower than CNG (4.8g/kWhr). The source of hydrocarbons emissions when using hydrogen as a fuel was probably from the lubricants and dependent on the quenching distance of the combustion flame to the cylinder walls. Although hydrogen was expected to have smaller quenching distance than CNG, the emission of hydrocarbons was still much lower.

The brake specific emission of carbon monoxide is also depicted in Figure 5-40. The CO emissions of the engine when using hydrogen was very low compared to CNG, between 0.02 to 0.08g/kWhr against 3 to 47 g/kWhr respectively. This was expected as hydrogen does not contain carbon and the combustion of the engine lubricant was minimal. It is also important to note that the emissions of CO for CNG increased rapidly as the speed went lower than 2500rpm. This indicates that the combustion became less complete at lower speed.

Of particular interest is the emissions of oxides of nitrogen which is dependent on the temperatures of the combustion and the presence of nitrogen in air. Figure 5-40 shows the comparison of the brake specific emission of NO_x of the engine when fuelled with hydrogen and CNG. When using hydrogen, the NO_x emission was between 4.3 to 9.8g/kWhr with a maximum value at 2500 rpm. For CNG, the NO_x emission was between 3.6 to 15.3g/kWhr with the peak value at 4000 rpm. At lower speeds of below 2500 rpm, NO_x emission was higher for hydrogen as compared to CNG. At higher speed, CNG produced more NO_x emission.

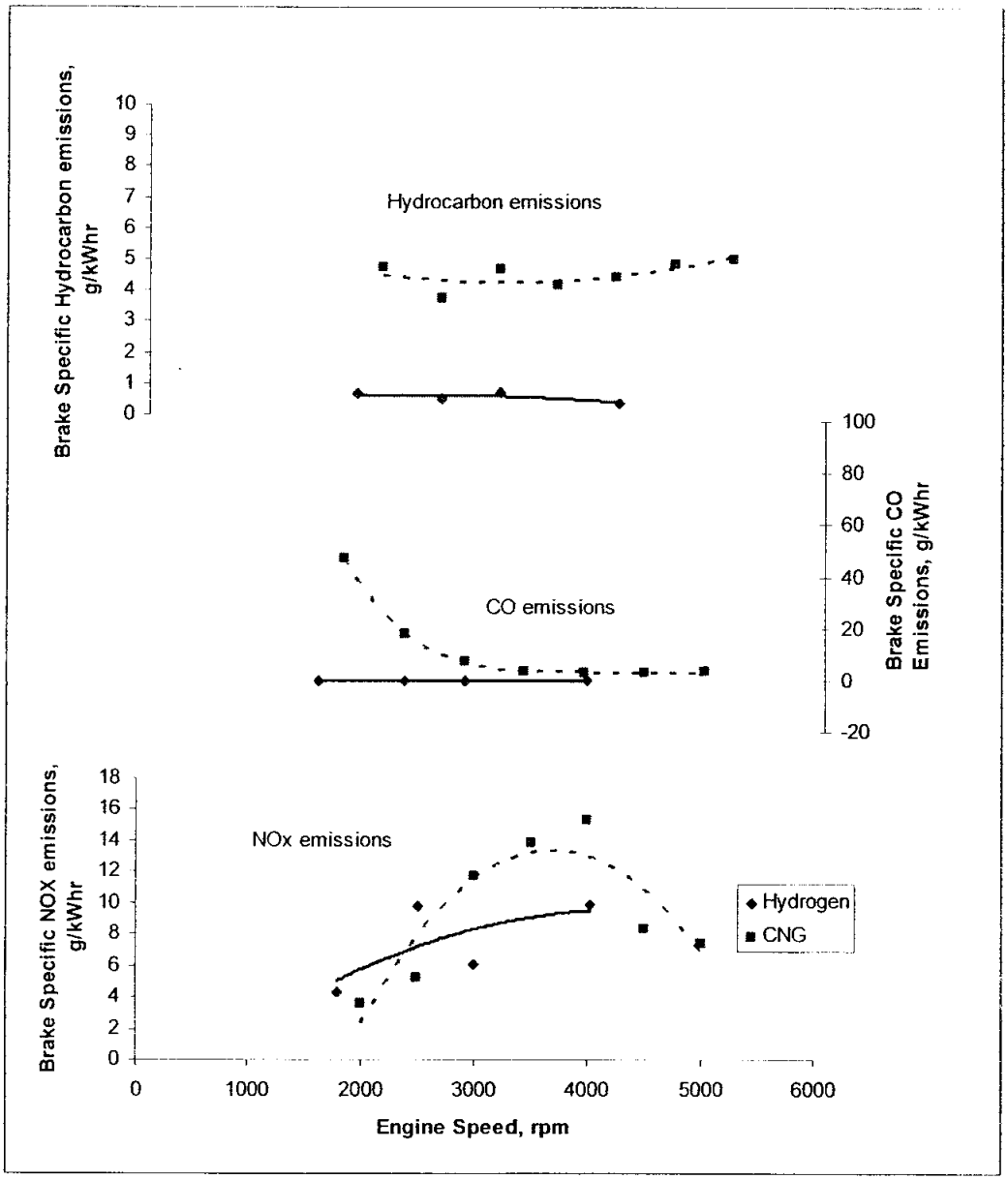

Figure 5-40 The comparison of bake specific emissions of hydrogen and CNG

Figure 5-41 shows the exhaust temperatures of the engine when using hydrogen and CNG. The exhaust temperatures are indicative of combustion temperatures. As expected, the combustion temperatures of hydrogen were higher than CNG at most speeds. At 4000rpm the exhaust temperatures of hydrogen was lower than CNG. This was due to the fact that at 4000rpm, the start of injection was earlier, 200BTDC which resulted in volumetric efficiency loss and thus lower heat is produced.

Figure 5-42 shows the peak cylinder pressure for both fuels which also signifies the peak cylinder temperature. At speed above 2000rpm, the peak cylinder pressure of hydrogen was less than that of CNG. As more ignition retard was needed at these speeds, the cylinder pressure and temperature was lower. Hence, the NO_x emissions was somewhat suppressed.

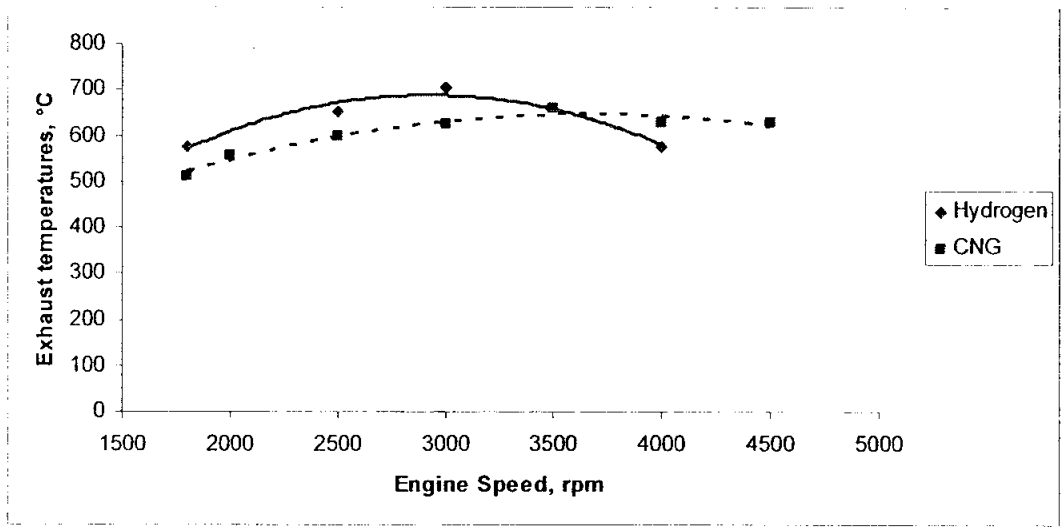

Figure 5-41 The exhaust temperature of the engine when operating with hydrogen and CNG

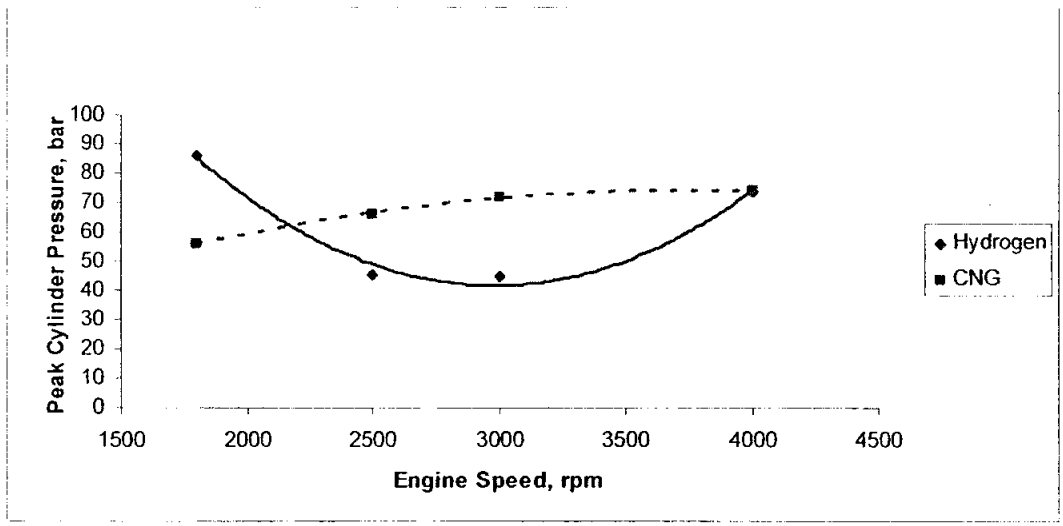

Figure 5-42 The peak cylinder pressure for hydrogen and natural gas

Summary

The hydrogen combustion was shown to be rapid and had low ignition delay in comparison to CNG even at low speeds where turbulence was less. As a result, at low speeds (<2000rpm) the performance of the engine was better than on CNG, with 10% torque increase at 1800rpm.

Alternatively, for fuel economy and efficiency, the engine can be operated leaner at lambda 1.1 to lambda 1.2 to give performance similar to the CNG engine at low speed (2000rpm and below). In this case, a 3% thermal efficiency gain is expected.

Hydrogen had 60% lower *BSFC* in comparison to CNG due to its high calorific value in mass basis. It is also interesting to note that at speeds below 2000 rpm, the indicated thermal efficiency and combustion efficiency of hydrogen was also higher than CNG (by approximately 10%). This shows that hydrogen remained efficient even at low speeds where turbulence and mixing was less.

Hydrogen combustion resulted in low THC and CO emissions, at almost an order of magnitude lower than CNG. For NO_x emissions, at lower speeds, hydrogen produced more NO_x than CNG as the combustion had higher peak temperatures. At higher speed, 3000 rpm however, the NO_x emissions for hydrogen was lower than that for CNG which was due to the retarded ignition timing which resulted in lower peak cylinder temperatures.

CHAPTER VI

CONCLUSIONS and RECOMENDATIONS

6.1 Conclusions

The experimental work investigating the performance and combustion characteristics of hydrogen in a single cylinder CNG direct injection engine was successfully conducted. Comparison with CNG operation was also carried out to demonstrate whether performance improvement can be achieved especially at low engine speeds. The following conclusions were drawn based on the investigation.

1. Direct injection hydrogen enables operation with stoichiometric air fuel ratio without abnormal combustion at low engine speed, below 2500rpm. At higher engine speed, abnormal combustion limits the operation of the engine to leaner ratios or retarded ignition with significant performance penalty.
2. At low end speed of below 2000 rpm, 10% improvement in power and torque over the natural gas operation was achieved by hydrogen combustion at stoichiometric. Alternatively, stock engine performance can be achieved using leaner hydrogen mixture with 3% thermal efficiency gain. This is due to the rapid and efficient combustion of hydrogen even though the low air motion at these speeds resulted in poor mixing.
3. Full direct and late direct injection (150°BTDC) proved to be able to maximise engine performance due to high volumetric efficiency. Although simulated port injection (300°BTDC) showed slightly higher thermal efficiency, the volumetric efficiency loss resulted in significant performance deficit.
4. Although MBT ignition timing can be achieved at slightly lean operation, the performance gained by the timing advance is not sufficient to overcome the loss due to the leaning effect. This is particularly obvious at low engine speed, 1800 rpm. Even though the efficiency and *BSFC* was minimum at lambda 1.2,

the torque deficit was almost 5 Nm. Thus, for full load operation, stoichiometric operation is preferred at low engine speed.

5. At intermediate engine speed, 3000rpm, the torque and power was relatively constant up to lambda 1.2 while the *BSFC* and efficiency was maximum. Thus, for this speed, operation at lambda 1.2 was optimum.
6. Lean unthrottled operation of the engine leads to 46% indicated thermal efficiency. This mode of operation is suitable for lower load application such as during cruising. At this load and low engine speeds, the engine performance is less sensitive to the injection timing.
7. In comparison to CNG, operating on hydrogen emits an order of magnitude lower CO and THC emissions.
8. In terms of NO_x emission, operation on hydrogen produces higher emission at low engine speeds where combustion is more efficient and has higher heat release. Operating leaner than lambda 1.3 could reduce NO_x emission of hydrogen engine, however, this results in lower performance.
9. At close to stoichiometric, the NO_x emission increases as the SOI is advanced, despite the lower peak cylinder pressure. This is due to the degree of stratification in which at late injections, the localised stoichiometric region is smaller resulting in lower NO_x.

In summary, low end speed performance improvement can be achieved by full direct injection or late partial direct injection of hydrogen at stoichiometric air fuel ratio. At this speed, hydrogen was shown to improve the performance of the original engine by 10%. For low load applications, high thermal efficiency can be obtained by unthrottled lean operation.

6.2 Recommendations

Further optimisation is required to fully operate the engine in hydrogen mode to cover the whole spectrum on engine operation. Figure 6-1 summarises the recommended future works on this engine. In particular, the abnormal combustion needs to be

eliminated. Cooler engine operations, reduction of hotspots in the combustion chamber or running a mixture of hydrogen-natural gas are among the options available to be explored.

Hydrogen and natural gas could be simultaneously introduced into the engine at different ratios trough port and direct injection respectively. The effects on the combustion and flame propagation properties could be an important area of study to further optimise the performance and emissions. Optimum mixture ratios and timing of the injections may be determined to overcome the abnormal combustion while gaining efficiency and performance.

For low load applications, unthrottled operation is recommended for thermal efficiency gain. In this mode, the injection duration is short and opportunity exists for optimisation in terms of injection parameters. Stratified charge could improve performance and allow very low loads such as idle to be run unthrottled. Flow and combustion visualisation as well as modelling would help understand the processes so that optimisation can be made.

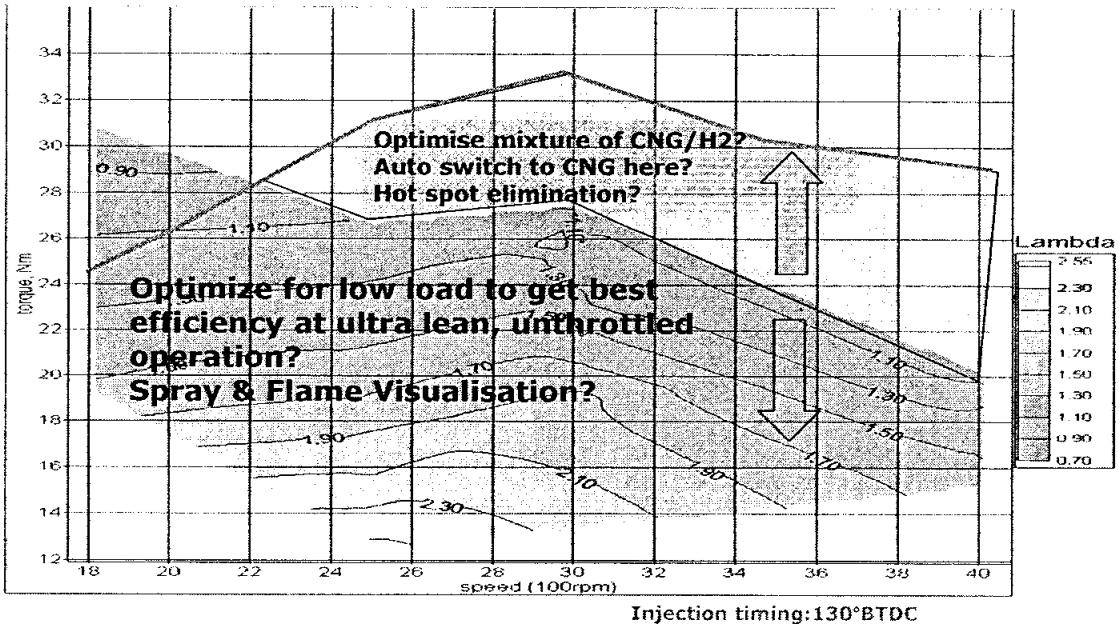

Figure 6-1 The recommended future works for optimising the hydrogen engine

REFERENCES

1. The National Hydrogen Association. *A Global Hydrogen Effort*, Fact sheets series www.HydrogenAssociation.org
2. Wan Ramli Wan Daud (2006).*Hydrogen Economy: Perspective From Malaysia*, presented at International Seminar on the Hydrogen Economy for the Sustainable Development, 28-29 September 2006.
3. The National Hydrogen Association. *The Hydrogen Economy*. Fact sheets series www.HydrogenAssociation.org
4. Georgia Institute of Technology (2007). *Improving Fuel Cells Durability: Research into Better Fuel Cell Materials and Designs Starts with Studying Failures*. Research News and Publication Office. November 28, 2007.
5. Wolf J.F. et. al., *BMW's Energy Strategy – Promoting the Technical and Political Implementation*, SAE Technical Paper Series, SAE2000-01-1324, 2000
6. Caley D., *Development of a Natural Gas Spark Ignited Direct Injection Combustion System DI CNG Engine System Development and DI CNG Engine Test Evaluation*, NGV2006, 2006
7. The National Hydrogen Association. *The History of Hydrogen*. Fact sheets series www.HydrogenAssociation.org
8. Argonne National Laboratory, *Argonne tests find near-zero emissions of BMW Hydrogen 7*, News Release, March28,2008.
9. College of the Desert, *Module 3: Hydrogen Use in Internal Combustion Engine*, US Department of Energy Hydrogen Fuel Cell Engines and Related Technologies Course Manual, www1.eere.energy.gov, 2001
10. Firmansyah (2007) *Optimization of Injection Parameters in Compressed Natural Gas Direct Injection (CNG-DI) Spark Ignition Engine*, MSc. Thesis, Universiti Teknologi Petronas,2007
11. Wicke V., et. al., *The potential for simulation of driveability of CVT vehicles, Society of Automotive Engineers Inc.*, 00PC-218, 1998
12. W F Stockhausen et.al. *Ford P2000 Engine Design and Vehicle Development Program*, SAE Technical Paper Series SAE2002-01-0240, 2002
13. Eischlseder H et. al., *The Potential of Hydrogen Internal Combustion Engines in a Future Mobility Scenario*, SAE Technical Paper Series, SAE2003-01-2267, 2003.
14. http://inventors.about.com/library/weekly/aacarsgasa.htm,2008
15. www.iangv.com (2008), NGV Statistics
16. www.gain.com (2008), LPG vehicles statistics
17. V Ganesan, *Internal Combustion Engines 2nd Edition*. 2003: Tata McGraw Hill Publishing Ltd.
18. Melendez M. et. al., *Emissions testing of Washington Metropolitan Area Transit Authority (WMATA) natural gas and diesel transit buses*, National Renewable Energy Laboratory technical report NREL/TP-540-36355, 2005
19. Heywood, JB., *Internal Combustion Engine Fundamentals*, McGraw Hill Book Company, 1988.

20. Yamada T. et. al. *Development of a New 1.8-Litter Lean Burn Engine for CNG*, poster paper, 7th International Conference and Exhibition on Natural Gas Vehicles, NGV2000, 2000
21. IANGV, *IANGV Emissions Report*, www.iangv.org, 2000
22. Durrel E., et.al., *Installation and Development of a Direct Injection System for a Gasoline and Compressed Natural Gas Engine*, NGV2000 conference, 2000
23. Oguchi M., et. al., *Development of a High Efficiency Natural Gas Engine*, NGV2000 conference, 2000
24. Shioji M., et. al., *Approaches to High Thermal-Efficiency in High Compression Ratio Natural Gas Engine*, NGV2000 conference, 2000
25. Wilhelm Hall, *Hydrogen Economy*, BMW Clean Energy Vision, Media Hydrogen Workshop, 2005
26. W F Stockhausen et. al. *Ford Hydrogen Powered P2000 Vehicle*, SAE Technical Paper Series SAE2002-01-0243, 2002
27. J Mackintosh, *Hydrogen is new hope to get gas-guzzlers off the road*, Financial Times, 8th June 2005.
28. Bluewater Network, *Hydrogen-fueled Hybrid Internal Combustion Engines – A potential near-term environmentally-sound bridge to hydrogen fuel cell vehicles*, undated document, www.bluewaternetwork.org
29. US Department of Energy, *Advanced Combustion and Emission Control Technical Roadmap*, Plan and Road Map documents by Energy Efficiency and Renewable Energy, http://www1.eere.energy.gov, 2006
30. Seth Dunn, *Hydrogen futures: towards a sustainable energy system*, International Journal of Hydrogen Energy 27, p. 235-264, 2002.
31. White CM et. al. *The hydrogen-fueled internal combustion engines: a technical review*, International Journal of Hydrogen Energy 31, p. 1292-1305, 2006.
32. Verhelst S. et. al., *A Critical Review of Experimental Research on Hydrogen Fueled SI Engine*, SAE Technical Paper Series, SAE2006-01-0430, 2006
33. Grabner P et.al., *Optimisation of a Hydrogen Internal Combustion Engine with Inner Mixture Formation*, In the report of the Institute for Internal Combustion engines and Thermodynamics, Graz University of technology - 1st International Symposium on Hydrogen Internal Combustion Engines. Published by Univ.-Prof Dr. Helmut Eichlseder., 2006
34. Green Car Congress, *Hydrogen-Enhanced Combustion Engine Could Improve Gasoline Fuel Economy by 20% to 30%.* www.greencarcongress.com, 2005
35. Fanhua Ma et.al., *Study on the extension of extension of lean operation limit through hydrogen enrichment in a natural gas spark-ignition engine* International Journal of Hydrogen Energy 33,p.1416-1424, 2008
36. Chapman K.S. et. Al., *Performance, Efficiency and Emissions Characterization of Reciprocating Internal Combustion Engines Fueled with Hydrogen/Natural Gas Blends*, Final Technical Report submitted to US Department of Energy by Kansas State University, 2007
37. Jorach R et. al., *Development of a Low-NO_x Truck Hydrogen engine with High Specific Power Output*, International Journal of Hydrogen Energy,Vol 22, p. 423-427, 1997
38. Sierens R.et.al., *An overview of hydrogen fuelled internal combustion engines*, Proceedings International Hydrogen Energy Congress and Exhibition IHEC 2005.

39. Das LM., *Hydrogen-oxygen reaction mechanism and its implication to hydrogen engine combustion*, International Journal of Hydrogen Energy vol.21, p. 703-715,1996
40. Szwaja S. et.al., *Comparison of hydrogen and gasoline combustion knock in a spark ignition engine*, International Journal of Hydrogen Energy, 2007
41. Verhelst S. et. al., *Aspects concerning the optimisation of a hydrogen fueled engine*. International Journal of Hydrogen Energy vol26, p. 981-985, 2001
42. Karim GA. et al., *Hydrogen Fueled Spark-Ignition Engines Predictive and Experimental Performance*, Transactions of the ASME vol 128,p 230-236, 2006
43. Das L.M., *Hydrogen engines: Research and development (R&D) programmes in Indian Institute of Technology (IIT) Delhi*, International Journal of Hydrogen Energy vol.27, p. 953-965, 2002
44. Subramaniam V.et. al., *Effect of water injection and spark timing on the nitric oxide emissions and combustion parameters on a hydrogen fuelled spark ignition engine*, International Journal of Hydrogen Energy, vol32p.1159-1173, 2007
45. Heffel JW., *NO_x emissions and performance data for a hydrogen fuelled internal combustion engine at 1500rpm using exhaust gas recirculation*, International Journal of Hydrogen Energy vol. 28,p.901-908, 2003
46. Shudo T. et.al., *Analysis of the degree of constant volume and cooling loss in a spark ignition engine fuelled with hydrogen*, Int J Engine Research, vol 2, p. 81-92, 2001.
47. Shudo T. et.al., *Reduction of Cooling Loss in Hydrogen Combustion by Direct Injection Stratified Charge*, SAE International, SAE2003-01-3094, 2003
48. Shudo T., *Improving the thermal efficiency by reducing cooling losses in hydrogen combustion engines*, International Journal of Hydrogen Energy, 2007
49. Ohira T. et. al., *Experimental Study of Emission Characteristics of a Small Hydrogen S.I. Engine*, SAE International, SAE2007-32-0074, 2007
50. Bleechmore C.et.al. *Dilution Strategies for Load and NO_x Management in a Hydrogen Fuelled Direct Injection Engine*, SAE Technical Paper Series, SAE2007-01-4097, 2007
51. Heffel JW., *NO_x emissions and performance data for a hydrogen fuelled internal combustion engine at 3000rpm using exhaust gas recirculation*, International Journal of Hydrogen Energy vol. 28,p.1285-1292, 2003
52. Peschka W., Hydrogen: *The future cryofuel in internal combustion engines*, International Journal of Hydrogen Energy vol. 23, p. 27-43, 1998
53. Guo LS. et. al., *A hydrogen injection system with solenoid valves for a four - cylinder hydrogen fuelled engine*, International Journal of Hydrogen Energy, vol. 24, p. 377-382, 1999.
54. Mohammadi A., *Performance and combustion characteristics of a direct injection SI hydrogen engine*, International Journal of Hydrogen Energy, vol. 32, p. 296-304, 2007
55. Knorr H., et.al., *The MAN Hydrogen Propulsion System for City Buses*, International Journal of Hydrogen Energy, vol. 23, p. 201-208, 1998
56. http://bmwgroup.com/ (2008), Roadmap of the BMW Group for sustainable mobility

57. Saravanan N. et. al., *An experimental investigation on DI diesel engine with hydrogen fuel*, Renewable Energy vol.33, p. 415-421, 2007
58. Saravanan N. et.al., *An experimental investigation on hydrogen as a dual fuel for diesel engine system with exhaust gas recirculation technique*, Renewable Energy vol. 33, p. 423-427, 2008
59. Saravanan N. et.al., *An experimental investigation of hydrogen-enriched air induction in a diesel engine system*, International Journal of Hydrogen Energy vol. 33, p. 1769-1775, 2008
60. Akansu S.O. et.al., *Internal combustion engine fuelled by natural gas-hydrogen mixtures*, International Journal of Hydrogen Energy vol.29, p.1527-1539, 2004
61. Dimopoulos P. et.al., *Increase of passenger car engine efficiency with low engine-out emissions using hydrogen-natural gas mixtures: a thermodynamic analysis*, International Journal of Hydrogen Energy vol. 32, p. 3073-3083, 2007
62. Huang Z.et.al., *Combustion characteristics of a direct injection engine fuelled with natural gas-hydrogen blends under different ignition timings*, Fuel vol.86, p. 381-387, 2007
63. Ortenzi F. et. al., *Experimental tests of blends of hydrogen and natural gas in light duty vehicles*, International Journal of Hydrogen Energy, 2008
64. www.hythane.com, 2008
65. Fontana G. et. al., *Performance and Fuel Consumption Estimation of a Hydrogen Enriched Gasoline Engine at Part-Load Operation*, SAE Technical Paper Series, SAE2002-01-2196
66. US Department of Energy, , Module 3: *Hydrogen Use in Internal Combustion Engines*, College of the Desert, Revision 0, December 2001, http://www1.eere.energy.gov, 2007
67. Heller K. et. al., *Optimisation of a hydrogen internal combustion engine with cryogenic mixture formation*, In the report of the Institute for Internal Combustion engines and Thermodynamics, Graz University of technology - 1st International Symposium on Hydrogen Internal Combustion Engines. Published by Univ.-Prof Dr. Helmut Eichlseder., 2006
68. Yi H.S., et. al., *The optimised mixture formation for hydrogen fuelled engines*, International Journal of Hydrogen Energy vol. 25, p. 685-690, 2000
69. Homan HS, et. al., *The effect of fuel injection on NO_x emissions and undesirable combustion for hydrogen-fuelled piston engines*. Int J Hydrogen Energy vol.8 p.131–46,1983
70. Tang X. et.al., *Ford P2000 Dynamometer Engine Development*, SAE Technical Paper Series, SAE2002-01-0242, 2002
71. Wallner T. et. al., *Evaluation of Injector Location and Nozzle Design in a Direct Injection Hydrogen Research Engine*, SAE Technical Paper Series, SAE2008-01-1785, 2008
72. White C.M., *A Qualitative Evaluation of Mixture Formation in a Direct-Injection Hydrogen-Fueled Engine*, SAE Technical Paper Series, SAE2007-01-1467, 2007
73. Kim Y.Y. et. al., *An investigation on the causes of the cycle variation in direct injection hydrogen fuelled engine*, International Journal oh Hydrogen Energy vol. 30, p. 69-76, 2005

74. Yi H.S., et. al., *Performance evaluation and emission characteristics of in-cylinder injection type hydrogen fuelled engine*, International Journal of Hydrogen Energy vol. 21, p. 617-624, 1996
75. Rottengruber H., et. al., *Direct-Injection Hydrogen SI Engine – Operation Strategy and Power Density Potentials*, SAE Technical Paper Series, SAE-2004-01-2927, 2004
76. Das L.M. et.al., *A comparative evaluation of the performance characteristics of a spark ignition engine using hydrogen and compressed natural gas as alternative fuels*, International Journal of Hydrogen Energy vol.25, p. 783-793, 2000
77. Bulla E., *The design and testing of a hydrogen fuelled internal combustion engine*, (MSc. Thesis, Graduate College of Nevada, Las Vegas), 2006
78. Gerke U. et. al., *Numerical analysis of the mixture formation and combustion process in a direct injected hydrogen internal combustion engine*, In the report of the Institute for Internal Combustion engines and Thermodynamics, Graz University of technology - 1st International Symposium on Hydrogen Internal Combustion Engines. Published by Univ.-Prof Dr. Helmut Eichlseder, 2006
79. Verhelst S., et. al., *A quasi dimensional model for the power cycle of a hydrogen-fuelled ICE*, International Journal of Hydrogen Energy, 2007
80. Pfitzner M. et. al., *Modelling of hydrogen and combustion in internal combustion engines*, In the report of the Institute for Internal Combustion engines and Thermodynamics, Graz University of technology - 1st International Symposium on Hydrogen Internal Combustion Engines. Published by Univ.-Prof Dr. Helmut Eichlseder., 2006
81. Colin O. et. al., *Adaptation of the ECFM combustion model to hydrogen internal combustion engines*, In the report of the Institute for Internal Combustion engines and Thermodynamics, Graz University of technology - 1st International Symposium on Hydrogen Internal Combustion Engines. Published by Univ.-Prof Dr. Helmut Eichlseder., 2006
82. Bender R. et. al., *Flamelet modelling of partially premixed hydrogen combustion in a direct fuel injection engine*, In the report of the Institute for Internal Combustion engines and Thermodynamics, Graz University of technology - 1st International Symposium on Hydrogen Internal Combustion Engines. Published by Univ.-Prof Dr. Helmut Eichlseder., 2006
83. Wallner T. et. al., *Endoscopic investigations in a hydrogen internal combustion engine*, In the report of the Institute for Internal Combustion engines and Thermodynamics, Graz University of technology - 1st International Symposium on Hydrogen Internal Combustion Engines. Published by Univ.-Prof Dr. Helmut Eichlseder., 2006
84. Braruer A. et. al., *Optical measurement techniques for the investigation of mixture formation and combustion in hydrogen internal combustion engines*, In the report of the Institute for Internal Combustion engines and Thermodynamics, Graz University of technology - 1st International Symposium on Hydrogen Internal Combustion Engines. Published by Univ.-Prof Dr. Helmut Eichlseder., 2006
85. Blotevogel T. et. al., *Developing planar laser-induced fluorescence for the investigation of the mixture formation process in hydrogen internal combustion engine*, SAE Technical Paper Series, SAE 2004-01-1408, 2004.

86. Ilbas M. et. al., *Laminar burning of hydrogen-air and hydrogen-methane-air mixtures: An experimental study*, International Journal of Hydrogen Energy vol 31, p. 1768-1779, 2006
87. G. Cussons Ltd, *The Ricardo/Cussons Standard Hydra Engine and Test Bed*, Issue 16, 1989
88. Emerson Process Management, *Product Datasheets Micro Motion® Meters Specification Summaries*, 2006
89. Temet Instruments Oy, *Gasmet™ CX-Series FT-IR Gas Analyser, On Line Series, Instruction and Operating Manual*, 2002
90. Ferguson C.R. and Kirkpatrick A.T., *Internal Combustion Engines Applied Thermosciences*, JWiley and Sons, 2001
91. ISO standard, *ISO1585 Road Vehicles- Engine test code – Net power*, International Organization for Standardization, Third Edition, 1992
92. Ishizawa S. et.al., *A Study of HC Emissions from a Spark Ignition Engine (The Influence of Fuel Absorbed into Cylinder Lubricating Oil Film)*, JSME International Journal vol. 30, No 260, p. 310-317, 1987
93. Li H. et. al., *Exhaust emissions form an SI engine operating on gaseous fuel mixtures containing hydrogen*, International Journal of Hydrogen Energy vol. 30, p. 1491-1499, 2005

APPENDIX 1

The Injector Calibration Curve